TREBALL DE FI DE CARRERA

TÍTOL DEL TFC: Use of Ram Air Turbines for electrical taxiing in Airbus 320

TITULACIÓ: Enginyeria Tècnica Aeronàutica, especialitat Aeronavegació

AUTORS: Dario Borhani Coca i Andreu Parés Prat

DIRECTOR: Joshua Tristancho Martínez

DATA: 18 de Juliol de 2012

Títol: Ús de Ram Air Turbines pel rodatge elèctric d'un Airbus 320
Autors: Dario Borhani Coca i Andreu Parés Prat
Director: Joshua Tristancho Martínez
Data: 18 de Juliol de 2012

Resum

El rodatge per pista d'un avió com l'Airbus 320, el qual té dos turboreactors, suposa no només un consum de combustible important, sinó que suposa també un consum notable en hores de funcionament dels motors, reduint el seu cicle de vida.

En aquest Treball de Final de Carrera s'estudia la possibilitat d'utilitzar uns aerogeneradors situats al fuselatge de l'aeronau que recarreguin unes bateries que permetin fer el rodatge de manera més eficient i que no gasti hores de funcionament dels motors principals. S'estudiaran possibles posicions per instal·lar el o els aerogeneradors, la idoneïtat d'aquestes propostes així com la seva eficiència.

Els estudiants hauran de tenir en consideració els efectes negatius sobre l'avió, com afecta a l'aerodinàmica d'aquest i quant d'eficient és tenint en compte el fet de que s'haurà de portar el pes extra de les bateries, així com del motor elèctric que mogui l'avió en terra.

El balanç energètic relaciona l'energia que s'obté durant l'aproximació amb la necessària pel procediment de taxi. L'objectiu és aconseguir una implementació viable del sistema en termes energètics i econòmicament desitjable per a la companyia aèria.

Paraules clau:
Ram Air Turbine, Airbus 320, Taxi Procedure, Approach Procedure, Electrical Taxiing.

Title: Use of Ram Air Turbines for electrical taxiing in Airbus 320
Authors: Dario Borhani Coca i Andreu Parés Prat
Director: Joshua Tristancho Martínez
Date: July, 18th 2012

Overview

Twin engine Airbus 320 taxi procedures involve not only a notable fuel consumption but an increment of engine hour operation, reducing its life cycle.

The possibility of using air generators is studied in this Bachelor Thesis. These air generators will be located in the aircraft fuselage so as to charge batteries. The energy stored will be used for an efficient taxiing but also for reducing main engines operating hours. Possible locations will be studied for one or more air generators, including its rightness and efficiency.

Students must consider all negative effects produced by air generators that may alter aircraft aerodynamics and operation. The extra weight added due to batteries and electrical generator needed must be taken into account so as to consider its efficiency.

The energetic balance relates the energy obtained during approach with the one needed for taxiing. The target is to achieve a viable implementation of this system in terms of energy and economically suitable for the airline as well.

Keywords:
Ram Air Turbine, Airbus 320, Taxi Procedure, Approach Procedure, Electrical Taxiing.

INDEX

LIST OF FIGURES

LIST OF TABLES

Acknowledgements

ACRONYMS, ABBREVIATIONS AND DEFINITIONS

A   Root Chord
AC   Alternate Current
AD   Airworthiness Directive
ADG   Air Drive Generator
AEO   All Engines Operating
ATC   Air Traffic Control
B   Tip Chord
C   Sweep distance
c   Mean chord
CG   Centre of gravity
CI   Cost Index
cn   Consumption
DC   Direct Current
DL   Disc Loading
DOW   Dry Operating Weight
Dv   Vertical Drag
EAS   Equivalent Air Speed
EPS   Emergency Power Sources
F   Force produced by the RAT blades
FCU   Flight Control Unit
FES   Flywheel Energy Storage
FMGS   Flight Management and Guidance System
FOD   Foreign Object Damage
FW   Fuel Weight
GW   Gross Weight
ISA   International Standard Atmosphere
KEAS   Knots Equivalent Air Speed
KIAS   Knots Indicated Air Speed
L   RAT blade length
M   Mach Number
MAC   Mean Aerodynamic Chord
OM   Outer Marker
PL   Payload
RAM   Ram Air Turbine
RPM   Revolutions Per Minute
S   Sweep Distance
SOP   Standard Operating Procedure
t   Time
TAS   True Air Speed
VHF   Very High Frequency

INTRODUCTION

This Bachelor Thesis came from the intention of taking part in the third edition of the contest *Fly Your Ideas,* proposed by the Airbus Company, which proposes contestants to develop environmental ideas applied to aeronautics.

The original idea was focused in taking advantage of the whirlwind created at the tip of the wing, due to pressure variations between lower and upper parts of it, by modifying the winglet. Conceptual preliminary analyses were done in order to check the viability of this idea. Some changes were applied to our earliest thoughts until it become our bachelor thesis, in which we take advantage of the RAT system used nowadays in emergency procedures, to obtain energy during common approach and landing procedures.

The energy obtained will be stored subsequently in the aircraft. The idea of implementing this system during approach came from the fact that in this procedure the intention of the aircraft is to decelerate, then, drag produced by RAT extraction will not be strictly restricting and it is going to be used for charging the batteries instead of being lost. The main target of this storage is being able to taxi electrically as an alternative of using fuel during ground movements' execution as it is done nowadays.

The aim of this project is to find an optimal solution that could be implemented in commercial aeronautics. Both students worked jointly during the entire project development due to the huge workload that entails the analysis of this new procedure and the implicit coordination it requires. Knowledge acquired during the degree was applied; such as physics, aerodynamics, graphic design and mathematics.

Referring to the work done, in chapter 1, a basic information research was arranged as an introduction from the most general concepts to the most detailed ones, which would be useful during the project development. In chapter 2 the state of the art was examined. It permits to show the actual use of RAT, in addition of storage and saving techniques. Once explained this basic information, chapter 3 aims to define a criterion for the optimal position selection as well as a final argument where the feasibility of the location where RAT is going to be positioned is evaluated. Once the options range has decreased, an accurate analysis related with the effects in the aircraft dynamics is going to be done in chapter 4, such as momentums and drag. Furthermore, simulations using SolidWorks Flow Simulation 2010 will be carried out in order to support the mathematical calculus commented previously. Eventually, in chapter 5 an energetic balance may demonstrate the validity of the system compared with the actual method using fuel to taxi.

CHAPTER 1. BASIC CONCEPTS

In this chapter some basic concepts will be introduced, from the most general to the most detailed ones leading its utility during the development of the project.

1.1   A320. Main features

Airbus launched its best-selling single-aisle product line with the A320, see Fig. 1.1, which continues to set industry standards for comfort and operating economy on short to medium-haul routes. Typically seating 150 passengers in a two-class cabin, or up to 180 in a high-density layout for low-cost and charter flights, the A320 is in widespread service around the globe on services that vary from short commuter sectors in Europe, Asia and elsewhere to transcontinental flights across the United States.

[1] The A320's advanced technology includes the extensive use of weight-saving composites, an optimized wing that is 20 per cent more efficient than previous designs, a centralized fault display for easier troubleshooting and lower maintenance costs, along with Airbus' fly-by-wire flight controls.
Advantages of the fly-by-wire controls, which were pioneered on the A320, are many. They provide total flight envelope and airframe structural protection for improved safety and reduced pilot workload, along improved flight smoothness and stability, and fewer mechanical parts.

Continuing its role as a pioneer, the A320 will be the first version in Airbus' single-aisle product line to be delivered with the new "Sharklets" large wingtip devices, which are designed to enhance the eco-efficiency and payload-range performance of the A320 Family.

The Sharklets, which completed their maiden flight outfitted on Airbus' A320 development aircraft in November 2011, are expected to result in at least a 3.5 per cent reduced fuel burn over longer sectors, corresponding to an annual reduction in CO_2 emissions of around 700 tonnes per aircraft. Sharklets also are incorporated in the A320neo, Airbus' fuel-efficient new engine option which brings enhanced range for its benchmark A320 jetliner.

Dimensions [2]

Wing span: 34.10 m
Overall length: 37.57 m
Height: 11 m
Cabin length: 27.51 m
Fuselage with: 3.95 m
Wheel base: 12.64 m

Capacity [2]

Pax: Typical seating 150 (2-class)
Max. 180

Freight: LD3 capacity underfloor: 7 LD3-46W
Max. Pallet number underfloor: 7
Bulk hold volume: 37.41 m³
Total volume: 25.8/31.7 m³ (LD3 / LD3+bulk)

Performance [2]

Range: 6,150 km with sharklets
Mach max: M0.82
Max ramp weight: 73.9 tonnes
Max take-off weight: 73.5 tonnes

Max landing weight: 64.5 tonnes   Max fuel capacity up to: 24,210 litres
Max zero fuel weight: 61.0 tonnes   Max Payload: 16.6 tonnes
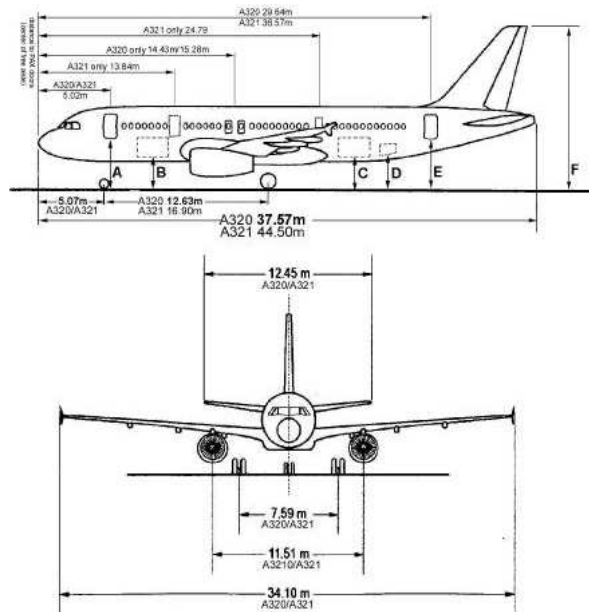
Fig. 1. 1 A320 dimensions and vertical clearances

Source: http://www.airbus.com/aircraftfamilies/passengeraircraft/a320family/a320/specifications/

1.2   Ram Air Turbine (RAT)

1.2.1   Function

Ram Air Turbines deal with supplying hydraulic emergency pressure as well as electrical energy to essential aircraft systems in case of breakdown in principal and support systems.

[3] When in this type of situations, RAT spreads into the relative wind in a brief time on the order of 2 seconds. The air dynamic pressure comes into contact with the propeller and causes a rotation movement which provides a final mean in order to obtain hydraulic power for the essential services.

[4] Nowadays, the greatest part of commercial aircrafts can create electric AC power using the RAT, which would swept along an electric AC current generator, commonly designated as ADG.

1.2.2   Situation and components

[3] RAT location depends on the aircraft model. It is allocated in a compartment into the ventral fuselage of many aircrafts and has an extension mechanism for the hatch, but also for the RAT unit.

RAT consists mostly on the following elements:

- Propeller blades
- Hydraulic pump
- Blades velocity governor
- Structure and extension support
- Hydraulic pressure supplier pipes

The propeller remains at constant speed (common values between 4,500 rpm and 6,000 rpm) but also it is able to keep the engine speed until a very low aircraft velocity, on the order of 115 KIAS.

The volume of hydraulic fluid flow that has to be supplied to the RAT depends on the aircraft where the unit is installed. E. g., for long range aircrafts about 40 litres of hydraulic fluid per minute and a pressure of 2,800 psi to 3,000 psi are needed.

1.2.3   RAT in commercial aircrafts

[3] In commercial aircrafts, RAT uses the fly-by-wire system and includes a generator conducive to provide emergency electrical energy for the flight control system. In case of emergency, RAT spreads automatically when:

- The aircraft is in Flight Mode
- Total loss of hydraulic pressure
- No combustion into the engine combustion chamber
- Total loss of electrical energy

[4] In an emergency situation, the AC generation adheres to assuring that the ADG generator will supply energy to the essential bars, in order to maintain the aircraft in controlled emergency flight conditions if any of the following conditions that causes the spread and start-up of the RAT occurs.

- Total failure of AC energy
- Engine generator failure while the second engine is not operating (twin-engine aircraft)
- Others

1.2.4   Deficiencies

[6] Ram Air Turbines have some recognized deficiencies:

- Such turbines are somewhat complex and expensive to manufacture.
- The mechanism of the governor apparatus may require calibration in order for the governor to maintain a substantially constant and predetermined rotor speed during flight of the aircraft.

- In military uses, the RAT is subject to operation and wears for a much longer period of time than its period of effective use. Such use leads to failures of RAT and to incapacitation of the auxiliary devices they power.
- If the RAT turbine blades are allowed to move to their fine pitch position, the parasitic drag of the RAT upon the aircraft is increased greatly. But if additional apparatus is provided to feather the turbine blades when the rotor is braked, the complexity and cost of the RAT are increased, as are the chances of its malfunctioning.

1.2.5   Operation procedures of a RAT

[6] The following steps describe the operation procedures of a RAT:

- Deploy signal commanded (automatic or manual)
- Up-lock releases
- Deployment actuator provides force to open RAT compartment doors and deploy RAT into airstream
- Turbine locked in position until blades clear aircraft
- Turbine is released and accelerates to rated speed
- Turbine governor maintains speed control
- RAT provides emergency power to aircraft
- RAT remains deployed for rest of flight

1.3   Taxi procedures

This procedure it is briefly introduced for the future need of data referring to taxi time, taxi speed and taxi distance.

1.3.1   Taxi procedure

[7] The airplane is normally taxied from the left seat only, using powered nose wheel steering. During taxi, at least one VHF radio shall be on, tuned to an appropriate frequency that would permit exchange of traffic information, and monitored by the pilot. Should it be necessary to have the co-pilot seat occupied by a person other than a pilot qualified on type; this person shall be fully briefed on duties and procedures. If necessary, a marshaller is to assist in taxiing in the vicinity of obstructions.

Taxi trajectory and speed are to be managed to operate the aeroplane safely and smoothly. Only the minimum thrust/power above idle that is required should be used to accelerate to taxi speed from a stop. All turns, accelerations, and decelerations shall be carried out smoothly. At taxi speeds the aeroplane is to be steered using the tiller and/or rudder pedals to control the powered nose wheel steering. Brakes should not be used for steering. Acceleration and deceleration during taxiing should be planned so as to minimize wear on brakes. When applying brakes to stop the aeroplane, brake pressure should

gradually be reduced as the aeroplane slows to prevent it from lurching to a stop.

1.3.2   Taxi speed

Taxi speed shall be appropriate to the conditions. When taxiing in congested areas the aeroplane shall be taxied at no more than walking speed. For taxiing in open areas taxi speed may be increased, but shall not be such that harsh braking or turning at high speed is required. For taxiing on surfaces contaminated by slush, snow, or standing water, speed shall be adjusted (increased or decreased) to minimize impingement of spray/snow on the aeroplane. For taxiing on gravel, loose surfaces, or unprepared surfaces, speed shall be adjusted (increased or decreased) to minimize FOD to engine intakes and propellers. For turns of more than a few degrees, the aeroplane shall not be taxied at more than walking speed. Reduced speed in turns is required (particularly in cold weather) to reduce lateral strain of the aeroplane and minimize the possibility of a tire losing air through the bead/wheel contact area. However, for forwardly calculus we are going to take as maximum taxi speed 16 knots [8].

1.3.3   Taxi time

Time has special relevance during taxi operations. Total fuel burn on the ground would be a function of the taxi time and number of accelerations made by the aircraft, see equation 1.1. Taxi time is a determinant of fuel consumption. In addition, the effect of taxi time on fuel is linear given that engines run at constant thrust for a large part of the taxi-out process. Stops are expected to affect fuel burn because of the breakaway thrust required to displace the aircraft once stopped.

$$\frac{f}{\sqrt{T_{amb}}} = a_2 + b_2 \cdot t + c_2 \cdot n_a$$

(1.1)

[9] In equation 1.1, f is the total fuel consumed, t is the total taxi time and n_a is the number of accelerations made by the aircraft during taxi. a_2, b_2 and c_2 are the parameters that depend exclusively on the aircraft.

The equation 1.1 would be useful for chapter 5 where the energetic balance is computed. Obviously, both time and fuel consumption depends on which airport we situate the taxi. Taking an approximation for any airport, 10 minutes for taxing-in [8] and 10 minutes for taxing-out will be considered.

1.3.4   Taxi distance

So as to calculate the taxi distance, an example route in Barcelona-El Prat airport and Madrid-Barajas airport will be drawn. See Fig. A.1 and Fig. A.2 in Annex A. Adopting large distances from gate until the threshold, a pessimistic example will be calculated, the slope though is going to be calculated in chapter 5.

According to the explanation in the previous paragraph, in order to calculate the worst case distances in Barcelona-El Prat airport and Madrid-Barajas airport, the ground movements map (GMC) from OACI [10] will be used.

Distance in Barcelona-El Prat: 3,136.36 m.
Distance in Madrid-Barajas: 3,000 m.

1.3.5   Taxiing without all engines operating

The aeroplane is not normally taxied with the intention of flight unless all engines are operating. However, it may be appropriate to reposition the aeroplane without starting all engines. This procedure is more likely to apply for taxiing after landing.

1.3.6   Reverse taxiing

[8] Taxiing in reverse should be kept to a minimum. Taxiing in reverse with asymmetric power is prohibited. Brakes shall not be used during reverse taxi. Rather the aeroplane shall be stopped or accelerated into forward taxi using forward thrust only.

- Caution that must be taken during taxiing

Application of brakes during reverse taxiing may cause the aeroplane to tip onto its tail, resulting in substantial damage.

If deciding to taxi in reverse, the following negative aspects should be considered:

  i.   Poor visibility behind the aeroplane
  ii. Increased FOD hazard to engines/propellers
  iii. High engine temperatures and reduced engine cooling

1.4   Approach procedures

We are going to focus on the approach sequence that may be of our interest in future calculus. The plane has to decelerate, loosing speed and descending to intercept the correct path for landing. We can take advantage of this deceleration by using the RAT and charging the batteries, which will possibly allow us to taxi electrically. Nevertheless, and bearing in mind that calculus will be done forwardly, we are going to describe approach in a physical procedure way, not focusing in communications with ATC, checklists, or emergency procedures. For theorical specifications points 12 and 13 of Rules of the Air and Air Traffic Services Doc 4444-RAC/501 may be consulted. Particularly 12.2.1; 13.2.2; 13.2.3; 13.2.4; 13.2.5

1.4.1   Specifications for a real case

Few useful characteristics of approach in a practical case will be described for our future study.

Taking Barcelona-El Prat airport as an example we see that often the minimum approach altitude starts at 7,000 ft. It is obvious that depending on the airport different values are going to be set out, but inquiring into other charts from Madrid-Barajas airport, can be seen that if an approach starts later (less altitude), the distance to the airport is less as well, keeping the descend angle in an approximately same value compared to the Barcelona-El Prat airport case.

Distances calculus will be split in two parts due to the angle of attack variation depending on the distance to the runway and the speed of the plane in those different moments; the first part goes from 7,000 ft to 2,000 ft altitude and the horizontal distance goes from the point in which the plane is at 7,000 ft until 6 nm from the header of the runway, the second part starts at 2,000 ft and 6 nm (called the OM point) from the header until the landing.

For this main purpose, we have looked up the Instrumental Approach Charts in the AENA webpage, particularly in AIP [11], in order to find out some values of distances from the beginning of the approach to the OM point.

Once we have the mean distance, we will consider an approach velocity in order to estimate the time until the plane has touched ground. Some routes are going to be computed using Google Earth, taking coordinates of the main points that define each route, to get the approach distances. An error is going to be committed, so that is an approximation. Three different approaches were considered to find this typical distance.

1.4.1.1   FROM 7,000 ft to 2000 ft

- **IAC/4-ILS RWY 07L (From RUBOT). See Fig 1.2.**
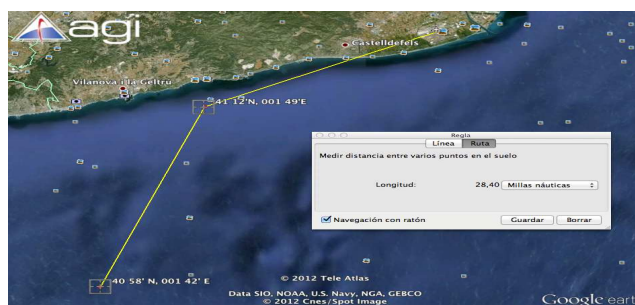
Fig. 1. 2 Distance from RUBOT to RWY 07L. See detail as 28.40 nm

As has been said, we start at 7,000 ft and we take approx. 28.40 nm – 6 nm until be stabilized at 2,000 ft so:
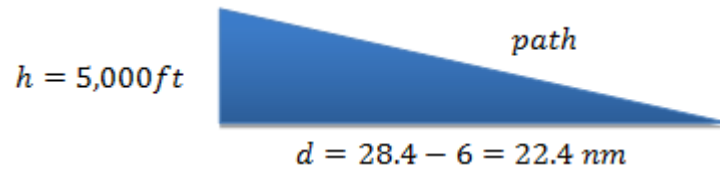
Hence,

$$d = 22.4\ nm = 41.48\ km = 41{,}480\ m \qquad\qquad \alpha = 2.1^{\underline{o}}$$

$$h = 5{,}000\ ft = 1{,}524\ m \qquad\qquad path = \frac{1{,}524}{\sin \alpha} \qquad (1.3)$$

$$\tan \alpha = \frac{1{,}524}{41{,}480} \qquad (1.2) \qquad\qquad \boxed{path = 41{,}590\ m}$$

- **IAC/10-ILS RWY 25L (From CALELLA). See Fig. 1.3.**
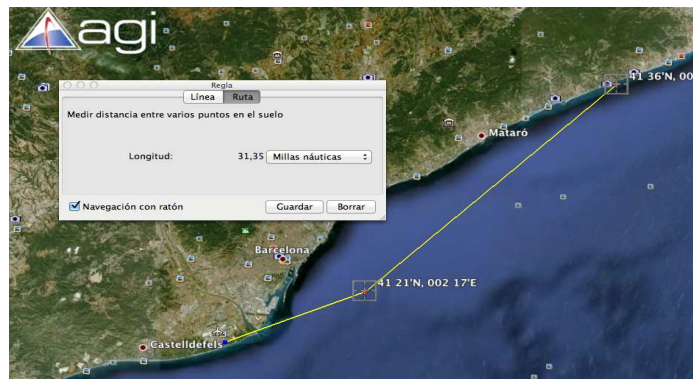
Fig. 1. 3 From CALELLA to RWY 25L. See detail as 31.35 nm

This route takes approximately 31.35 nm. – 6 nm. until being stabilized at 2,000 ft.
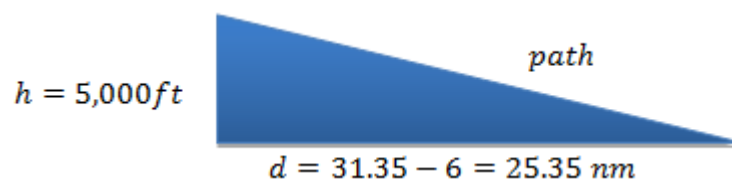
So:

$$d = 31.35\ nm = 58.07\ km = 58{,}070\ m \qquad\qquad \alpha = 1.5^{\underline{o}}$$

$$h = 5{,}000\ ft = 1{,}524\ m \qquad\qquad path = \frac{1{,}524}{\sin \alpha} \qquad (1.5)$$

$$\tan \alpha = \frac{1{,}524}{58{,}070} \qquad (1.4) \qquad\qquad \boxed{path = 58{,}219\ m}$$

- **IAC/9-VOR RWY 07R (From SABADELL). See Fig. 1.4.**
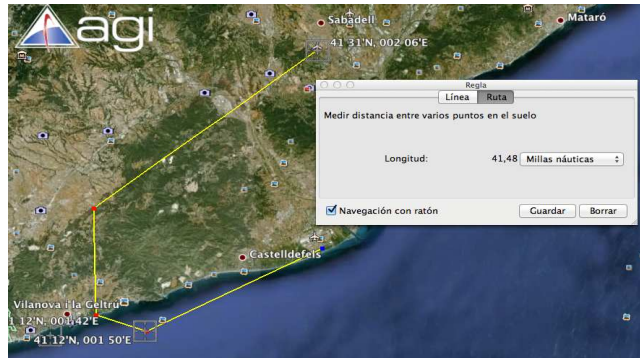
Fig. 1. 4 From SABADELL to RWY 07R. See detail as 41.48 nm

As has been said, we start at 7,000 ft and we take approx. 41.48 nm – 6 nm until be stabilized at 2,000 ft so:

$$h = 5,000 ft$$
$$d = 41.48 - 6 = 35.48\ nm$$
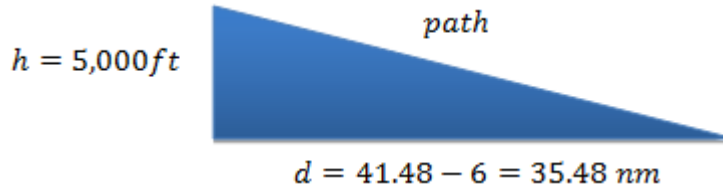
So:

$$d = 31.35\ nm = 76.82\ km = 76,820\ m \qquad\qquad \alpha = 1.14^{\circ}$$

$$h = 5,000\ ft = 1,524\ m \qquad\qquad\qquad path = \frac{1,524}{\sin \alpha} \qquad\qquad \textbf{(1.7)}$$

$$\tan \alpha = \frac{1,524}{76,820} \qquad\qquad \textbf{(1.6)} \qquad\qquad \boxed{path = 76,600\ m}$$

Brief table:

Approach Name	Distance [m]	Angle of descent [⁰]
IAC/4-ILS RWY 07L	41,590	2.1
IAC/10-ILS RWY 25L	58,219	1.5
IAC/9-VOR RWY 07R	76,600	1.14

Table 1. 1 Distances and angles of descent for each approach

Doubtlessly we cannot say values exposed in table 1.1 are enough to obtain an accurate mean of distances and angles but we can assume the solution as typical values of approach. However, a mean is going to be worked out to have only one number.

Typical distance from 7,000 ft to 2,000 ft [m]	Typical angle of descent [⁰]
58,803	1.58

Table 1. 2 Typical distances and angles of descent

Once we have the mean of distances and descending angles, approach speed will be computed. Due that our RAT cannot work over some velocities, see section F.1. from Annex F for all RAT specifications, 200 knots for the approach are considered.

Starting from the basic formula:

$$v = \frac{x}{t} \ m/s \qquad (1.8)$$

We can find the time we will take until being at 2,000 ft:

200 kt = 102.88 m/s

$$t = \frac{58{,}808}{102.88} = 571.57 \ s \approx 572 \ s \ \rightarrow \ t = 9 \ minutes \ 32 \ seconds$$

1.4.1.2   FROM 2,000 ft to Landing

[12] Although deceleration characteristics largely depend on the aircraft type and gross-weight, the following typical values can be considered for a quick assessment and management of the aircraft deceleration capability:

Deceleration in flight level:

- With approach flaps extended: 10 to 15 kt per nm
- With landing gear down and flaps full: 20 to 30 kt per nm

Deceleration on a 3 degree glide path:

- With landing flaps and gear down: 10 to 20 kt per nm.

When established on a typical 3 degree glide slope path with only slats extended (i.e., with no flaps), it takes approximately 3 nm (1,000 ft) to decelerate down to the target final approach speed and to establish the landing configuration. See Fig. 1.5 for more clarity.

Speed brakes may be used to achieve a faster deceleration, as allowed by the aircraft type (i.e. speed brakes inhibition).

Usually the use of speed brakes is not recommended when below 1,000 ft above airfield elevation and/or in the landing flaps configuration.

The following conditions are considered:

- IMC (stabilization height 1,000 ft above airfield elevation)
- Final approach speed (VAPP) = 130 kt

The maximum deceleration achievable between the OM (typically 6 nm from the runway threshold) and the stabilization point (1,000 ft above airfield elevation / 3 nm) is: 10 kt per nm · (6 – 3) nm = 30 kt.

In order to be stabilized at 130 kt at 1,000 ft above airfield elevation, the maximum speed that can be accepted and maintained down to the OM is: 130 kt + 30 kt = 160 kt.
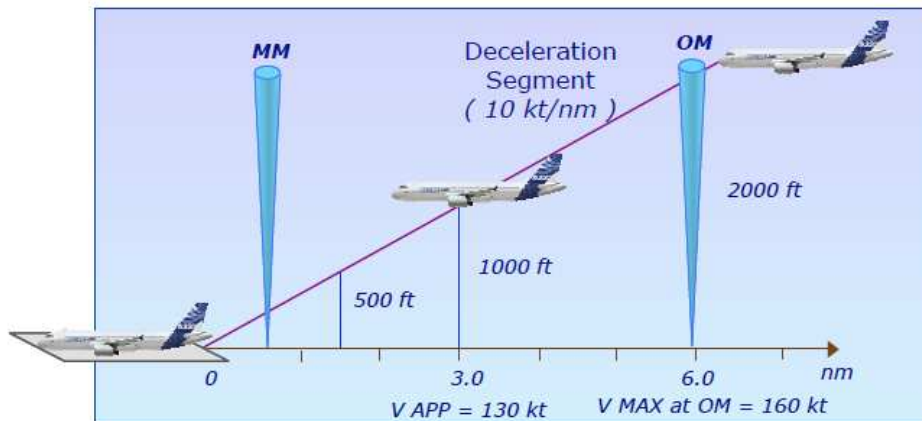
Fig. 1. 5 Approach profile

Source: http://www.smartcockpit.com/pdf/flightops/flyingtechnique/2

It will be considered that the aircraft descends continuously from OM to the height of 1,000 ft at 160 kt from there on, at 130 kt to the threshold so as to calculate reference time. All paths are at 3 degrees from the threshold.

3 nm = 5,556 m; 1,000 ft = 305 m; 160 kt = 82.3 m/s; 130 kt = 66.9 m/s

The first and second line measure 5,564 m each one.

A measure of the time that takes us to complete the descent at correct speeds must be done. The equation 1.8 will be used.

$$v = \frac{x}{t} \ m/s \qquad \qquad \textbf{(1.8)}$$

The estimated time in the first part (at 160 kt) will be calculated using:

$$t = \frac{5.564}{82.3} = 67.6 \ s \qquad \qquad \textbf{(1.9)}$$

For the second sector at 130 kt, using the same formula:

$$t = \frac{5.564}{66.9} = 83.2 \ s \qquad \qquad \textbf{(1.10)}$$

So, a reference time of approach will be taken as the sum of both values. Then, the result is:

$$\boxed{t = 150.8 \ seconds \approx 2 \ minutes \ 30 \ seconds}$$

1.4.2 Summary for the total values

Following, total approach time and total distance is computed.

1.4.2.1   Total approach time

$$t_{TOTAL} = 2\ minutes\ 30\ seconds + 9\ minutes\ 32\ seconds =$$
$$= 12\ minutes\ 2\ seconds$$

1.4.2.2   Total distance

$$\begin{aligned} Total\ distance \\ = [d(From\ 7{,}000\ ft + 2{,}000\ ft) \\ + d(From\ 2{,}000\ ft\ to\ Landing)]\ km \end{aligned} \tag{1.11}$$

$$Total\ distance = 58.803\ km + 11.112\ km = 69.915\ km$$

CHAPTER 2. STATE OF THE ART

In this chapter we delve into the state of the art, where it is shown which is the actual use of RAT on military applications, a non-military application, energy storage techniques and taxiing saving techniques.

2.1   RAT applications

2.1.1   Military applications

2.1.1.1   Vulcan B2

[13] First **Vulcan B 2s**, see Fig. 2.1, were powered by **Olympus 201** engines, set behind enlarged air intakes and in front of toed-out jet pipes.

The introduction of a main AC system was not only much more reliable; it also meant that more effective back-up facilities could be built into the aircraft. The main Vulcan electrical system was divided into two halves so even if two alternators on one side failed, the two on the other side could carry all loads. If all four alternators failed at height, pilots would pull a handle that lowered a Plessey RAT into the airstream below the port engine intake.

Fig. 2. 1 Vulcan Bomber

Source: Vulcan units of the cold war. Andrew Brookes. Osprey Combat Aircraft. No.72

This wind-driven alternator would provide power for the flying controls until the bomber descended to less rarefied levels, where the AEO could start the Rover gas turbine Airborne Auxiliary Power Plant, positioned outboard of engine number four, to take over all the essential services until the main alternators could be brought back on line.

2.1.1.2   F-4 Phantom

[14] The F4-Phantom emergency equipment consists of a pneumatically extended and retracted RAT, and a comprehensive set of warning and indicator lights.

A RAT in the upper left side of the aircraft fuselage is a power source for an emergency generator. The turbine assembly consists of a housing that contains two variable pitch turbine blades, a governing unit that controls the pitch of the blades, and the gearing to transfer blade rotation to a vertical drive shaft.

The RAT acts as a constant speed drive unit for the emergency generator providing the airspeed over 90 knots. The RAT is extended and retracted pneumatically by a handle in the forward cockpit. Pushing down on the handle extends the turbine, pulling up on the handle retracts it.

2.1.2   A non-military application. EPS

[15] All hydraulic systems have some form of emergency power source (EPS). It simplest form will be an accumulator. It is mandatory for wheel-brake systems including a standby accumulator capable of supplying power for a predetermined number of brake applications when all other sources of power are inoperative. Cockpit canopies are frequently opened and closed hydraulically. Emergency openings can be achieved by using the energy stored in accumulators.

For longer periods of emergency power supply, an electric motor driven pump may be provided. The available flow is usually kept as low as possible to operate only batteries and minimize its limitations such as weight and size. Weight may be kept to minimum using one-shot batteries.

For continuous emergency supply a RAT may be used. A location into the aircraft structure must be found to stow the turbine and carriage assembly. Also, a small accumulator is needed to deploy the turbine in case of emergency.

Hydraulic pumps and/or emergency electrical generators can be mounted immediately behind the turbine on the same shaft. Anyhow, it is more common to mount them at the bottom of the carriage arm close to the deployment hinge axis. This involves the use of drive shafts and gears. Deployment of the RAT is done through the electric motor-driven pump.

In spite of these drawbacks, RATs have proved their worth several times, particularly on civil aircrafts, providing the only means of hydraulic and electric power until an emergency has been solved and the aircraft has been recovered to a safe attitude.

2.2   Taxiing saving techniques

2.2.1   Engine shut down

[16] Disengaging one engine is a usual procedure for fuel saving while taxiing. Nevertheless, it has its disadvantages:

- This procedure is not recommended for uphill slopes or slippery runways.
- No fire protection from ground staff is available when starting engine away from the ramp.

- Mechanical problems may occur during start-up of the other engine, requiring a gate return for maintenance and delaying departure time.

After landing, it is required not less than a defined time before shutting down the engine. Cooling time after reverse operation, prior to shut down, has a significant effect on engines life.

It is recommended that once the runway is cleared, engine 1 is feathered, and once the appropriate cooling time has expired, it is shut down, even if parking stand has not been reached.

When taxiing with one engine cut off, the electrical supply of the hydraulic system is done by the operating engine. Some precautions have to be taken to check that the entire hydraulic system, notably in charge of the braking and the steering, remains correctly supplied by the remaining engine. The SOPs have to be changed accordingly.

2.2.2   Sectorization

[17] Another technique used for reducing fuel consumption is distributing efficiently the platforms along the airport in order to reduce the taxi time the less as possible. This matter belongs of how an airport is designed. An efficient airport will be the one whose distribution allows the correct and fast positioning of the aircrafts along its platform.

2.3   Energy storage techniques

2.3.1   Batteries

Batteries main purposes:

- To assist in damping transient loads in the DC system.
- To provide power in system start-up modes when no other power source is available.
- To provide a short-term high-intensity source during emergency conditions while alternative/backup sources of power are being brought on line.

[15] Most modern aircraft systems utilize battery chargers to maintain the battery charge at moderately high levels during normal system operation thereby assuring a reasonable state of charge. In Fig. 2.2 an example of aeronautical batteries is shown.

Fig. 2. 2 Aeronautical Batteries

Source: Sistemas eléctricos y electrónicos de las aeronaves. Jesús Martínez Rueda. Thomson Paraninfo. 2007. Pages 4-18

Battery parameters extracted from [18]:

- **Capacity:** It is measured in Amperes per hour [A*h]. Depends on the electrolyte quantity, active material quantity into the plates and its surface.
- **Internal resistor:** It is measured in Ohms [Ω]. Varies significantly with the electrolyte type, the area of the plates, the material of the plates and the separation space between positive and negative plates.
- **Voltage:** It is measured in Volts [V]. Depends on the number of accumulators (if they are in series), the components chemical settings, the concentration of the electrolytes and temperature of the electrolytes.

2.3.1.1   Accumulators

Most accumulators are assembled in order to reinforce parameters like voltage and capacity. They can be put into groups using serial or parallel methods.

2.3.1.1.1 Lead-Acid batteries

[18] Lead-acid batteries have been an important standard as continuous energy sources. But nowadays most systems with a great energy demand, such as turbine engine aircrafts, use Ni-Cd batteries rather than Lead-Acid ones.

The accumulator that constitutes this type of batteries contains dissolution of sulphuric acid plus distilled water as an electrolyte. Positive and negative electrodes are joined into a series of alternated plates buried into this electrolyte.

Lead-acid batteries are not favoured in modern applications due to corrosive effects. To preserve battery health it is usual to monitor its temperature which gives useful indications of over-charging and thermal runaways.

2.3.1.1.2 Ni-Cd batteries

[18] Due to an increasing demand of current intensity in turbine engines it is necessary to reduce the batteries internal resistor. This objective is accomplished by Ni-Cd batteries because of his low level of internal charge,

which assures an almost constant output voltage until the battery is practically flat.

Ni-Cd batteries need air ventilation because of a temperature upturn when its internal resistor is reduced. This boost can produce a thermal overflow during the battery discharge. In order to avoid such temperature increment, maintenance procedures are needed dealing with manufacturer specifications.

In Table 2.1, composition and voltage of most usual accumulators is shown. This information is extracted from [18]:

Type	Accumulator	Positive Plate	Negative Plate	Electrolyte	Voltage (V)
Acid	Lead-Acid	Lead oxide	Lead	H_2SO_4	2
Alkaline	Ag-Zn	Silver oxide	Zinc	KOH	1.6
	Ni-Fe	Nickel peroxide	Iron	KOH	1.4
	Ni-Cd	Nickel hydroxide	Cadmium hydroxide	KOH	1.3

Table 2. 1 Composition and voltage of most common accumulators

Source: Sistemas eléctricos y electrónicos de las aeronaves. Jesús Martínez Rueda. Thomson Paraninfo. 2007. Pages 4-18

> **Cell replacement during battery life:**

It is normal for a number of cells to require replacement during the battery life. There is no significant effect on the life of a new cell from mixing it with older cells. Cell failure follows the usual "bathtub" curve. See Fig. 2.3: [19]
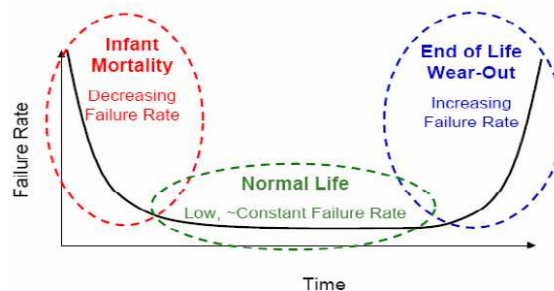
Fig. 2. 3 Bathtub curve

Source: SAFT batteries technical notes. TN6 Rev0 – March 2008. Page 1

[15] Summing up, the most commonly used battery is the Ni-Cd type, which depends upon the reaction between nickel oxides for the anode, cadmium for the cathode and operates in a potassium hydroxide electrolyte.

2.3.2   Flywheels

[20] Flywheels, also known as mechanical batteries, consist of a mass which is rotating around an axis. Kinetic energy is stored mechanically into a flywheel. See Fig. 2.4 for a graphic scheme. The energy is supplied to the flywheel by an

electric engine coupled to the axis, which raises its velocity to its nominal value. If the electric machine is used as a generator, the flywheel reduces its velocity to a minimum design value and causes an energy return.

Flywheels are one of the most promising technologies in order to substitute conventional batteries as energy storage systems. Recently there has been a step forward in this field, by evolving mechanical composites characteristics.
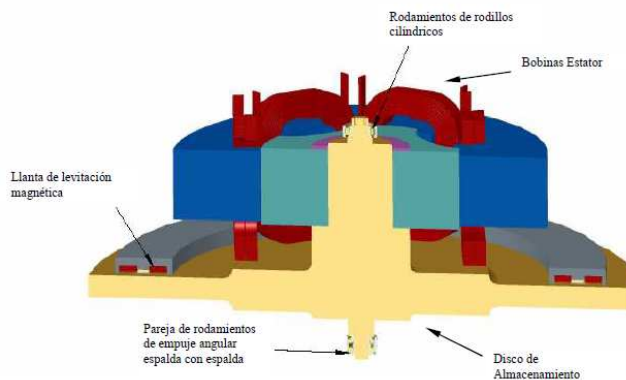
Fig. 2. 4 Flywheel scheme

Source: Desarrollo de un almacenador cinético de energía. David Ugena González. September 2008

FES also offers many important advantages over other energy storage methods. Power is only limited by the electric engine coupled at the flywheel, and so it is possible to exchange great quantities of energy in a shorter period of time than traditional chemical batteries. It is also possible to charge mechanical batteries faster than chemical ones.

2.3.3   Hydrogen batteries

[21] Nickel-hydrogen is a newer cell technology than nickel-cadmium. A nickel-hydrogen cell is characterized by a solid nickel electrode, similar to the one used in nickel-cadmium cells, and a negative platinum gas electrode containing catalysed sites. Since the negative active material is hydrogen gas, the entire cell is contained in a pressure vessel forming the cell case.

Nickel-hydrogen cells come in a large number of possible combinations of internal components as well as a variety of internal configurations. The most important consideration for a cell design is that it has to be tolerant to the expected changes that may take place during its storage in its intended application.

[22] The nickel-cadmium cell, which also uses the nickel electrode, suffers from the relatively poor lifetime and reliability of the cadmium electrode. The nickel-hydrogen cell concept combined the highly reliable nickel electrode with the advanced hydrogen electrode concepts that came from fuel cell development programs. Both nickel and hydrogen electrodes were seen as very robust, for that reason early nickel-hydrogen cell development effort identified few failure modes that were expected to limit the life of these battery cells.

CHAPTER 3. OPTIMAL LOCATION SELECTION

Criterion for the optimal selection of the location has been defined in this chapter, plus a final argument where the feasibility of the location where RAT is going to be positioned is evaluated.

3.1   Optimal location selection criteria

3.1.1   Non-Turbulent air in RAT inlet

First of all, we might define turbulence using the following Corrsin's suggestion (1961) as follows:

Incompressible and hydrodynamic turbulence is a spatially complex distribution of vorticity which advects itself in a chaotic manner. The vorticity field is random in both space and time, and exhibits a wide and continuous distribution of length and time scales [23]*.*

In fluid dynamics, a turbulent flow is a regime characterized by chaotic and stochastic property changes. While there is no theorem relating the non-dimensional Reynolds Number (Re) to turbulence, flows at Re larger than $1 \cdot 10^5$ are typically turbulent, while those at low Re usually remain laminar. Moreover, the turbulence [24] is generally interspersed with laminar flow until a larger Re of about 3,000.

Turbulent air flow at the inlet of our RAT will reduce its performances. Our main objective is to minimize the turbulences effect on our RAT and so it is interesting for us to choose a location where the air that comes into contact with our RATs inlet was as clean as possible. When we are introducing air fluxes and turbulences facts and performances, the meaning of the word "clean" refers to an air flow without turbulence.

3.1.2   Some operational limitations

3.1.2.1   Vibrations

The RAT [25] is a back-up device which means that it is rarely used. Although being mostly unused, an efficient and proper operation it is important when deployed.

Although RATs are used as back-up devices, our idea is just the opposite of its normal use. We are studying the possibility of using it during normal operations of the aircraft, not only for emergency situations.

Conventional RATs can encounter self-induced vibrations caused by turbine imbalance [25]. The turbine imbalance is primarily caused by motion of the governor components and governor springs. Self-induced vibrations increase when a structural resonance within the operating speed range of the turbine appears.

3.1.2.2 Effect of temperature and altitude

One of the most important parameters on the RAT performance is the density of the air that hits the RAT blades (ρ), which changes slightly with air temperature and elevation. Using ratings for wind turbines based on standard conditions at 59° F (15° C) at sea level, a density correction sh ould be made for higher elevations, as shown in Fig. 3.1 [26]. A temperature correction it is typically not needed for predicting long-term wind turbine performances on the ground.
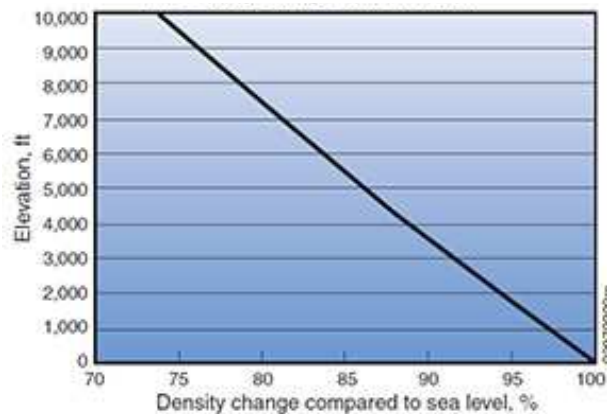
Fig. 3. 1 Air density change with elevation

Source: http://winds-energy.blogspot.com.es/

3.1.2.3 Structural limitations

Some RAT specifications [27] shall be listed in order to keep in mind the some nominal values.

- Speed and direction of rotation
  - ➢ Direction of rotation .... Clockwise
  - ➢ Minimum airspeed at the turbine for rated output .... 135.5 KEAS
- Environmental conditions
  - ➢ Maximum operational altitude .... 12.5 km
  - ➢ Ambient temperatures range .... -65ºC to 90ºC
- Weight and overall dimensions
  - ➢ Weight .... 81.65 kg
  - ➢ Height .... 1.220 m
  - ➢ Length .... 0.660 m
  - ➢ Width .... 0.178 m
  - ➢ Turbine Diameter .... 0.7493 m

KEAS value must be emphasized due to the main limitation that will cause when deploying the RAT. Using equation 3.1 we can make sure that the TAS value is correct at 7,000 ft since at this altitude the aircraft will start a normal approach procedure.

$$EAS = TAS \cdot \sqrt{\frac{\rho_{7000ft}}{\rho_0}} \rightarrow TAS = \frac{EAS}{\sqrt{\frac{\rho_{7000ft}}{\rho_0}}} = \frac{135.5}{\sqrt{\frac{0.59}{1.225}}} = 195.24 \; kt$$

(3.1)

We are now sure that deploying the RAT at 7,000 ft it is possible, since a normal approach TAS is around 200 kt.

Due to its weight, the location where it is installed will vary the aircraft mass centre. Also its size will dismiss some possible locations. For example, if we focus on the landing procedure, we have to take into account the following geometry of the A320 so as to avoid the tail strike:

Tail strike pitch attitude	
Landing gear compressed	Landing gear extended
11.7^0	13.5^0

Table 3. 1 Tail strike pitch attitude

Source: Airbus A318/A319/A320/A321 Flight Crew Training Manual

Main factors that could cause a tail strike in an A320 are the early rotation, the rotation technique, the configuration, the landing trim setting, crosswind landing and oleo inflation.

3.1.2.4 *Maximum air velocity at the inlet*

Following the Airworthiness Directive (AD) number 2006-0135, issued in 22 May 2006, during a flight test performed by Airbus with an A320 aircraft, high vibration and noise were reported two minutes after RAT deployment. Investigations revealed that the counterweights material of the RAT governing system was not in compliance with specifications. These counterweights fractured leading to a severe imbalance and an over speed of the RAT. In an aircraft high speed configuration this situation could lead to the rupture of the RAT blades.

Therefore, the AD 2006-0135 renders mandatory a speed limitation [28] only during flight tests with the RAT deployed, by limiting the speed to 250 knots IAS from RAT deployment to landing.

Other speed limitations [29] will be bounded by the various stages of the flight. This is due to the fact that the RAT has to ensure its full availability during the entire route.

a) Climb speed
    a. Managed: is computed by the FMGS and provides the most economical climb profile as it takes into account weight, actual and predicted winds, ISA deviation and Cost Index (CI).

    Example: 250 kts up to 10,000 ft.

     b. Selected: if necessary, the climb speed can be either pre-selected on ground or selected on the FCU once airborne.

b) Cruise speed

     a. Managed: the optimum cruise Mach number is automatically targeted. Its value depends on CI, cruise flight level, temperature deviation, weight and headwind component.

     Example: It will increase with an increasing wind. +50 kt headwind equates to +0.01 Mach.

     b. Selected: should ATC require a specific cruise speed or turbulence penetration is required.

c) Descent speed

If selected speed is used, the descent profile remains unchanged. As the selected speed may differ from the speed taken into account for pre-computed descent profile and speed deviation range does not apply, the aircraft may deviate from the descent profile.

Example: If the pilot selects 275 kts with a pre-computed descent profile assuming managed speed equal to 300 kts vertical deviation will increase.

d) Approach speed

[29] The approach speed (V_{app}) is defined by the crew to perform the safest approach. It is function of gross weight, configuration, headwind, A/THR ON/OFF, icing and downburst as it is shown in Fig. 3.2.
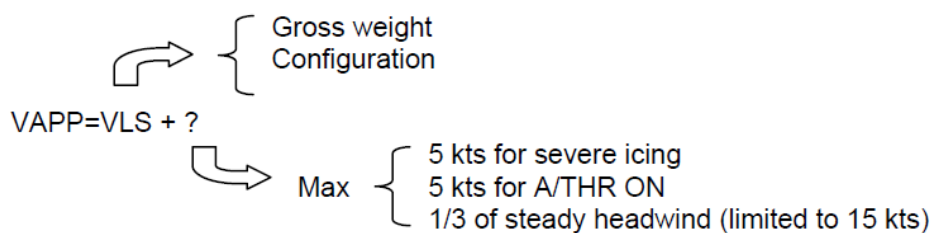
Fig. 3. 2 Approach speed dependences

Source: Airbus A318/A319/A320/A321 Flight Crew Training Manual.

3.1.3 Symmetry

We will have to study if the energy obtained with one RAT is enough to achieve our objective, which is using this energy for taxi procedures. If it is not, we will have to consider the possibility of installing more than one single RAT.

Our main thought about symmetry when installing more than one RAT device is motivated basically in the modification of the mass centre position. If we add

more weight into the aircraft it is obvious that it has to be well distributed since modifications added into the aircraft must vary its performance and actuation as less as possible.

3.1.4   Non-turbulent RAT air trail

As it was introduced in 3.1.3, our principal aim is not to alter the aircraft flight and performance in normal conditions by installing one or more RATs into it. Hence, another aspect to take into account is the RAT trail and its effect on actuators, control surfaces and the part of the aircraft which is located behind of it. Using the information from the study of *wind turbine wake aerodynamics* by L.J. Vermeer, J.N. Sørensen and A. Crespo [30], we can divide the case of study in two great parts:

   a) Near wake computations

Near wake computations can be carried out with various numerical techniques, ranging from inviscid lifting line/surface methods to viscous Navier–Stokes based methodologies. Each method has its own advantages and limitations. While e.g. prescribed vortex wake methods [30] are fast to run on a computer but leave much of the physics to a priori given assumptions, Navier–Stokes based methods offer very detailed insight in the flow behaviour but are very computing costly.

In Fig. 3.3 a) and b) it is possible to visualize the flow and its tip vortices during flow visualization experiments at **TUDelft**. http://home.tudelft.nl/
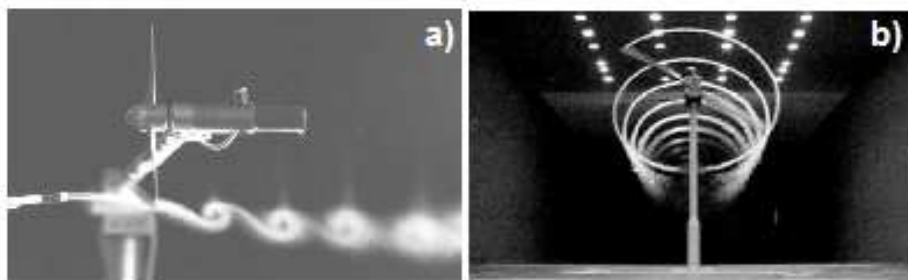
Fig. 3. 3 a) Flow visualization experiment at TUDelft, showing two revolutions of tip vortices for a two-bladed rotor. **b)** Flow visualisation with smoke grenade in tip, revealing smoke trails for the NREL turbine in the NASA-Ames wind tunnel

Source: Study of wind turbine wake aerodynamics. L.J. Vermeer, J.N. Sørensen and A. Crespo. Pergamon. 2003

   a) Far wake computations

Some aspects of individual wake modelling, such as near wake representation, influence of atmospheric stability, appropriate turbulence modelling, or convergence problems, are still issues of active research. Some of these aspects are more relevant to the offshore wind farms, which are not our case of study.

Models which depend on the least simplifying assumptions [30] are better suited in dealing with different configurations and in reproducing wake development in more detail. Therefore, far wake computations are not such decisive as near wave computations.

3.1.5 Retractable or fixed

There are two well deferred options regarding to RAT installation into the aircraft. RAT can be fixed or retractable, and this condition will be set by studying it further in this paper. As we cannot assure which *status quo* will be used in our implementation in advance, we have to heed in mind both possibilities.

Both alternatives will require a delimited area into the aircraft structure so as to store RAT system devices, wires and mechanisms. Even so, the most delicate case is the retractable RAT, since not only will need an unpressurized well delimited area to store its system elements, but it will have to store the blades, rotor and the hydraulic arm that extends and retracts the RAT.

3.1.6 Pressurized and unpressurized areas

As it is shown in Fig. 3.4, unpressurized areas are located on the nose, landing gear delimited area, belly-fairing and tail.
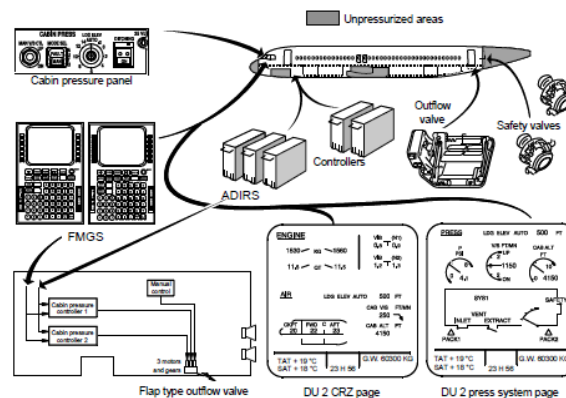
Fig. 3. 4 A319/320/321 ECS. Cabin pressure control

Source: Airbus A319/A320/A321 Flight deck and systems briefing for pilots

In order to install a retractable RAT and not varying the A320 structure, we shall place the RAT into one of these four locations. It is clear that a fixed RAT has many more possible locations than the retractable RAT, because it does not require an unpressurized area so as to install the RAT system.

Some important facts about pressurization [31] in the A320 series are added below:

- The pressurization control system operates fully automatically without any crew action.

- Dual system with automatic switchover after failure.
- In normal operation, cabin altitude and rate of change are automatically controlled from FMGC flight plan data.
- In case of dual FMGC failure, the cabin altitude varies according to a pre-programmed law.
- In case of failure of both pressurization system auto controllers, the manual back-up mode is provided through the third outflow valve motor.

3.1.7   Easy implementation

Our main purpose on this paper is to study one modification on the Airbus A320 with enough consistency in order to achieve its implementation in future Airbus A320 series.

This purpose requires an easy implementation so as to minimize fabrication costs, certification costs, and others due to the fulfilment of a really incident modification into the aircraft dynamics. Despite this great quantity of alterations that should be carried out, if our system is reliable, easy to set up and safe, it can bring considerable benefits for the airlines.

We recall that the objective of adding one or more RATs into the Airbus A320, is to store enough energy for the taxiing procedures, using electrical energy and consequently save vast quantities of fuel which is translated to saving costs as well as being environmentally friendly.

3.1.8   Cleared placement area

As we can see in the *Airbus A319/A320/A321 Ground Operations Manual* [32], we have to consider the physically interference with other systems. On section 3.1.11 we will see that there must be some safety analysis to ensure these criteria, but in this point, we are going to use the Airbus A320 manual to determine which sockets, grounds, intakes, etc. exist along the aircraft fuselage. All these inputs/outputs will restrict the range of possibilities of RAT locations, since we try to interfere as less as possible in the already existing systems.

The Fig. 3.5 [32] shows the service points in the A320/A321:
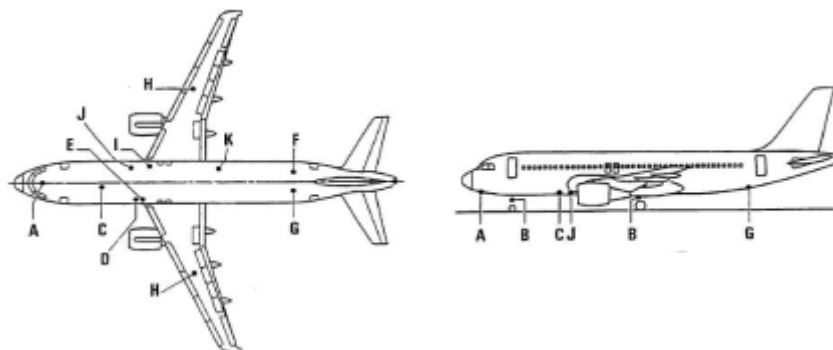
Fig. 3. 5 Service points in A320/A321

Source: Airbus A319/A320/A321 Ground operations manual. 2002

A – Electrical power receptacle
B – Aircraft grounding
C – Potable water drain panel (forward)
D – Conditioned air connector.
E – Air starter connector
F – Toilet servicing panel

G – Potable water fill and drain panel
H – Fuelling connector.
I – Fuelling panel
J – Potable water drain/overflow panel (centre)
K – Yellow ground service panel

3.1.9   Positioning depending on centre of gravity

When establishing a possible location for RAT, special attention will have to be paid on the gravity centre since its variation affects the aircraft pitch momentum. In order to keep momentum low the system will be installed as close as possible to the aircraft centre of gravity.
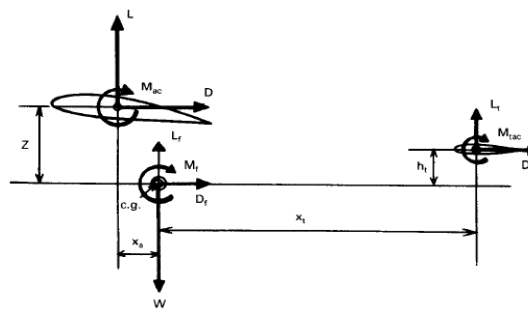
Fig. 3. 6 Centre of gravity and momentums

Above all, an important point would be the calculus of the main surfaces momentums, see Fig. 3.6. Once main surfaces are analysed, RAT will be our study target.

Obviously, the desired value for the sum of momentums must be equal to zero in order to affect the less possible the aircraft attitude. During position testing forwardly, our main interest will be to compensate the momentum due to the weight and the momentum due to the drag.

Even so, not every place for RAT positioning in relation with our momentum calculus will be practical or reasonable for final location or studying because other restrictions may be our priority.

3.1.10   Easy access to the system

RAT positioning must allow an easy access for maintenance and checking. Therefore, some good positioning proposals may be extracted:

1. The location should be close enough to touch by an operator in order to check the system status.
2. Possibility to reach all parts of the system in order to last less time during rotation.
3. Operator access. Two modes of opening recommended: One done by the pilot from the cabin and the other one done by the operator from the

platform in the same way that operator can open the electric supply once the aircraft is landed.

3.1.11   Safety considerations

3.1.11.1 General safety considerations

First of all we shall describe what a failure is according to CS 25 1309 [33]:

A failure condition is defined at each system level by its effects on the functioning of the system. It is characterized by its effects on the other systems and on the aircraft. All single failures or combination of failures including failures of other systems that have the same effect on the considered system are grouped together in the same Failure Condition.

When analysing safety on board we should consider all general requirements related to devices implemented in an aircraft. In order to do so, the Safety Assessment Process Model; see Fig. 3.7, it is used. With this model, the critical level of each system failure is quantified so as to establish the failure probability of each element.

A top-down analysis called System Safety Analysis shall be done in order to consider possible failures and the value of probability that we can afford them to occur. Once the entire structure is defined the final step will be a bottom-up analysis to verify if the structure designed fulfils the probability we established at the beginning for the device (in our case in RAT).
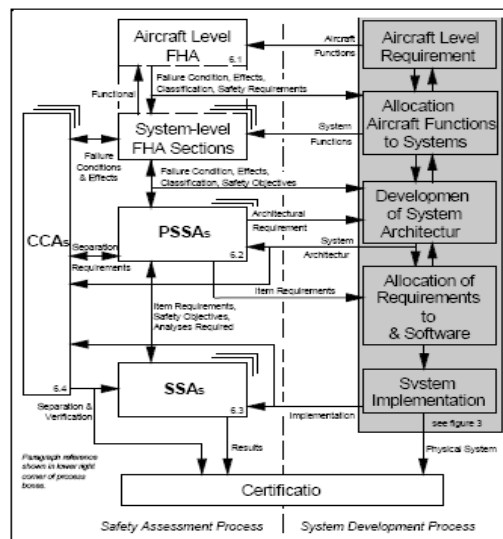
Fig. 3. 7 Safety Assessment Process Model

Source: Industrial Considerations. Avionics class notes. EETAC. 2012

3.1.11.2 Interference with other systems

Another process is going to be needed in order to verify the independence between other systems on board. This process is called Common Cause Analysis and it is fundamental in order to keep systems independent one from

the other. If it does not happen, a non-important failure can lead to a catastrophic event.

Many different analyses can be distinguished:

> ➤ Common Mode Analysis
> ➤ Human Hazard Analysis
> ➤ Particular Risk Analysis
> ➤ Zonally Safety Analysis

3.1.11.3 Interference with other systems

We have to assure that no problems are going to be found during an emergency operation. The following list checks all we will have to verify during the design:

- Landing on the sea

After an emergency sea landing, what we will take in account while designing, is not to make sinking faster, so the zone in which we will work must be sealed to guarantee an established floating time enough for the passengers to evacuate.

- Clearance with doors and evacuation slides

During evacuation process, unfolded RAT must not interfere in the way out of slides, see Fig. 3.8 [34], so when designing the positioning will depend on the number of exits, the size of the slides, and the movement they could have during its way out, passengers jumping on them or if there are wheels out or the plane is in the sea.

Fig. 3. 8 Evacuation slide

Source: http://www.airspacemag.com/flight-today/HTW-evacuation.html#

- Braking system

If a malfunction is found during RAT operation, a system is going to be needed

in order to stop RAT and not damaging other possible devices or parts of the aircraft as wings or landing gear.

3.2   Location selection

The following selection of location is based mainly on the optimal position criteria exposed on section 3.1.

3.2.1   Tail

The first location selection is the tail. If we consider the air flow that strikes this area, the wake turbulence that is caused because of this hit is limited. Also, the air flow turbulence generated by the engines is not fully decisive, in view of the fact that the outflow of the engines does not have a great effect on the performance of the horizontal and vertical stabilizers of the aircraft, given that the air follows its body.

When characterising the RAT our goal is reducing the operational restrictions that it would cause. For example, possible tail strikes must be avoided during landing procedures. We are going to elude those collisions by calculating its optimal location on the tail area. The RAT weight it is noticeable but not confining, given that by redistributing the entire weight configuration (baggage, fuel…) the mass centre deviation caused by the RAT shall be corrected.

The air speed at the intake of the RAT should not be emphasized during approach and landing procedures, since it is not too high. Also, the air flow loses part of its velocity on the impact against the aircraft, as well as during its displacement to the end of the aircraft.

The outflow of the RAT has to be as less agitated as possible in order to reduce its effect on subsequent control surfaces. Anyhow, in chapter 4 a deeper analysis will be realized.

As mentioned in the optimal location selection criteria outlined above, we have to ensure that if we set the RAT on the tail area, during limit procedures we will guarantee that emergency exits will not be obstructed and the speed of collapse will not be increased in case of sea accident due to poor sealing, among others.

Another important fact is realizing that, if we take a look onto the Fig. 3.9, we can clearly see that, in G location, we have a potable water fill and drain panel, which demands that the RAT has to be installed between B and G locations, or in a location upper than G, considering that there is an emergency door.
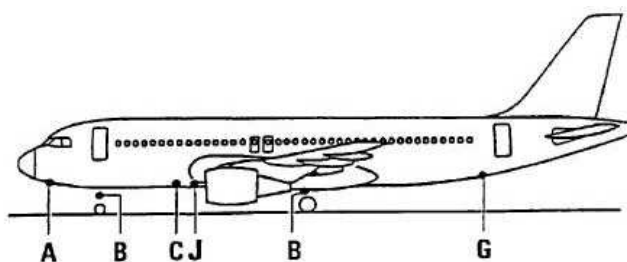
Fig. 3. 9 Airbus A320 service points

Source: Airbus A319/A320/A321 Ground operations manual. 2002

At last, we can specify that locating the RAT on the tail it is a logical decision, for the reason that the area above G location is non-pressurized, which permits a study of a retractable RAT if needed.

By extending flaps and slats we cannot allow that the air variation affects the operation of RAT due to a change in the wing chord. We are going to consider the worst case when simulating and assure that the RAT is not extremely affected.

3.2.2   Nose

By placing the RAT in the nose area we can guarantee that the airflow which is going to impact into it, will have better laminar properties than in any other location along the rear part of the aircraft.

As we have mentioned, in an ideal case, the air flow will reach the RAT in laminar conditions, but the maximum speed at which RAT could operate remains constant. This is not a decisive factor, since varies slightly from one end to the other of the aircraft, regardless of the air expelled by the engine behind the RAT.

In order to check whether there may be symmetry or not, a deeper study should be done, as in this zone there is located the landing gear, which will limit the space where the RAT could be set. Furthermore, we will have to analyse whether the turbulence created by the RAT is important or not, because by installing it into the nose, all air flow variations will have some role in the performance of control surfaces located behind of it.

As previously specified, in front of the aircraft there are two non-pressurized areas, so that the placement of one or more RATs in that space can be investigated in order to avoid possible interferences with existing systems.

Another important fact is realizing that, if we take a look onto Fig. 3.9, we can clearly see that, in the A location we have an electrical power receptacle, which demands that the RAT has to be installed in a location between A and B, where B is the aircraft grounding. We do not discard positioning the RAT in front of the A location, but it should be analysed in detail.

In the end, we have to probe the momentum created by locating the RAT in the nose area, as we shall have done with the tail case, because it will be essential to know how much extra engine power will be required so as to compensate the additional weight, especially in the pursuit of pitch and other aircraft movements during approach and landing.

3.2.3   Belly-fairing

First, we can determine that the air flow reaching the belly-fairing and in consequence the RAT, does not have a striking component of turbulence, as it has not trespassed the imaginary line that engines delimit yet. From this imaginary line, some turbulence may appear in the air flow. If we focus in the belly-fairing we can notice that the air flow at the RAT intake will be almost laminar, led by the aircraft fuselage to the location of the RAT.

As it happens in the tail and nose cases, vibrations are remarkable only during landing procedures. That is why vibrations are not considered as critical. Temperature and weather variations are not an aspect to be considered in order to dismiss this option.

Some possible locations of the RAT would be suited by main structural constraints for placing it, as the belly-fairing is really wide, so that gives the symmetry option by using two RATs. Although the belly-fairing is not a primary structure, it is subject to aerodynamic loads which the panels transmit to the supporting structure, and so it is important to maintain safety. It is noteworthy that the RAT does not cause major turbulence in the airflow at its outlet, as in the nose case, rear control surfaces may suffer lift reduction or dynamics variation due to this non-laminar flow condition.

It should be emphasized that the area of the belly-fairing is non-pressurized, so in this case there is a possibility the RAT was a retractable device. The belly-fairing compartment could be modified in order to include a sealed space to allow the deployment of the RAT. Also, it is known that the actual emergency RAT is installed in the belly-fairing of the A320 aircraft.

Another important fact is realizing that, if we take a look onto Fig. 3.9, in the B location, we have an aircraft grounding, which demands that the RAT has to be installed in a point between J and B locations, where J is a potable water drain/overflow panel (centre), or between B and G locations.

As mentioned in the optimal location selection criteria outlined above, we have to ensure that if we set the RAT on the belly-fairing area, the speed of collapse in case of sea accident will not be increased due to poor sealing, among others. It is very important especially in the belly-fairing location, since in case of emergency landing on water its main function is to slow down gradually the aircraft, and so it reduces the impact considerably.

3.2.4   Winglet

When analysing the winglet location we must keep in mind that we are not designing a specific small turbine. For this reason placing our RAT in this part of the aircraft is a non-viable option for many different reasons.

First of all, there is not enough space to place the whole system into the wing. Another important issue is that we will need to make our system retractile and as we said there is no space for this procedure. Furthermore, an extra weight in this location may lead to structural inconvenient due to the momentum produced by its separation from the main body of the plane that we cannot allow.

If a system was developed here, we have to assure that when splashing down during emergency, the wings (place that mostly contributes to make plane float due to its surface) do not sink faster due a variation of it. As it has been mentioned, this location has a lot of disadvantages so is going to be probably refused as a candidate to the positioning for the RAT.

3.2.5   Symmetry

When designing RAT, one of the most interesting points about positioning is the fact of symmetrizing its position on the plane. Some issues have to be considered when adding more than one RAT. Weight is a very important fact to be considered when adding an extra RAT in our design because we will have to analyse if it is better adding the symmetric system rather than taking a passenger out or limiting our fuel quantity. As mentioned on the previous section the momentum produced by a variation of centre of gravity has a very important effect, so adding two RATs for symmetrizing has a very important impact that has to be taken into account.

The energy produced is fact of interest as well. In chapter 5 the energy needed for a typical taxi procedure will be computed and then the need of symmetry may or may not appear. When symmetrizing RATs, some points have to be avoided in order to not interfere with electrical power receptacles, sinks and other locations specified in Fig. 3.10.
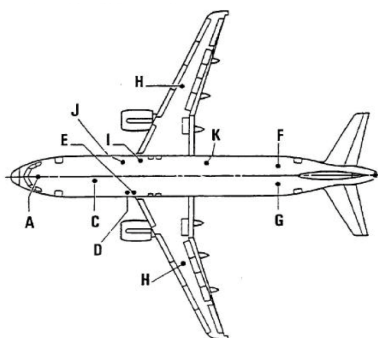
Fig. 3. 10 Airbus A320 service points

Source: Airbus A319/A320/A321 Ground operations manual. 2002

3.3 Options summary

This options summary reorganizes the ideas that have been developed in this chapter, so as to give a clear vision of the available options and indicate the most important points in each possible RAT position. Also, this summary pretends to obtain a graphic illustration of the importance of each selection criteria.

	Tail	Nose	Belly-fairing	Winglet
3.1.1 Non-turbulent air in RAT inlet	Medium	Low	Low	Medium
3.1.2.1 Vibrations	Medium	Medium	Medium	Medium
3.1.2.2 Effect of temperature and altitude	Low	Low	Low	Low
3.1.2.3 Structural limitations	Medium	Very	Medium	Very
3.1.2.4 Maximum air velocity at the inlet	Low	Low	Low	Low
3.1.3 Symmetry	Low	Medium	Low	Low
3.1.4 Non-turbulent RAT air trail	Low	Medium	Medium	Low
3.1.5 Retractable or fixed	Medium	Low	Low	Very
3.1.6 Pressurized and unpressurized areas	Medium	Low	Low	Very
3.1.7 Easy implementation	Medium	Medium	Low	Very
3.1.8 Cleared placement area	Low	Medium	Low	Medium
3.1.9 Positioning depending on centre of gravity	Very	Very	Low	Low
3.1.10 Easy access for maintenance procedures	Low	Low	Low	Medium
3.1.11 Parasite drag produced	Low	Medium	Medium	Medium
3.1.12.1 General safety considerations	Very	Very	Very	Very
3.1.12.2 Interference with other systems	Very	Very	Very	Very
3.1.12.3 Positioning caring emergency and limit procedures	Very	Very	Very	Very

Table 3. 2 Options summary

Colour code:

Low restrictive consideration	Medium restrictive consideration	Very restrictive consideration

CHAPTER 4. OPERATIONAL RESTRICTIONS DUE TO RAT EFFECTS

In this chapter an accurate analysis related with the effects in the aircraft dynamics will be done, such as momentums and drag. Furthermore, simulations using SolidWorks Flow Simulation 2010 will be used in order to support mathematical calculus commented previously.

4.1   Centre of Gravity Calculation

In order to calculate the centre of gravity of the A320 we are going to use the equation 4.1 [35]:

$$CG = \%MAC \cdot MAC + c \qquad \text{(4.1)}$$

If we take a look into the Fig. 4.1, we are able to notice which parameters are necessary to calculate the CG position:
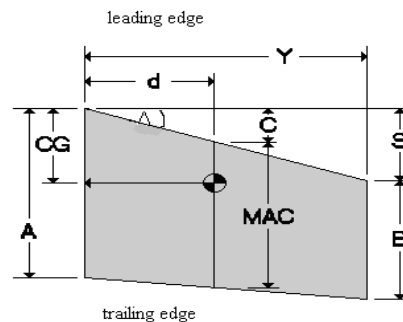
Fig. 4. 1 Most important parameters when calculating CG

Source: http://www.nasascale.org/howtos/mac-calculator.htm

First of all, we need to calculate the MAC and c values; therefore we are going to use equations 4.2 and 4.3

$$MAC = A - \frac{2 \cdot (A - B) \cdot (0.5 \cdot A + B)}{3 \cdot (A + B)} \qquad ; \qquad c = \frac{S \cdot (A + 2 \cdot B)}{3 \cdot (A + B)} \qquad \text{(4.2);(4.3)}$$

Using the table 4.1 we are going to calculate the CG in three different configurations, in order to see if its variation is noticeable or not. Also, we are going to use the CG position of one of those three configurations in the following sections in order to calculate the momentum generated by the RAT.

Configuration	Weight (Kg)	CG (%)	Other Parameters
Dry Op. Weight	42,500	27	S = 0.416 m, A = 10.5 m,
Zero Fuel Weight	60,280	32.7	B = 2.5 m, Y = 14 m
Take Off Weight	73,280	30.5	

Table 4. 1 A320 Configurations

Source: Airbus A320 Landing Gear. Project Report from Hogeschool van Amsterdam, AIT. 2007/2008

$$MAC = 10.5 - \frac{2 \cdot (10.5 - 2.5) \cdot (0.5 \cdot 10.5 + 2.5)}{3 \cdot (10.5 + 2.5)} = 7.32 \; m \qquad c = \frac{0.416 \cdot (10.5 + 2 \cdot 2.5)}{3 \cdot (10.5 + 2.5)} = 0.165 \; m$$

Now we can calculate the centre of gravity for those configurations:

$$CG_1 = \frac{27}{100} \cdot 7.32 + 0.165 = 2.1414 \; m \qquad CG_2 = \frac{32.7}{100} \cdot 7.32 + 0.165 = 2.5586 \; m$$

$$CG_3 = \frac{30.5}{100} \cdot 7.32 + 0.165 = 2.3976 \; m$$

Distances of centre of gravity from nose:

$$d_{CG_1} = 13.073 + 2.1414 = 15.214 \; m \qquad d_{CG_2} = 13.073 + 2.5586 = 15.632 \; m$$

$$d_{CG_3} = 13.073 + 2.3976 = 15.470 \; m$$

4.2   Momentum Analysis

In the following section we are going to set the equations used in order to obtain momentum generated by the wing and tail, see Fig. 4.2. Two different situations will be considered, flying at 7,000 ft during the approach procedure, and flying at sea level during the landing procedure.
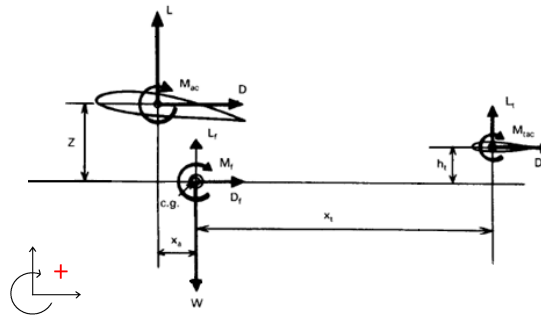
Fig. 4. 2 Momentums analysis scheme

Source: A. I. Carmona, "Estabilidad Longitudinal", Chap. 13 in *Aerodinámica y actuacions del avión*, 11th Ed., Thomson Paraninfo, pp.415, Madrid (2002)

Most important values:

Concept	7,000 ft	Sea Level
Density (Kg/m³)	0.59	1.225
Temperature (K)	242.55	293
Max. velocity (m/s)	100.35	75.56/57.57
Air dynamic viscosity (Kg/m s)	$1.488 \cdot 10^{-5}$	$1.983 \cdot 10^{-5}$

Table 4. 2 Important values flying at 7,000 ft and SL

Essential equations:

$$\Sigma F_x = 0 \quad \rightarrow \quad \Sigma F_x = T - D - D_f - D_t = 0 \tag{4.4}$$

$$\Sigma F_y = 0 \quad \rightarrow \quad \Sigma F_y = L - W + L_f + L_t = 0 \tag{4.5}$$

$$M_{CG} = 0 \quad \rightarrow \quad M_{wing} + M_f + M_{tail} = 0 \tag{4.6}$$

4.2.1   Wing momentum analysis

Momentum produced by the wing:

$$M_{wing} = \left(L_{wing} \cdot x_a\right) - \left(D_{wing} \cdot z\right) \tag{4.7}$$

It has to be remarked that the momentum component generated by the lift force is positive because the wing is below the centre of gravity, which is not exactly what is represented in Fig. 4.2, because that is a general case.

4.2.1.1   Wing momentum analysis at 7,000 ft

Lift and drag calculus:

$$L_{wing} = \frac{1}{2} \cdot \rho \cdot S \cdot c_l \cdot v^2 \qquad ; \qquad D_{wing} = \frac{1}{2} \cdot \rho \cdot S \cdot c_d \cdot v^2 \tag{4.8 ; 4.9}$$

There are some values that must be found:

- Surface (S) [36]

$$S = 122.6 \ m^2$$

- Lift coefficient (c_l)

We are going to consider that the A320 wing air foil follows the NACA 4412 [37, 38] in order to obtain the lift coefficient. Also, analysing the approach procedure, we will consider an angle of attack equal to 3⁰ since it is a commonly used value in this situations.

In order to use the graphic shown in Fig. B.1 from Annex B, we must calculate the Reynolds number in our situation:

$$Re = \frac{\rho v c}{\mu} = \frac{0.59 \cdot 100.35 \cdot 3.5953}{1.488 \cdot 10^{-5}} = 14 \cdot 10^{-6} \tag{4.10}$$

Where: ρ is density, v is velocity, c is the root chord of the wing and μ is the dynamic viscosity of the air.

- Drag coefficient (c_d)

In order to obtain the drag coefficient we are going to consider the same as the lift coefficient by using the NACA 4412 [37, 38]. Using the graphic that relates the lift and drag coefficients shown in the Fig. B.1 in the Annex B, the last one will be obtained.

$$D_{wing} = \frac{1}{2} \cdot \rho \cdot S \cdot c_d \cdot v^2 = 0.5 \cdot 0.59 \cdot 122.6 \cdot 0.00625 \cdot 100.35^2 = 2.276 \ kN$$

$$L_{wing} = \frac{1}{2} \cdot \rho \cdot S \cdot c_l \cdot v^2 = 0.5 \cdot 0.59 \cdot 122.6 \cdot 0.725 \cdot 100.35^2 = 264.049 \ kN$$

In pursuance of finding the vertical and horizontal distances from the wing to the CG, we are going to use the distances in Fig. 4.3, previously used.
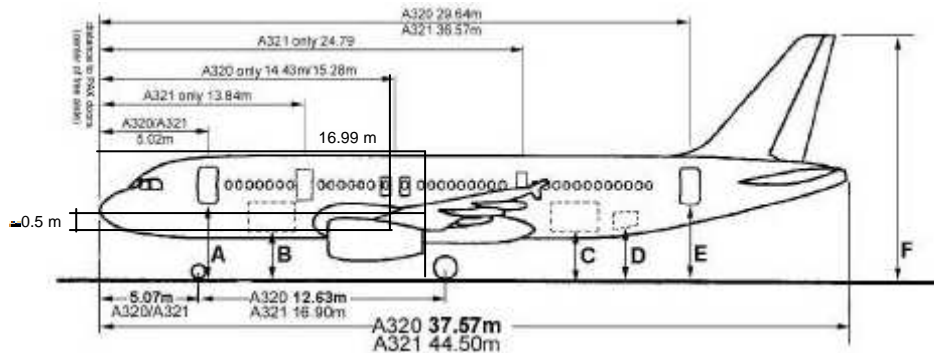
Fig. 4. 3 Aircraft CG distances

$$
\begin{aligned}
M_{wing_{T,000ft}} &= \left(L_{wing} \cdot x_a \right) - \left(D_{wing} \cdot z \right) \\
&= \left(264.049 \cdot 10^3 \cdot (16.99 - 15.28) \right) - \left(2.276 \cdot 10^3 \cdot 0.5 \right) \\
&= \boxed{450.386 \ kN \cdot m}
\end{aligned}
$$

4.2.1.2 Wing momentum analysis at sea level

Lift and drag calculus:

$$L_{wing} = \frac{1}{2} \cdot \rho \cdot S \cdot c_l \cdot v^2 \qquad ; \qquad D_{wing} = \frac{1}{2} \cdot \rho \cdot S \cdot c_d \cdot v^2 \qquad \textbf{(4.8) ; (4.9)}$$

There are some values that do not need to be calculated again, such as the surface, but the lift and drag coefficients must be found again at sea level.

- Lift coefficient (c_l)

We are going to use the NACA 4412 [37, 38] and consider an angle of attack equal to 10⁰, which is lower than the geometry limit at 13.5⁰ [39].

Aircraft	Geometry limit at touchdown	Pitch attitude at touchdown (Vapp - 8) *	Clearance
A319	15.5°	7.7°	7.8°
A320	13.5°	7.6°	5.9°
A321	11.2°	6.6°	4.6°

Table 4. 3 Factors affecting the margin during landing

Source: http://www.smartcockpit.com/data/pdfs/flightops/flyingtechnique/Avoiding_Tailstrikes_by_Airbus.pdf

So as to use the graphic shown in Fig. B.2 in the Annex B, we must calculate the Reynolds number in our situation:

$$Re = \frac{\rho v c}{\mu} = \frac{1.225 \cdot 100.35 \cdot 3.5953}{1.983 \cdot 10^{-5}} = 22 \cdot 10^{6} \tag{4.11}$$

- Drag coefficient (c_d)

To obtain the drag coefficient we are going to consider the same as the lift coefficient by using the NACA 4412. [37, 38] Using the graphic shown in Fig. B.2 in the Annex B that relates the lift and drag coefficients, the last one will be obtained.

$$L_{wing_{MAX}} = \frac{1}{2} \cdot \rho \cdot S \cdot c_l \cdot v_{MAX}^{2} = 0.5 \cdot 1.225 \cdot 122.6 \cdot 1.675 \cdot 75.56^{2} = 718.117 \; kN$$

$$L_{wing_{min}} = \frac{1}{2} \cdot \rho \cdot S \cdot c_l \cdot v_{min}^{2} = 0.5 \cdot 1.225 \cdot 122.6 \cdot 1.675 \cdot 57.57^{2} = 416.873 \; kN$$

$$D_{wing_{MAX}} = \frac{1}{2} \cdot \rho \cdot S \cdot c_d \cdot v_{MAX}^{2} = 0.5 \cdot 1.225 \cdot 122.6 \cdot 0.0125 \cdot 75.56^{2} = 5.359 \; kN$$

$$D_{wing_{min}} = \frac{1}{2} \cdot \rho \cdot S \cdot c_d \cdot v_{min}^{2} = 0.5 \cdot 1.225 \cdot 122.6 \cdot 0.0125 \cdot 57.57^{2} = 3.110 \; kN$$

For the vertical and horizontal distances from the wing to the CG, we are going to use the values previously calculated.

$$
\begin{aligned}
M_{wing_{MAX}} &= \left(L_{wing_{MAX}} \cdot x_a\right) - \left(D_{wing_{MAX}} \cdot z\right) \\
&= \left(718.117 \cdot 10^{3} \cdot (16.99 - 15.28)\right) - (5.359 \cdot 10^{3} \cdot 0.5) \\
&= \boxed{1225.300 \; kN \cdot m}
\end{aligned}
$$

$$
\begin{aligned}
M_{wing_{min}} &= \left(L_{wing_{min}} \cdot x_a\right) - \left(D_{wing_{min}} \cdot z\right) \\
&= \left(416.873 \cdot 10^{3} \cdot (16.99 - 15.28)\right) - (3.110 \cdot 10^{3} \cdot 0.5) \\
&= \boxed{711.298 \; kN \cdot m}
\end{aligned}
$$

4.2.2   Tail momentum analysis

Momentum produced by the tail:

$$M_{tail} = -(L \cdot x) + (D_{tail} \cdot h_{tail}) \tag{4.12}$$

4.2.2.1   Tail momentum analysis at 7,000 ft

Lift and drag formulas:

$$L_{tail} = \frac{1}{2} \cdot \rho \cdot S \cdot c_l \cdot v^{2} \qquad ; \qquad D_{tail} = \frac{1}{2} \cdot \rho \cdot S \cdot c_d \cdot v^{2} \tag{4.8 ; 4.9}$$

In the same way that happens in wing, many parameters must be found:

- Surface (S) [36]

$$S = 31 \, m^2$$

- Lift coefficient (c_l)

With the aim of obtaing the lift coefficient we are going to consider that the A320 wing air foil follows the NACA 0009. [37, 38] Also, since we are analysing the approach procedure we will consider an angle of attack equal to 3^0 since it is a commonly used value in this situations.

In order to use the graphic shown in Fig. B.3 in the Annex B, we must calculate the Reynolds number in our situation:

$$Re = \frac{\rho v c}{\mu} = \frac{0.59 \cdot 100.35 \cdot 2.4899}{1.488 \cdot 10^{-5}} = 9.4 \cdot 10^6 \tag{4.13}$$

Where: ρ is density, v is velocity, c is the root chord of the wing and μ is the dynamic viscosity of the air.

- Drag coefficient (c_d)

To obtain the drag coefficient we are going to consider the same as the lift coefficient by using the NACA 0009. [37, 38] Using the graphic shown in Fig. B.3 in the Annex B that relates the lift and drag coefficients, the last one will be obtained.

$$L_{tail} = \frac{1}{2} \cdot \rho \cdot S \cdot c_l \cdot v^2 = 0.5 \cdot 0.59 \cdot 31 \cdot 0.3 \cdot 100.35^2 = 27.627 \, kN$$

$$D_{tail} = \frac{1}{2} \cdot \rho \cdot S \cdot c_d \cdot v^2 = 0.5 \cdot 0.59 \cdot 31 \cdot 0.006 \cdot 100.35^2 = 0.553 \, kN$$

For the vertical and horizontal distances from the wing to the CG, we are going to use the values previously calculated.

$$M_{tail_{ropoft}} = -(L \cdot x) + (D_{tail} \cdot h_{tail}) =$$
$$= (27.627 \cdot 10^3 \cdot (37.57 - 15.28 - 2.5)) + (0.553 \cdot 10^3 \cdot 1.5) = \boxed{-545.938 \, kN \cdot m}$$

4.2.2.2   Tail momentum analysis at sea level

Lift and drag calculus:

$$L_{tail} = \frac{1}{2} \cdot \rho \cdot S \cdot c_l \cdot v^2 \qquad ; \qquad D_{tail} = \frac{1}{2} \cdot \rho \cdot S \cdot c_d \cdot v^2 \tag{4.8 ; 4.9}$$

There are some values that do not need to be calculated again, such as the surface, but the lift and drag coefficients must be found.

- Lift coefficient (c_l)

As computed in the wing case, we are going to use the NACA 0009 [37, 38] and consider an angle of attack equal to 10^0, which is lower than the geometry limit

at 13.5⁰ as has been explained previously. The table where the angles are shown is the same as used in the wing.

We must calculate the Reynolds number in the tail to use the graphic shown in Fig. B.4 in the Annex B,; this one is different due to the change in the chord length:

$$Re = \frac{\rho v c}{\mu} = \frac{1.225 \cdot 100.35 \cdot 2{,}4899}{1.983 \cdot 10^{-5}} = 15{,}4 \cdot 10^{6}$$

(4.14)

- Drag coefficient (c_d)

In order to obtain the drag coefficient we are going to consider the same graphic as the lift coefficient by using the NACA 0009. [37, 38] Using the graphic shown in Fig. B.4 in the Annex B that relates the lift and drag coefficients, the last one will be obtained.

$$L_{tail_{MAX}} = \frac{1}{2} \cdot \rho \cdot S \cdot c_l \cdot v_{MAX}^2 = 0.5 \cdot 1.225 \cdot 31 \cdot 1.1 \cdot 75.56^2 = 119.246 \ kN$$

$$L_{tail_{min}} = \frac{1}{2} \cdot \rho \cdot S \cdot c_l \cdot v_{min}^2 = 0.5 \cdot 1.225 \cdot 31 \cdot 1.1 \cdot 57.57^2 = 69.223 \ kN$$

$$D_{tail_{MAX}} = \frac{1}{2} \cdot \rho \cdot S \cdot c_d \cdot v_{MAX}^2 = 0.5 \cdot 1.225 \cdot 31 \cdot 0.0128 \cdot 75.56^2 = 1.388 \ kN$$

$$D_{tail_{min}} = \frac{1}{2} \cdot \rho \cdot S \cdot c_d \cdot v_{min}^2 = 0.5 \cdot 1.225 \cdot 31 \cdot 0.0128 \cdot 57.57^2 = 0.806 \ kN$$

Using the distances from the Fig. 4.3, we compute momentums using the values obtained in the few above written lines.

$$M_{tail_{MAX}} = -\left(L_{tail_{MAX}} \cdot x\right) + \left(D_{tail\ MAX} \cdot h_{tail}\right)$$
$$= -\left(119.246 \cdot 10^3 \cdot (37.57 - 15.28 - 2.5)\right) + (1.388 \cdot 10^3 \cdot 1.5) =$$
$$= \boxed{-2\ 357.796 \ kN \cdot m}$$

$$M_{tail_{MIN}} = -\left(L_{tail_{MIN}} \cdot x\right) + \left(D_{tail\ MIN} \cdot h_{tail}\right) =$$
$$= -\left(69.223 \cdot 10^3 \cdot (37.57 - 15.28 - 2.5)\right) + (0.806 \cdot 10^3 \cdot 1.5)$$
$$= \boxed{-1\ 368.714 \ kN \cdot m}$$

4.2.3   RAT momentum analysis

When computing RAT momentum, it is going to be divided in two parts. In one hand, we are going to study the weight and its effects. On the other hand, the drag effect caused by its rotation is going to be analysed.

4.2.3.1   Nose

First of all, before start doing numeric calculus we have to guarantee that the sum of momentums compensates or keeps a low value between weight and the drag momentums.

In the nose, some positions are going to be analysed starting from the one that apparently seems the best one in terms of simplicity and easiness of implementation

4.2.3.1.1 Momentum due to the weight

4.2.3.1.1.1 Below the CG position

Positioning RAT in the nose, in Fig. 4.4 could be observed that weight contribute with a negative momentum.
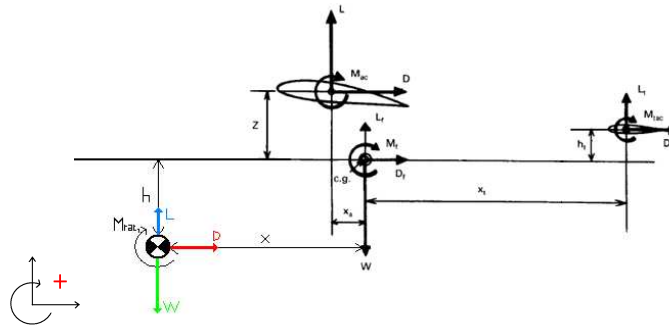
Fig. 4. 4 RAT located at nose below the CG

Equation 4.15 that describes the momentum done by RAT weight.

$$M_{RAT_W} = -(W \cdot x)$$
(4.15)

The x variable references the distance to the centre of gravity and W is the total weight of the system.

The position to the centre of gravity is 13.047 m and the total weight of the RAT is 81.65 kg, with this, we can compute the value of the momentum due to weight in the nose:

$$M_{RAT_W} = -(81.65 \cdot 9.8 \cdot 13.047) = -10.440 \ kN \cdot m$$

Lift has not much influence in the calculus of momentum due to its small component so it is going to be despised. Aside from this, due that we have an already stabilized plane; we will try to achieve a value of momentum equal to zero. In this case, however, it is going to be impossible because we have two components in the same direction.

$$M_{RAT} = -(W \cdot x) - (D \cdot h)$$
(4.16)

This option is not going to be discarded directly, we are going to find the numeric calculus instead, in order to compare the different numeric values and find a solution afterwards.

It is obvious that this placement does not compensate of momentums.

4.2.3.1.1.2 Two RAT located below the CG

In order to compensate the momentum created in the same direction we can opt for installing one RAT in the nose and another in the tail keeping the same distance from the centre of gravity, see Fig. 4.5. It is obvious that the nose RAT may create non-desired turbulence at the inlet of the RAT located in the tail, so, they are going to be added keeping an angle between each other.
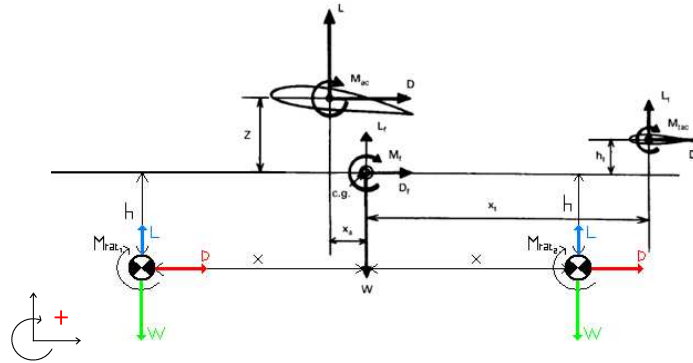
Fig. 4. 5 Two RAT located below the CG

$$M_{RAT_W} = -(W \cdot x) + (W \cdot x) \qquad (4.17)$$

Its resulting momentum:

$$M_{RAT_W} = 0 \; N \cdot m$$

The lateral momentum is compensated because RATs are placed with a symmetrical angle.

During the design process at nose position, another placing was thought in order to solve the problem of momentum with single RAT. See Fig. 4.6. Positioning RAT at the top of the cabin we might achieve a compensation of momentums due to the drag component. The problem came across at the cabin structure itself, so that cabin is totally pressured and we cannot allow having a system in this position, having to modify and change the plane main fuselage.
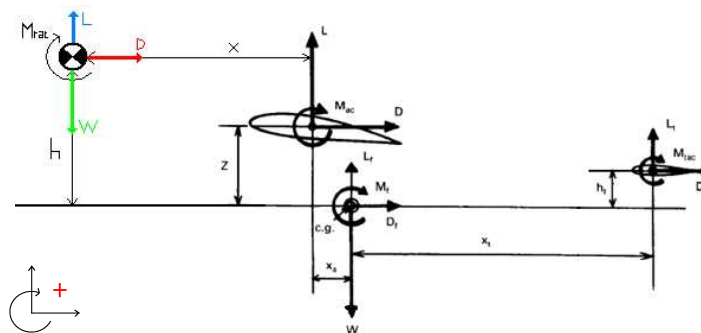
Fig. 4. 6 RAT located at nose above the CG

The momentum here will not be computed because there is no real chance to add any sort of system in that position as has been mentioned.

4.2.3.1.2 Momentum due to the drag

In order to calculate the drag generated by the rotation of the RAT blades, and consequently the momentum that it is generating, we will focus onto the autorotation of a helicopter since it represents the same situation for our case by changing the reference axis, see Fig. 4.7.

The procedure that we are going to use in order to find the drag it is identical in the different possible positions of the RAT, so the equations will be written only once.

Fig. 4. 7 Helicopter in autorotation

Source: Helicopter Flying Handbook. U.S. Department of Transportation. FAA. 2012

One method for making a rough estimate of the vertical drag penalty in hover is stated as follows [40]:

$$\frac{D_V}{GW} = \frac{0.3 \cdot DL \cdot projected\ area}{DL \cdot disc\ area} \tag{4.18}$$

An equivalent expression for our case based on the Fig. 4.8 is found.
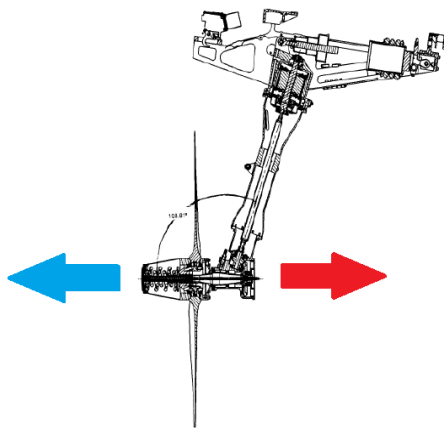
Fig. 4. 8 Main forces affecting the RAT

Source: Hamilton Sundstrand. Dossier resource de la RAT. A320

$$\frac{D_{RAT}}{F} = \frac{0.3 \cdot DL \cdot projected\ area}{DL \cdot disc\ area} \quad \rightarrow \quad D_{RAT} = \frac{F \cdot 0.3 \cdot projected\ area}{disc\ area}$$

Where F is the force produced by the RAT blades, painted in blue in Fig. 4.8. The drag of the RAT is the contrary force painted in red. First of all, we are going to calculate the F [41] force and after we are going to find out the drag of the RAT.

$$F = \frac{1}{2} \cdot \rho \cdot S \cdot v^2 \cdot c_F$$

(4.19)

The S variable is the surface of the RAT blades. In order to obtain this value we are going to reduce the size of an A380 RAT blade due to the lack of information of its dimensions in the A320 aircraft, see Fig. 4.9.
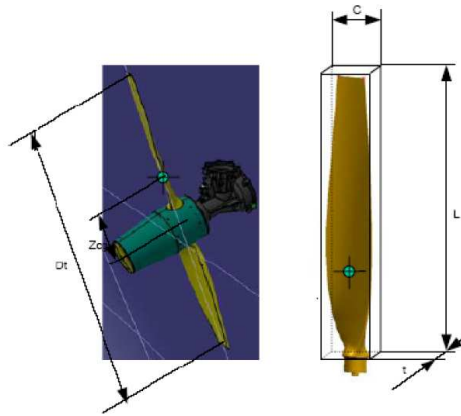
Fig. 4. 9 A380 RAT blades dimensions

Source: Hamilton Sundstrand. Dossier resource de la RAT. A320

If we know the L value for both A380 and A320 RATs and the value of c of the A380 RAT, we can obtain its surface in the A320 aircraft [27].

$$c_{A320} = \frac{c_{A380} \cdot L_{A320}}{L_{A380}} = \frac{100 \cdot 285.65}{701.20} = 40.74\ mm$$

(4.20)

Therefore, approximating the RAT blade to a rectangle we can obtain its surface:

$$S = c_{A320} \cdot L_{A320} = 40.74 \cdot 285.65 = 11,637.38\ mm^2 = 0.012\ m^2$$ (4.21)

We will take the value of $c_F = 8/9$, which is the worst case caused by the deceleration of the wind caused by the RAT. [41] Finally we have to calculate the F force into three different situations, as we have done in previous sections:

1. **Flight at sea Level ($\rho = 1.225\ Kg/m^3$)**
    a. At maximum speed ($v = 75.56\ m/s$)

$$F_{SL_{MAX}} = \frac{1}{2} \cdot 1.225 \cdot 0.012 \cdot 75.56^2 \cdot \frac{8}{9} = 37.30\ N$$

    b. At minimum speed ($v = 57.57\ m/s$)

$$F_{SL_{min}} = \frac{1}{2} \cdot 1.225 \cdot 0.012 \cdot 57.57^2 \cdot \frac{8}{9} = 21.65\ N$$

2. **Flight at 7,000 ft ($\rho = 0.59\ Kg/m^3, v = 100.35\ m/s$)**

$$F_{7,000 \, ft} = \frac{1}{2} \cdot 0.59 \cdot 0.012 \cdot 100.35^2 \cdot \frac{8}{9} = 31.69 \, N$$

Now modifying the drag formula stated previously we can calculate the drag produced by the rotation of the RAT blades.
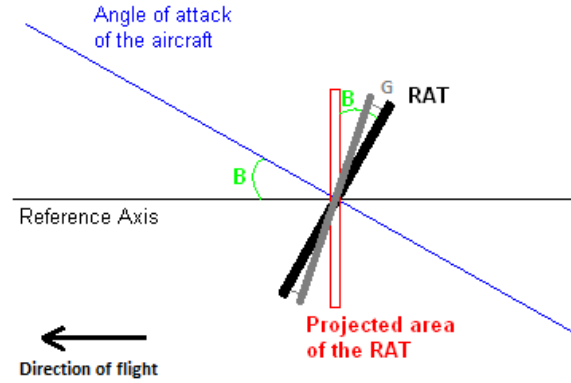
Fig. 4. 10 Scheme about the projected area of the RAT

If we have a look at the Fig. 4.10 we can see that the projected area of the RAT is going to depend on the angle of attack of the airplane during approach and landing (B), but also the angle between the RAT and the aircraft longitudinal axis (G) when situated in the tail, which is the most limiting case.

$$D_{RAT} = \frac{F \cdot 0.3 \cdot \pi \cdot R^2 \cdot \cos(B - G)}{\pi \cdot R^2} = F \cdot 0.3 \cdot \cos(B - G) \qquad \textbf{(4.22)}$$

1. **Flight at sea Level $(\alpha = 10°)$**
   a. At maximum speed $(v = 75.56 \, m/s)$
   $$D_{RAT_{SL \, MAX}} = 37.30 \cdot 0.3 \cdot \cos(10 - 0.5) = 11.03 \, N$$

   b. At minimum speed $(v = 57.57 \, m/s)$
   $$D_{RAT_{SL \, MAX}} = 21.65 \cdot 0.3 \cdot \cos(10 - 0.5) = 6.41 \, N$$

2. **Flight at 7,000 ft $(\alpha = 3°)$**
   $$D_{RAT_{7,000 \, ft}} = 31.69 \cdot 0.3 \cdot \cos(3 - 0.5) = 9.50 \, N$$

4.2.3.1.2.1 Below the CG position

If we now focus in the Fig. 4.4 we can obtain the following equation:

$$M_{RAT_d} = -(D \cdot h) \qquad \textbf{(4.23)}$$

In order to find the value of h, we are going to estimate a distance from the centre of gravity looking at the Fig. 4.3. Hence,

$$h \simeq 2.14 \, m$$

Also, we will have to calculate different drag momentums for each flight situation:

1. **Flight at Sea Level**
    a. At maximum speed

$$M_{RAT_{d\,SL_{MAX}}} = -(11.03 \cdot 2.14) = -23.60 \; N \cdot m$$

    b. At minimum speed

$$M_{RAT_{d\,SL_{min}}} = -(6.41 \cdot 2.14) = -13.72 \; N \cdot m$$

2. **Flight at 7,000 ft**

$$M_{RAT_{d\,7,000\,ft.}} = -(9.50 \cdot 2.14) = -20.33 \; N \cdot m$$

4.2.3.1.2.2 Two RAT located below the CG

Now we are going to obtain the momentum equation related to the Fig. 4.5:

$$M_{RAT_d} = -(D \cdot h) - (D \cdot h) \qquad\qquad (4.24)$$

Following the same pattern as the previous case, we will obtain the drag momentums for each flight situation:

1. **Flight at sea Level**
    a. At maximum speed

$$M_{RAT_{d\,SL_{MAX}}} = -(11.03 \cdot 2.14) - (11.03 \cdot 2.14) = -47.20 \; N \cdot m$$

    b. At minimum speed

$$M_{RAT_{d\,SL_{min}}} = -(6.41 \cdot 2.14) - (6.41 \cdot 2.14) = -27.48 \; N \cdot m$$

2. **Flight at 7,000 ft**

$$M_{RAT_{d\,7,000\,ft}} = -(9.49 \cdot 2.14) - (9.49 \cdot 2.14) = -40.66 \; N \cdot m$$

As said previously and observing the obtained results we can see that locating a single RAT in the nose both momentums are negative. Shall be said that the momentum created due to drag is quite low compared with the one created by the weight. However, we will try to keep the momentum as less as possible, for this main reason different studies. In the second case we have tried to compensate the momentum of the weight and it has been achieved, but, we have the compromise of adding the double of weight in the plane because another RAT is going to be needed. Energetic balance in chapter 5 is of our need to see if it worth or does not.

4.2.3.2   Tail

The tail positioning keeps the same distance than the first analysis of the single nose RAT.

4.2.3.2.1 Momentum due to the weight

4.2.3.2.1.1 Below the CG position
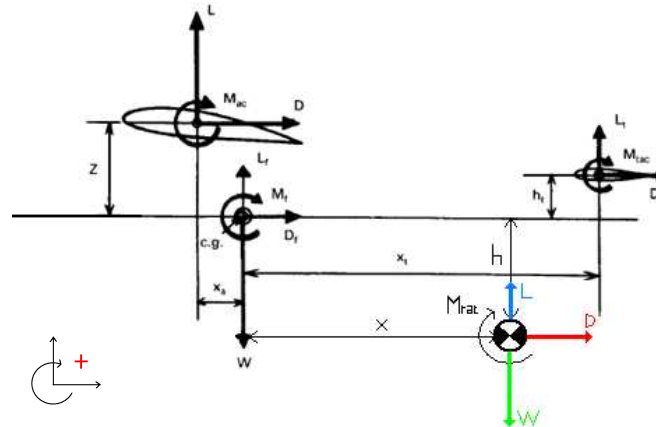
Fig. 4. 11 RAT located at tail below the CG

The distance to the tail is the same as the one calculated in the nose and it is obvious that the weight remains constant. The only change that appears here in the nose is the change of sign due to the position in the front side, see Fig. 4.11. So the formula:

$$M_{RAT_w} = (W \cdot x) \qquad \textbf{(4.25)}$$

$$M_{RAT_w} = (81.65 \cdot 9.8 \cdot 13.047) = 10.440 \; KN \cdot m$$

4.2.3.2.2 Momentum due to the drag

4.2.3.2.2.1 Below the CG position

Understanding the scheme of this tail momentum analysis, we can obtain the equation 4.26:

$$M_{RAT_d} = -(D \cdot h) \qquad \textbf{(4.26)}$$

The RAT will be located in the opposite direction as it was in the nose case, but at the same height. For this reason, the value of h will be exactly alike. Also, the different drag momentums for each flight situation will be the same as the previous case:

1. **Flight at Sea Level**
   a. At maximum speed
$$M_{RAT_{d\,SL_{MAX}}} = -(11.03 \cdot 2.14) = -23.60 \; N \cdot m$$
   b. At minimum speed
$$M_{RAT_{d\,SL_{min}}} = -(6.41 \cdot 2.14) = -13.72 \; N \cdot m$$

2. **Flight at 7,000 ft**
$$M_{RAT_{d\,7,000\,ft}} = -(9.49 \cdot 2.14) = -20.31 \; N \cdot m$$

4.2.3.3 Belly-fairing

4.2.3.3.1 Momentum due to the weight

4.2.3.3.1.1 Below the CG position

The position in the belly-fairing remains at the point of the centre of gravity, see Fig. 4.12. As analysed in the optimal position selection, there are some points where some connections are placed not allowing the placement of RAT in some points of belly-fairing. Due to those limitations a location is found in the centre of gravity making easy the calculus so that we do not have a momentum due to the weight.

$$M_{RAT_w} = (W \cdot x)$$
$$M_{RAT_w} = 0\ N \cdot m$$

(4.27)

We must consider that the centre of gravity is going to vary during the flight, but in order to simplify the calculus we consider that is going to be fixed, which is an approximation.
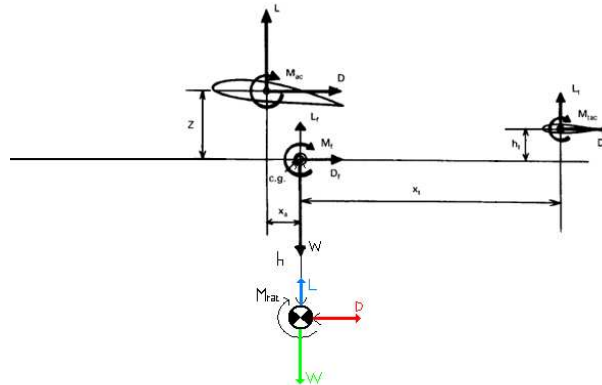
Fig. 4. 12 RAT located at the belly-fairing

4.2.3.3.2 Momentum due to the drag

4.2.3.3.2.1 Below the CG position

Understanding the scheme of this tail momentum analysis, we can obtain the equation 4.28:

$$M_{RAT_d} = -(D \cdot h)$$

(4.28)

The value of h will be found graphically in order to avoid the collision of the RAT blades against the fuselage, and also prevent rear actuators from turbulences. This is showed in the Fig. 4.13.
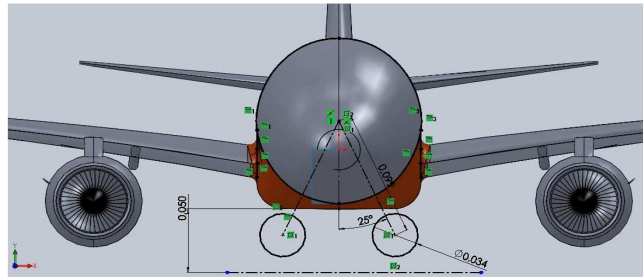
Fig. 4. 13 Front view of the A320 with the sketch of the RAT in the belly-fairing

It is obvious that all measurements are scaled in respect to the real dimensions of the A320; therefore the value of h real sized is 2.5 m. The different drag momentums for each flight situation will be calculated below:

1. **Flight at sea Level**
   a. At maximum speed
$$M_{RAT_{d\,SL_{MAX}}} = -(11.03 \cdot 2.5) = -27.58\ N \cdot m$$
   b. At minimum speed
$$M_{RAT_{d\,SL_{min}}} = -(6.45 \cdot 2.5) = -16.13\ N \cdot m$$

2. **Flight at 7000 ft**
$$M_{RAT_{d\,7000\,ft.}} = -(9.49 \cdot 2.5) = -23.73\ N \cdot m$$

4.2.4   Momentums summary

Concept	7,000 ft (kN·m)	Concept	Sea Level (kN·m)	
4.2.1.1 Wing 7,000 ft	450.39	**4.2.1.2 Wing at sea level**	**Max**	1225.30
			Min	711.29
4.2.2.1 Tail 7,000 ft	-545.94	**4.2.2.2 Tail at sea level**	**Max**	-2357.80
			Min	-1368.71

	Momentum due to the weight		Momentum due to the drag		
Concept	**(kN·m)**	**Concept**	**7,000 ft (N·m)**	**Sea Level (N·m)**	
4.2.3.1.1.1 Nose, below the CG.	-10.44	**4.2.3.1.2.1 Nose, below the CG.**	-20.33	**Max**	-23.60
				Min	-13.72
4.2.3.1.1.2 Nose, 2 RAT below the CG.	0	**4.2.3.1.2.2 Nose, 2 RAT below the CG.**	-40.66	**Max**	-47.20
				Min	-27.48
4.2.3.2.1.1 Tail, below the CG.	10.44	**4.2.3.2.2.1 Tail, 2 RAT below the CG.**	-20.33	**Max**	-23.60
				Min	-13.72
4.2.3.3.1.1 Belly-fairing, below the CG.	0	**4.2.3.3.2.1 Belly-fairing, below the CG.**	-23.73	**Max**	-27.58
				Min	-16.13

Table 4. 4 Momentums summary

4.3   Simulations Analysis

All the velocity and pressure simulations shown below were set to represent 1 second. Due to the time it took and the precision that required, more time was not configured.

In all force graphics, during first iterations can be seen very different values with a variable slope. This is due to the time that the force analysis requires to stabilise. First of all we will take the values of A320 lift and drag without RAT in two cases, see Fig. 4.14 and Fig. 4.15, one at sea level and the other one at 7,000 ft in order to have values to compare with all RAT positions analysed in chapter 3.

Goal Name	Averaged Value
🟥 GG Z - Component of Force 1	-45585.2 N
🟩 GG Y - Component of Force 1	11194 N

Fig. 4. 14 Lift (green) and Drag (red) values for A320 without RAT at sea level

Goal Name	Averaged Value
🟥 GG Z - Component of Force 1	-40378.6 N
🟩 GG Y - Component of Force 1	8678.43 N

Fig. 4. 15 Lift (green) and Drag (red) values for A320 without RAT at 7,000 ft

Pictures at the beginning of each location analysis at sea level and 7,000 ft give an idea about which part of the aircraft is involved. If more detail is desired, the Annex D contains all simulations graphics and figures.

4.3.1   Tail analysis. Sea Level

Specifically in the tail, we have the influence of the wings which leverages the flow at the inlet reducing its velocity and giving us a velocity margin to take RAT out. So we can use RAT safely when the pilot is at the velocity that permits the extraction of the RAT, because the velocity in it will be less than the velocity that the pilot sees.

The only variation remarkable comes when varying altitude. The values of drag and lift are shown in Fig. 4.16:

Goal Name	Averaged Value
🟥 GG Z - Component of Force 1	-48385.7 N
🟩 GG Y - Component of Force 1	13769.5 N

Fig. 4. 16 Lift (green) and Drag (red) values for RAT in the tail at sea level

If more image quality is desired, Fig. D.4 and Fig. D.5 in Annex D show the pressure and velocity changes, which leads to a turbulent flow. Focusing on pressure, we can clearly see a hollow in the back of RAT. In the same way that happens to pressure, a deceleration might be perceived in the front when air strikes against RAT and another deceleration in the back due to the frontal one.

In the sea level case, the movement of the fluid cannot be seen clearly due to its low velocity but if we have a look to the 7,000 ft case, the track that the air follows is better defined. The turbulent flow generated is not enough then, to affect the rear control surfaces such as horizontal stabilizer and elevator, because it returns quite quickly to its nominal velocity movement and the turbulences of RAT and elevator are not in the same plane, which helps to maintain a margin if the angle of attack changes. Shall be said, that devices such as flaps or ailerons are not influenced by the frontal deceleration or the increment of pressure.

We have considered a solid object that does not totally allow the circulation of air through it. This supposition magnifies all the numbers calculated in this chapter. For this reason, in section 4.2.3 the resistance created by its rotation has been calculated, instead of the resistance produced by a solid cylinder.

4.3.2   Tail analysis. 7,000 ft

Goal Name	Averaged Value
■ GG Z - Component of Force 1	-46765.9 N
■ GG Y - Component of Force 1	9657.27 N
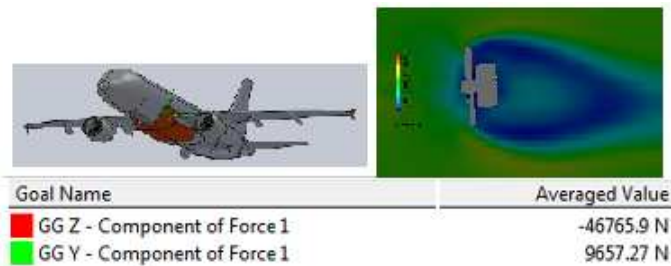
Fig. 4. 17 Lift (green) and Drag (red) values for RAT in the tail at 7,000 ft

At 7,000 ft, Fig. D.9 and Fig. D.10 in the Annex D show that we have to bear in mind that velocity is about 100.35 m/s so decreases reaching values of 36 m/s at some points. In this case, the pressure variation increases between the front part and the back. It reaches values approximately of 43,000 Pa in the front and 38,000 Pa in the back. Comparing the results shown in Fig. 4.17 to the ones obtained in 4.3.1 section we can notice that a decrement in the resistance is produced. This reduction is due to the change of density of the air, which is less than at sea level.

4.3.3   Tail analysis. Sea level at full flaps

Goal Name	Averaged Value
🟥 GG Z - Component of Force 1	-56106.9 N
🟩 GG Y - Component of Force 1	145664 N
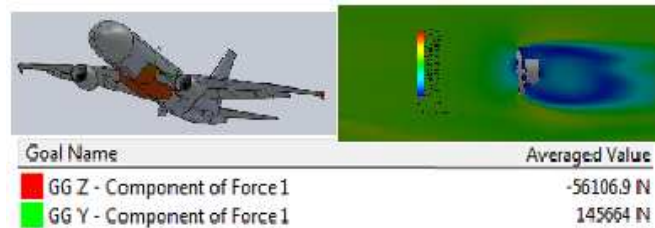
Fig. 4. 18 Lift (green) and Drag (red) values for RAT in the tail at sea level with full flaps

In Fig. D.14 and Fig. D.15 of Annex D flap extension is shown. When extending flaps it is obvious that drag increases because there is an augmentation of surface, for the same reason Y force increases which means an increment of lift. Our interest is to see if the extension of the flaps affect excessively to the flow at RAT inlet. The flow when extracting flaps follows the chord of the wing driving the air below the RAT and leading a non-effect as shown in the simulations. It might happen that when pulling up at great angles of attack the effect of flaps appears.

In the pressure case, remains almost equal to the previous case, having an increment in the front and a decrement in the back without affecting any other control surface.

The differences comparing with the A320 without RAT start being large at 7000 ft but them decrease when the plane starts losing altitude and speed, being speed the conditioning value.

4.3.4 Nose analysis. Sea level

Goal Name	Averaged Value
🟥 GG Z - Component of Force 1	-46302.7 N
🟩 GG Y - Component of Force 1	17391.3 N
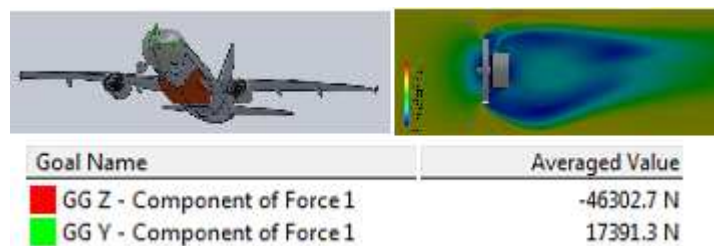
Fig. 4. 19 Lift (green) and Drag (red) values for RAT in the nose at sea level

Locating RAT in the nose, shown in Fig. D.17 and Fig. D.18 in Annex D, the drag obtained is approximately 2 kN less than if we place it in the tail at the same distance. In this case the plot starts at the iteration 35 so the stabilizations are not shown.

Analysing the velocity simulation, the main and most important point is the fact that we do not have any effect coming from any surface of the plane such as wings or flaps. This has its advantages and disadvantages. In one hand, if we do not have any perturbation in front, we can assure a non-turbulent flow at inlet of the RAT. On the other hand, if we do not have any reduction of velocity, the

velocity that sees the pilot at which we can take the RAT out safely, lightly decreases.

The velocity effect is clearly large. A decrement in velocity of the flow as big as this one may affect slightly the engines and posterior control surfaces, which is not of our interest. Compared with the tail position this solution would be clearly discarded.

In the case of pressure and comparing values with the tail position, the variation of pressure increases due to the great difference between the high pressure at inlet an the low pressure at the rear part of RAT. In the tail case, we had the wing effect so the variation was not so large. We cannot allow having this magnitude of low pressure at the underneath part of fuselage at an important distance of the centre of gravity, so it may lead to a down pitch movement that we are not interested to have.

4.3.5   Nose analysis. 7,000 ft

Goal Name	Averaged Value
■ GG Z - Component of Force 1	-44221.8 N
■ GG Y - Component of Force 1	15856.8 N
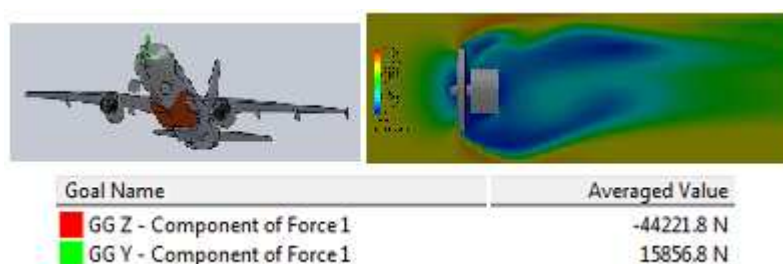
Fig. 4. 20 Lift (green) and Drag (red) values for RAT in the nose at 7,000 ft

As seen in the tail simulations the resistance decreases due to the density of the air at this altitude.

In this case, Fig. D.20 and Fig. D.21 in Annex D the impact of velocity is more relevant that in the study at sea level. We can see that the reduction of velocity due to the RAT at this altitude affects going under values of about 21 m/s and this velocity does not return to its nominal velocity likely affecting the whole below part of the plane. At the tips of the RAT appear and acceleration causing instability between the inner flow and the outer, once the flow has overshot the RAT leaving it behind. This may affect to the engines inner flow.

In the case of pressure the same as at sea level happens, but the difference here between the front and the back is greater. So the limitation case is the 7,000 ft instance.

4.3.6   Nose and tail analysis. Sea level

Goal Name	Averaged Value
🟥 GG Z - Component of Force 1	-53523.4 N
🟩 GG Y - Component of Force 1	22296.9 N

Fig. 4. 21 Lift (green) and Drag (red) values for RAT in the nose and tail at sea level

This disposition was proposed when the nose study was done. In Fig. D.23, Fig. D.24, Fig. D.25 and Fig. D.26 in Annex D the simulations are shown with more quality and extension. The resistance is approximately 54 kN, reaching values almost equal than the full flaps configuration. The nose RAT has a very close effect than the one studied in 4.3.4, the only difference though, is that we only place one. The one in the rear part has the same effect as the simulation done in the tail placement. The advantage that gives us this disposition is the compensation of momentums in the case of weight. The momentum due to the drag it is not going to be the same because of the increment in air velocity at inlet of each RAT. Pressures do not have a relevant effect, as in the other cases increment of pressure appears in the front and a decrement in the rear side.

4.3.7   Nose and tail analysis.7,000 ft

Goal Name	Averaged Value
🟥 GG Z - Component of Force 1	-49298.5 N
🟩 GG Y - Component of Force 1	10529.4 N
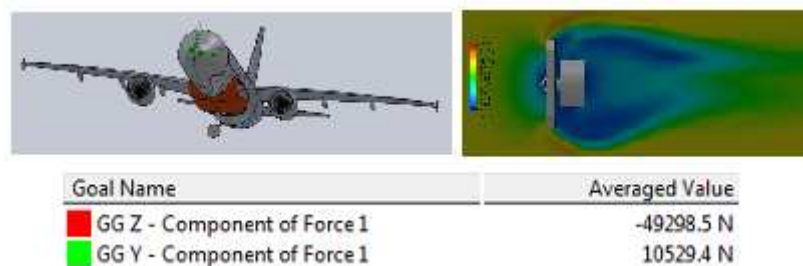
Fig. 4. 22 Lift (green) and Drag (red) values for RAT in the nose and tail at 7,000 ft

Looking at Fig. D.32, D.33, D.34, D.35 in Annex D at this altitude, we have a great velocity so the reduction is larger. The value of resistance decreases but is approximately 2 kN and 5 kN higher than tail and nose locations at this altitude. Even this reduction of velocity, pressure has not a relevant effect. Comparing those simulations with others, we can clearly see that this solution is not as good as belly-fairing or tail placement referring to drag created.

4.3.8 Belly-fairing analysis. Sea level

Goal Name	Averaged Value
GG Z - Component of Force 1	-49093.8 N
GG Y - Component of Force 1	9461.85 N
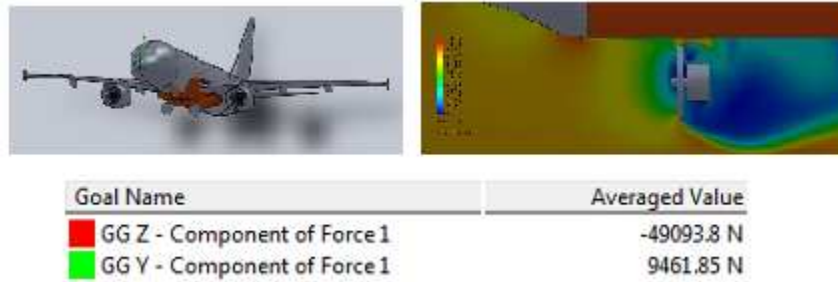
Fig. 4. 23 Lift (green) and Drag (red) values for RAT in the belly-fairing at sea level

In the case of belly-fairing at sea level, shown in Fig. D.41 and Fig. D.42 in Annex D, a clearly reduction of velocity is produced between the blades cylinder and the fuselage and also in the rear part of the RAT. The first reduction might be partially underestimated because the distance from the cylinder to the fuselage is really short and has not been studied in detail. We have to remember that the cylinder is an approximation, so in the upper part would not exist a decrement as large as the one shown. Although this reduction, the trajectory of the flow in the engines inlet does not vary because the RAT is located at its vertical same plane.

An important issue appears in the simulation in the lower part of the RAT where flow spreads its non-velocity area out due to the reduction of the upper narrowing.

In the case of pressure, no relevant changes are produced.

4.3.9 Belly-fairing analysis. 7,000 ft

Goal Name	Averaged Value
GG Z - Component of Force 1	-48033.3 N
GG Y - Component of Force 1	11367.1 N

Fig. 4. 24 Lift (green) and Drag (red) values for RAT in the belly-fairing at 7,000 ft

Looking at the same positioning at 7,000 ft as it is simulated in Fig. D.44 and Fig. D.45 in Annex D, the variation of velocity is not as important and large as in the case of sea level and the velocity recovers in few meters almost its nominal velocity.

Pressure though, decreases more than at sea level, but it keeps irrelevant anyway in comparison with some pressures simulated in other positions.

4.3.10 Simulations summary

Concept		Concept		Concept	
4.3.1 Tail analysis. Sea level.	🟧	4.3.4 Nose analysis. Sea level.	🟥	4.3.7 Nose and tail analysis. 7,000 ft.	🟥
4.3.2 Tail analysis. 7,000 ft.	🟧	4.3.5 Nose analysis. 7,000 ft.	🟥	4.3.8 Belly-fairing analysis. Sea level.	🟩
4.3.3 Tail analysis. Sea level at full flaps.	🟧	4.3.6 Nose and tail analysis. Sea level.	🟥	4.3.9 Belly-fairing analysis. 7,000 ft.	🟩

Table 4. 5 Simulations summary

Colour code:

🟩	Accepted options	🟧	Needs modifications or some problems appear	🟥	Discarded options

The analysis of all positions leads us to choose the best position of the ones proposed.

In the case of nose positioning, the results show a clear deceleration of velocity at any altitude affecting all the lower part of the plane, which could affect the aircraft performances commented on section 4.1.4 and 4.1.5. The unpressurized areas are not a problem here, but we cannot allow having such a decrement in velocity positioning RAT in this location. This option then is going to be discarded.

In the tail positioning, the reduction of velocity is not as large as in the nose case and we assure that the turbulent flow does not affect any control surface and has no contact with the plane fuselage. This positioning is good in this aspect; at the end of the fuselage no effect of placement is produced. The problem comes when we look for unpressurized areas to implant the system; the fuselage in this zone has not this sort of areas where we can add safely and easily the whole system. If other solution could not be found, this position could be deeply studied; finding for example a possible solution by modifying the A320 main structure in order to create a non-pressurized area in that zone. This option then is going to be discarded.

The nose plus tail case came out as a solution to compensate the momentums due to the weight, but concluding what was seen in the simulations, the problem in the tail of finding an unpressurized area persists and the little momentum created by the two RAT drags appears. The last mentioned could be compensated by the pilot with the trimmer. Even though this possible solution, other options may be better, so this option then is going to be discarded.

Belly-fairing is the next and the last studied case, this position has an effect on the last half of the fuselage but the reduction in velocity is not as large as the one commented in the nose, so this is not going to be considered as a sizeable problem. The sum of momentums in the case of weight here is the best of all cases studied so that the distance to the gravity centre is almost zero, then the momentums will have a small variation during the entire flight. The resistance

here is a bit higher than tail or nose cases but it keeps being a possibility so that the system is going to be used in approach procedures when the plane needs to lightly decelerate. Referring to the placement, non-pressurized areas exist, so the placement is possible. Therefore, this position is the one selected for placing RAT system.

In conclusion, the position that best satisfies the criteria specified in chapter 3, and also fulfills the desired specifications defined in chapter 4 is the belly-fairing.

4.4 Selected position versus A320 without RAT

4.4.1 Comparison at sea level

If we compare the values with the corresponding ones on the belly-fairing, see 4.3.8 section, we can clearly see that, without the RAT there is a difference of almost 4 kN in the drag force generated by the entire aircraft between the A320 without the RAT and when the RAT is installed in the belly-fairing.

Now comparing the lift values there is a difference of 2 kN between each configuration, which leads us to determine that the RAT does not vary the performance of the aircraft in an extremely limiting way, as commented previously on 4.3.8 section.

Finally, it is also evident that the flow simulations in respect to velocity and pressure will be better in the A320 without RAT, but as we have commented before, the difference is noticeable but still desirable.

4.4.2 Comparison at 7,000 ft

If we compare the values with the corresponding ones on the belly-fairing, see 4.3.9 section, we can clearly see that, without the RAT there is a difference of almost 8 kN between the drag force generated by the entire aircraft and the one generated when the RAT is installed in the belly-fairing.

Now comparing the lift values there is a difference of 3 kN between each configuration, which is greater than in the previous comparison at sea level, but still does not vary the performance of the aircraft in an extremely limiting way.

Finally, as it happened previously, the flow simulations of velocity and pressure showed an obvious improvement in the aircraft performances with the A320 without RAT rather than the RAT in the belly-fairing case, which it is normal.

4.5 Drag Analysis

In this section, the fuselage drag will be calculated and a summary of all drags calculated previously will be done.

4.5.1   Fuselage drag

We are going to use the fuselage drag coefficient obtained by Marc Julbe Poca in his study [42] of the repercussion of weight and balance over the final fuel consumption in the A320.

$$c_{D_{fuselage}} = c_{D_{0_{fus}}} + c_{D_{L_{fus}}} = 0.0081 \tag{4.29}$$

It is clear that the transversal section of the fuselage it is not constant, therefore it should be convenient to use a subroutine in order to take this variation into account. Nevertheless, so as to simplify the calculus of the fuselage drag we will approximate the fuselage to a cylinder.

We obtain the diameter of the cylinder that we suppose as a fuselage from the Fig. 4.25 [32]. Also, the fuselage length is 37.57 m.
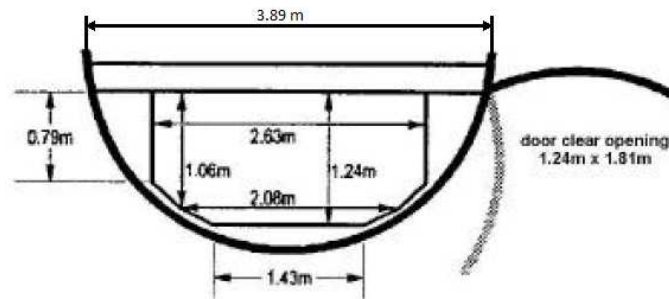
Fig. 4. 25 Fuselage section

Source: Airbus A319/A320/A321 Ground operations manual. 2002

$$S_{fuselage} = 2 \cdot \pi \cdot \left(\left(\frac{D}{2}\right)^2 + \left(\frac{D}{2}\right) \cdot l \right) = 2 \cdot \pi \cdot \left(\left(\frac{3.89}{2}\right)^2 + \left(\frac{3.89}{2}\right) \cdot 37.57 \right)$$
$$= 482.90 \ m^2 \tag{4.30}$$

4.5.1.1   Fuselage drag at sea level

$$D_{fuselage_{SLMAX}} = \frac{1}{2} \cdot \rho \cdot S_{fuselage} \cdot c_{D\_fuselage} \cdot v_{MAX}^2$$
$$= 0.5 \cdot 1.225 \cdot 482.9 \cdot 0.0081 \cdot 57.57^2 = 7.940 \ kN$$

$$D_{fuselage_{SL_{min}}} = \frac{1}{2} \cdot \rho \cdot S_{Fuselage} \cdot c_{D\_fuselage} \cdot v_{min}^2$$
$$= 0.5 \cdot 1.225 \cdot 482.9 \cdot 0.0081 \cdot 75.56^2 = 13.678 \ kN$$

4.5.1.2   Fuselage drag at 7,000 ft.

$$D_{fuselage_{7,000ft}} = \frac{1}{2} \cdot \rho \cdot S_{fuselage} \cdot c_{D\_fuselage} \cdot v^2$$
$$= 0.5 \cdot 0.59 \cdot 482.9 \cdot 0.0081 \cdot 100.35^2 = 24.125 \ kN$$

4.5.2   Drag summary

As it is shown in the table 4.6, the most noticeable on it is the fact that the fuselage produces much more drag force than the wing, tail or RAT, which is normal because we have considered the fuselage as a cylinder, and it has a rough aerodynamic profile.

Concept	7,000 ft (kN)	Sea Level (kN)	
Fuselage	24.125	Max	7.940
		Min	13.678
Wing	2.276	Max	5.359
		Min	3.110
Tail	0.553	Max	1.388
		Min	0.806
RAT rotation	0.0095	Max	0.0110
		Min	0.0064

Table 4. 6 Drag summary from previous sections

CHAPTER 5. ENERGETIC BALANCE

In order to compute costs and quantity of fuel for taxi, a difference is going to be made between taxiing-in and taxiing-out. The first one references to the way the plane makes on its way from the gate to the runway. The taxiing-out means the way done in the other way round.

For the ideal energy that we need while taxiing, we took as example values as if we fly from Barcelona to Madrid. Consequently, the taxiing-out is the one from the Gate C in Barcelona until the threshold of runway 07L. In the arrival the taxing-in is considered L1 exit until the Gate 1.

5.1   Typical taxiing ideal energy required

Some analyses will be done about this required energy. As it was specified previously, there shall be a differentiation between the energy waste during taxi-out and taxi-in procedures.

5.1.1   Taxi-out analysis

In chapter 1 we have already calculated the taxi-out distance in the Barcelona-El Prat airport, and we consider that the maximum altitude that reaches the entire airport platform is 10 meters, see Fig. 5.1.
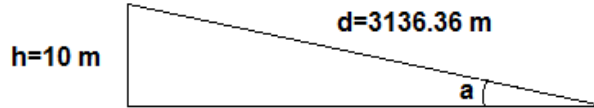
Fig. 5. 1 Barcelona-El Prat simplified platform slope

Looking at Fig. A.1 in the Annex A, can be seen that the aircraft will have to accelerate 13 times, where 8 of those accelerations are due to the intersections with other taxi ways and the 5 left are due to possible stops at the proximity of the threshold due to queues. Also we will determine three different velocities (v_1, v_2, v_3) during the taxi procedure in order to approximate as much as possible the performance of this acceleration from the aircraft. Those velocities are: v_1 = 16 kts, v_2 = 8 kts and v_3 =3 kts.

$$E = E_P + E_K = mgh + \frac{1}{2} \cdot m \cdot v_1^2 + \left(\frac{1}{2} \cdot m \cdot v_2^2 \right) \cdot 7 + \left(\frac{1}{2} \cdot m \cdot v_3^2 \right) \cdot 5 \quad \text{(5.1)}$$

We need to obtain the mass of the aircraft at take-off, so we must consider the value of Dry Operating Weight of the aircraft [43] plus the payload considering a 70% of occupation of the aircraft and the fuel quantity needed for a flight [42] such as Barcelona-Madrid.

$$m_{Take-Off} = DOW + PL + FW = 42599 + 11340 + 6200 = 60139 \, kg \quad \text{(5.2)}$$

Finally, we obtain the total energy needed for the taxi-out procedure in Barcelona-El Prat airport:

$$E_{taxi-out} = E_p + E_K = 5.89 \cdot 10^6 + 5.97 \cdot 10^6 = 11.87 \; MJ$$

5.1.2   Taxi-in analysis

We have to calculate the maximum altitude of the Madrid-Barajas airport. The same slope as the previous case can be considered but modifying the maximum distance that the aircraft must travel. Therefore, using simple mathematics we obtain the value of h as it is shown in Fig. 5.2:
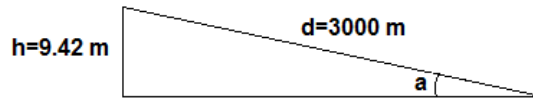
Fig. 5. 2 Madrid-Barajas simplified platform slope

Following the same steps done before, by looking at the figure A.2 at the Annex A, we can see that the aircraft will have to accelerate 10 times, where 7 of those accelerations are due to the intersections with other taxi ways and the 3 left are due to possible stops due to queues. The same three velocities used in the first case will be used in order to approximate as much as possible the performance of this acceleration from the aircraft.

$$E = E_p + E_K = mgh + \frac{1}{2} \cdot m \cdot v_1^2 + \left(\frac{1}{2} \cdot m \cdot v_2^2\right) \cdot 6 + \left(\frac{1}{2} \cdot m \cdot v_3^2\right) \cdot 3 \tag{5.3}$$

We need to obtain the mass of the aircraft at landing, so we only have to subtract the fuel that has been burned during the flight. If we know the consumption and the flight time [44] the mass at landing will be calculated:

$$m_{fuel\;loss} = cn \cdot t = 2,500 \frac{kg}{h} \cdot \frac{1\;h}{60\;min} \cdot 43\;min = 1,791.67 \; kg \tag{5.4}$$

$$m_{Landing} = m_{Take-Off} - m_{fuel\;loss} = 60,139 - 1,791.67 = 58,347.33 \; kg \tag{5.5}$$

Finally, we obtain the total energy needed for the taxi-in procedure in Madrid-Barajas airport:

$$E_{taxi-in} = E_p + E_K = 5.39 \cdot 10^6 + 5.15 \cdot 10^6 = 10.55 \; MJ$$

So as to obtain the total energy that requires the taxi-in and taxi-out procedures we just have to sum both values. The value of the energy generated by the RAT will have to be greater than this value in order to our system to be feasible, which is commented in the following sections.

$$E_{total} = E_{taxi-in} + E_{taxi-out} = 11.87 \cdot 10^6 + 10.55 \cdot 10^6 = 22.42 \; MJ \tag{5.6}$$

5.2   Fuel quantity

Starting with the formula proposed in the taxi procedures in chapter 1, the quantity of fuel needed [9] to make a taxi during 10 minutes will be found.

$$\frac{f}{\sqrt{T_{amb}}} = a_2 + b_2 \cdot t + c_2 \cdot n_a$$

(5.7)

As explained in the first chapter coefficients a_1, b_2 and c_2 depend on the aircraft taking the following values:

$$a_1 = -0.0896 \; ; \; b_2 = 0.0124 \; ; \; c_2 = 0.1174$$
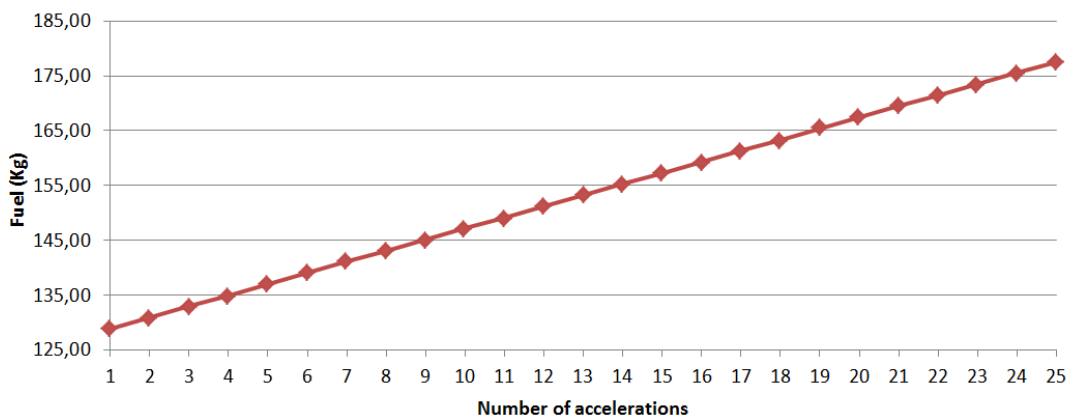
Fig. 5. 3 Fuel consumption evolution

Using Microsoft Excel [45] we compute different values of fuel consumption (Kg) depending on the number of accelerations done by the aircraft. Looking at the Fig. 5.3 we can observe that the fuel consumption evolution is linear.

5.3   Price of taxi

Consulting IATA's webpage [46] we get the current price of the fuel, being 884.4 cts/gal. Then this unit is converted to €/liters knowing first of all the actual value of the dollar and the relation between the gallon and the liter:

$$884.4\frac{cts}{gal} \cdot \frac{1\$}{100\,cts} \cdot \frac{0.794849376€}{1\$} \cdot \frac{1gal}{3.7854118\,liters} = 1.857\frac{€}{kg}$$

Once in this point, and having a look to a fuel provider as CLH we can obtain the density of the fuel Jet A1. The specifications give us the density at 15℃, being 0.775 kg/liter.

$$1.857\frac{€}{liter} \cdot \frac{liter}{0.775\,kg} = 2.39613\frac{€}{kg}$$

Computing the price of a taxi getting different values for taxi-in and taxi-out we obtain:

$$price\ of\ taxi = fuel\ price\ \frac{€}{kg} \cdot kg\ of\ fuel$$

(5.8)

$$Total\ price\ of\ taxi - out = 2.39613\frac{€}{kg} \cdot 153.23\ kg = 367.16\ €\ per\ taxi$$

$$Total\ price\ of\ taxi - in = 2.39613\frac{€}{kg} \cdot 147.15\ kg = 352.59\ €\ per\ taxi$$

For the next calculus the worst case is going to be taken to assure that with the greatest cost per taxi we can obtain a benefit. Consequently, we are going to take the taxi-out total cost.

5.4   Energy obtaining

We will start the energy study extracted from our RAT, knowing that at 130 KEAS we get 54 HP [47]. Also remembering the time calculated on chapter 1, a value of energy can be estimated knowing that our approach will last 12 minutes more or less.

$$54\ HP \cdot \frac{745.7\frac{J}{s}}{1HP} \cdot 720\ s = 28.99\ MJ \approx 29\ MJ$$

(5.9)

This is the value of the energy obtained when approaching from 7,000 ft until landing using the velocities calculated with the suppositions made in chapter 1. This energy must be stored in batteries weighting the less possible and a study of costs is going to be done in order to know if it worth or if it is not.

Furthermore, using the criterion that our generator does not provide the 100% of the energy produced, we are going to suppose that our generator delivers to the batteries the 40% of the energy achieved.

$$29\ MJ \cdot \frac{40}{100} = 11.6\ MJ$$

(5.10)

Comparing with the value of energy that we need for our taxi in section 5.1, one RAT is not enough. The solution is to add another RAT to achieve a value of energy for which the taxi-in and taxi-out would be possible. This result is not a problem so the simulations were tested with symmetric RATs and the limiting parameters were studied.

Energy obtained by adding another RAT:

$$11.6\ MJ \cdot 2 = 23.2\ MJ\ ;\ 23.2\ MJ \geq 22.4\ MJ$$

(5.11)

Theoretically, with two RATs the demand of energy can be satisfied without any problem assuming a low efficiency in the suppliancy of energy to the batteries.

5.5   Batteries

Once we know the exact amount of energy that the RAT generates, we have to choose the correct batteries so as to store this energy. We are going to compare three types of batteries that could be used in order to show a possible solution for this system.

Shall be said that during the choice of the number of batteries we took as efficiency the 100% in order to oversize the storage in the case we had a higher efficiency.

5.5.1   SAFT 2758. At present used in A320

- Technical data from [48]:

    o Nominal voltage: 24 V
    o Rated capacity: 23 Ah
    o Maximum weight: 25.5 kg

- Storable energy

$$E = P \cdot t \quad ; \quad P = I \cdot V \qquad \text{(5.12) ; (5.13)}$$

$$E = I \cdot V \cdot t = 23 \cdot 24 \cdot 3600 = 1.98 \cdot 10^6 \approx 2 \text{ MJ} \qquad \text{(5.14)}$$

- Number of batteries needed and total weight

We are going to calculate the number of batteries needed to store the energy that is produced by the RAT considering the quantity of energy that can be stored in each battery.

$$\text{Number of batteries} = \frac{29 \text{ MJ}}{2 \text{ MJ}} = 15 \quad \rightarrow \quad 15 \text{ batteries} \cdot \frac{25.5 \text{ } Kg}{1 \text{ } battery} = 382.50 \text{ kg} \qquad \text{(5.15)}$$

5.5.2   Super B 7800. For aircraft use

- Technical data from [49]:

    o Nominal voltage: 13.2 V
    o Rated capacity: 7.8 Ah
    o Maximum weight: 1.3 kg

- Storable energy

$$E = I \cdot V \cdot t = 13.2 \cdot 7.8 \cdot 3600 = 370.66 \text{ kJ}$$

- Number of batteries needed and total weight

$$\text{number of batteries} = \frac{29 \text{ MJ}}{370.66 \text{ kJ}} = 79 \;\rightarrow\; 79 \text{ batteries} \cdot \frac{1.3 \text{ } kg}{1 \text{ } battery} = 102.70 \text{ kg}$$

5.5.3   Super B 10 P. For aircraft use

- Technical data from [50]:

   o Nominal voltage: 13.2 V
   o Rated capacity: 10 Ah
   o Maximum weight: 1.75 kg

- Storable energy

$$E = I \cdot V \cdot t = 13.2 \cdot 10 \cdot 3600 = 475.20 \text{ kJ}$$

- Number of batteries needed and total weight

$$\text{number of batteries} = \frac{29 \text{ MJ}}{475.20 \text{ kJ}} = 62 \;\rightarrow\; 62 \text{ batteries} \cdot \frac{1.75 \text{ } kg}{1 \text{ } battery} = 108.50 \text{ kg}$$

5.5.4 Batteries data summary

Concept	SAFT 2758	Super B 7800	Super B 10P
Nominal voltage (V)	24	13.2	13.2
Rated capacity (Ah)	23	7.8	10
Maximum weight (kg)	25.5	1.3	1.75
Storable energy (kJ)	2000	370.66	475.2
Number of batteries needed	15	79	62
Total weight (kg)	382.5	102.7	108.5

Table 5. 1 Batteries data summary

5.6   Batteries and saving costs

We are going to relate the weight added by the batteries and try to compensate it by taking off a certain number of passengers [44] (baggage per person included).

5.6.1   Using SAFT 2758 batteries

$$382.5 \text{ } kg \text{ of batteries} \cdot \frac{1 \text{ } passanger}{90 \text{ } kg} = 5 \text{ } passengers \tag{5.16}$$

If we now consider a standard price of 90€ for a ticket per passenger, a cost will be obtained for carrying those batteries.

$$5 \text{ } pax. \cdot \frac{90€}{1 \text{ } pax.} = 450 € \tag{5.17}$$

Comparing the cost per taxi obtained with fuel consumption, we can see that this type of batteries cannot be used since no profit is obtained.

Cost using fuel: 367.16 €/taxi
Cost using SAFT 2758 batteries: 450 €/taxi

5.6.2   Using Super B 7800 batteries

We are going to do the same analysis [44] as the previous section.

$$102.7\ Kg\ \cdot \frac{1\ passanger}{90\ Kg} = 2\ passengers \qquad 2\ pax. \frac{90€}{1\ pax.} = 180\ €$$

In this case we can see that the cost per taxi using this type of batteries is lower than using fuel.

Cost using fuel: 367.16€/taxi
Cost using Super B 7800 batteries: 180 €/taxi

If we know the initial cost of each battery and the number of batteries that we need [49], comparing it with the cost using fuel, we can calculate the number of flights that will take us in order to recoup this inversion.

$$profit\ = 2 \cdot (367.16 - 180) = 374.32\ €/flight \tag{5.18}$$

$$initial\ cost = 79 \cdot 474.81\ = 37,509.99€ \tag{5.19}$$

$$number\ of\ flights\ to\ recoup\ = \frac{37,509.99}{374.32} = 101 \tag{5.20}$$

5.6.3   Using Super B 10P batteries

Repeating the same analysis [44] for this new type of batteries:

$$108.5\ Kg\ \cdot \frac{1\ passanger}{90\ Kg} = 2\ passengers \qquad 2\ pax. \frac{90€}{1\ pax.} = 180\ €$$

We obtain the same number of passengers as the previous section; therefore the cost per taxi using this type of batteries is also lower than using fuel.

Cost using fuel: 367.16 €/taxi
Cost using Super B 10 P batteries: 180 €/taxi

As it was calculated before [50]:

$$profit\ = 2 \cdot (367.16 - 180) = 374.32\ €/flight$$

$$initial\ cost = 62 \cdot 593.81\ = 36,816.22€$$

$$number\ of\ flights\ to\ recoup\ =\ \frac{36,816.22}{374.32} = 99$$

Finally, we have to notice that those cost values and recouping only include the battery price. It also should be taken into account the RAT, structural modifications, maintenance, design and other costs, which are not included in this analysis.

5.6.5 Batteries selection summary

Concept	
5.6.1 SAFT 2758	
5.6.2 Super B 7800	
5.6.3 Super B 10 P	

Table 5. 2 Batteries selection summary

Colour code:

	Accepted options		Discarded options

In conclusion for this summary, the Super B 10 P batteries have been selected despite its higher initial cost because the number of flights to recoup this cost is the lowest since this type of batteries permit obtaining a greater profit per flight. This profit per flight will be positive for the airline after 99 flights because the initial cost of the system will be already assumed and the airline will obtain approximately 374.32 € of benefit per flight.

Other types of energy storage methods, like flywheels or hydrogen batteries could be considered to be implemented so as to reduce the extra weight added by the batteries or obtaining greater energy values. Anyhow, using regular batteries we obtain a positive conclusion for this system and we let this point for further studies.

CHAPTER 6. CONCLUSIONS

The Bachelor Thesis carried out in these 4 months, intends to be an entrepreneur essay, which shows the knowledge acquired during the last three years. The innovative idea implements extra Ram Air Turbines in A320. Once implemented, the air generators may obtain enough energy to taxi electrically and replace the actual taxiing propulsion method.

From our point of view, the environmentally friendly world could be improved in aeronautics. It could be accomplished by the addition of modifications into the aircrafts using systems that already exist with relatively low cost. RAT system reduces the fuel waste and leads to a decrement of emissions and can therefore provide a more efficient engine use. Despite these advantages, batteries used by the system are highly contaminant so precautionary measures need to be upheld.

Furthermore, security measures on the ground have to be considered as well, so RAT can damage airport personnel on its way out during maintenance routines. Therefore, regulations have to be overhauled. Moreover, regular operation procedures must be modified in order to supply RAT operational information to the pilots.

The main conclusion of our entire project has been the best position for locating the proposed system is the belly-fairing. Through simulations made by using CFD (Computational Fluid Dynamics) helpful results have been carried out. The combination of those results plus momentums and drag analysis lead to this selection. In addition, the energetic study put into practice demonstrated the reasonable viability of this system in commercial aeronautics.

Some aspects were not taken into account when the analysis has been done. The authors of this thesis consider that it would be convenient as a detailed study, if a future extension of this investigation would be considered. An example could be the effect of the friction while taxiing in the energetic balance calculated in chapter 5. Also in this chapter, another example would be the extra consumption of fuel that the aircrafts needs on its way to the runway. Students considered the efficiency of the generator that provides energy to the batteries as 40%. Shall be said that it could be lower, then, other type of batteries or energy storage systems may be found, offering higher performances.

As said in the previous paragraph, the solution we cope with, is not definitive. Posterior studies should be done in many specific topics of the system e.g. the concrete electric generator needs, the correct placement of batteries, the specific procedures when approaching or security limitations.

CHAPTER 7.   BIBLIOGRAPHY

[1] http://www.airbus.com/aircraftfamilies/passengeraircraft/a320family/a320/

[2] http://www.airbus.com/aircraftfamilies/passengeraircraft/a320family/a320/ specifications/

[3] Oñate, A.E., "APU y Turbina de aire de impacto", Chap. 41 in *Conocimientos del avión*, Thomson Paraninfo, 4th Ed., pp. 1006-1009, Madrid (2003)

[4] F. Gato, "Generación de suministro de emergencia", Chap. 11.6 in *Sistemas de Aeronaves de Turbina II*, Ed. Club Universitario, 1rst Ed., pp. 58-62. Alicante (2010)

[5] United States Patent. Number 4,578,019. Date of Patent: Mar. 25, 1986.

[6] Hamilton Sundstrand. Electric Systems PowerPoint presentation.

[7] http://www.tc.gc.ca/eng/civilaviation/standards/commerce-manuals-singlecrewsop-chapter3-section5-1996.htm

[8] http://www.oaklandairport.com/masterplan_oak/pdf/masterplan/march2006/chapters/chapter_5.pdf

[9] H. Khadilkar and H. Balakrishan, "Estimation of aircraft taxi-out fuel burn using flight data recorder archives", *Massachusetts Institute of Technology*, 2010.

[10] http://www.aena.es/csee/Satellite/navegacionaerea/es/Page/1078418725163/?other=1083158950596&other2=1083857757906&other3=1096014689955#ancla373

[11] http://www.aena.es/csee/Satellite/navegacionaerea/es/Page/1078418725163/?other=1083158950596&other2=1083857757906#ancla37

[12] http://www.smartcockpit.com/pdf/flightops/flyingtechnique/2

[13] A. Brookes, "Vulcan units of the cold war", *Osprey Combat Aircraft*. No.72, 2009.

[14] F-4 PHANTOM II Pilot's Flight Operating Instructions. Originally Published by the U.S. Navy. Reprinted by PeriscopeFilm.com

[15] I. Moir and A. Seabridge, "Emergency Power Sources", Chap. 8.4 in *Aircraft systems: mechanical, electrical, and avionics subsystems integration*, Ed. Wiley. 3rd Edition, pp. 203, Chichester (2008)

[16] http://www.atraircraft.com/media/downloads/fuelsaving2011_1.pdf

[17] D. Galíndez, "Planificación", Cap.1 in *Aeropuertos modernos. Ingeniería y certificación*. Instituto Politécnico Nacional-Aeropuertos y Servicios Auxiliares, pp. 3-89, Mexico (2006)

[18] J. Martínez, "Fuentes eléctricas de la aeronave", Chap. 1 in *Sistemas eléctricos y electrónicos de las aeronaves*, Thomson Paraninfo, 1rst Edition, pp. 4-18, Madrid (2007)

[19] SAFT batteries technical notes. TN6 Rev0, pp. 1 (2008)

[20] PFC, D. Ugena González, "Desarrollo de un almacenador cinético de energía", Universidad Carlos III, Madrid (2008)

[21] L.Thaller and A.Zimmerman, "Overview of Nickel-Hydrogen Cell Technology", Chap.1 in N*ickel-Hydrogen Life Cycle Testing: Review and Analysis*, AIAA Press (2003)

[22] A. Zimmerman, "Fundamental Principles", Chap. 2 in *Nickel-Hydrogen Batteries: Principles and Practice*, AIAA Press (2009)

[23] Turbulence. An introduction for scientists and engineers. P.A. Davidson. Ed. Oxford. 2007. Page 52.

[24] Avila, K.; D. Moxey, A. de Lozar, M. Avila, D. Barkley, B. Hof, "The Onset of Turbulence in Pipe Flow". Science 333 (6039), pp. 192–196, 2011.

[25] http://www.faqs.org/patents/app/20100158698

[26] http://winds-energy.blogspot.com.es/

[27] Hamilton Sundstrand. Dossier resource de la RAT. A320.

[28] AD No.: 2006-0135. 22 May 2006. Flight Tests

[29] Airbus A318/A319/A320/A321 Flight Crew Training Manual.

[30] L.J. Vermeer, J.N. Sørensen and A. Crespo, "Study of wind turbine wake aerodynamics", *Progress in Aerospace Sciences*, Ed. Pergamon (2003)

[31] Airbus A319/A320/A321 Flight deck and systems briefing for pilots.

[32] Airbus A319/A320/A321 Ground operations manual. 2002.

[33] http://www.thesameinnovation.com/Publi/Fichier/Airbus_embedded_system

[34] http://www.airspacemag.com/flight-today/HTW-evacuation.html#

[35] Airbus A320 Landing Gear. Project Report from Hogeschool van Amsterdam, AIT. 2007/2008

[36] PFC, J. Martínex Chapín, "Estudio de la ampliación del campo de vuelos del aeropuerto de Girona en el máximo horizonte previsto en su plan director", Universitat Politècnica de Catalunya (2012)

[37] http://www.smartcockpit.com/data/pdfs/flightops/flyingtechnique/Avoiding_ Tailstrikes_by_Airbus.pdf

[38] http://www.aerosquare.com/en/Airbus-A320/Page-2.html

[39] http://www.smartcockpit.com/data/pdfs/flightops/flyingtechnique/Avoiding_ Tailstrikes_by_Airbus.pdf

[40] A. A. Wahab and M.Hafiz Ismail, "Estimating Vertical Drag on Helicopter Fuselage during Hovering", Universiti Teknologi Malaysia (2006)

[41] C. Beller, "Energy Output Estimation for a Small Wind Turbine Positioned on a Rooftop in the Urban Environment with and without a Duct", Risø DTU (2011)

[42] TFC, "Influencia de la carga y centrado sobre el consume final en A320", Marc Julbe Poca, Universitat Politècnica de Catalunya (2009)

[43] TOPCAT User manual. Take-Off and Landing Performance Calculation Tool.

[44] Air Space Management notes. EETAC. Professor Maria Huerta (2011)

[45] http://office.microsoft.com/es-es/excel/

[46] http://www.iata.org/whatwedo/economics/fuel_monitor/Pages/index.aspx

[47] M. J. Zolidis, "Emergency Airplane RATs", Hamilton Sundstrand. (2006)

[48] SAFT F6177. Component Maintenance Manual With Illustrated Parts List. Aircraft Battery. P/N 2758. Oct. 01/87.

[49] http://www.super-b.com/products/super-B-7800-%252d-Aircraft.html

[50] http://www.super-b.com/products/super-B-10P-%252d-Aircraft.html

ANNEXOS

ANNEX A – TAXI DISTANCES

A.1 Barcelona-El Prat airport

Fig. A. 1 Example of taxi in order to calculate the typical distance in Barcelona-El Prat airport

A.2 Madrid-Barajas airport

Fig. A. 2 Example of taxi in order to calculate the typical distance in Madrid-Barajas airport

ANNEX B – NACA 4412 AND 0009 GRAPHICS

B.1 NACA 4412. Coefficient obtaining at 7,000 ft
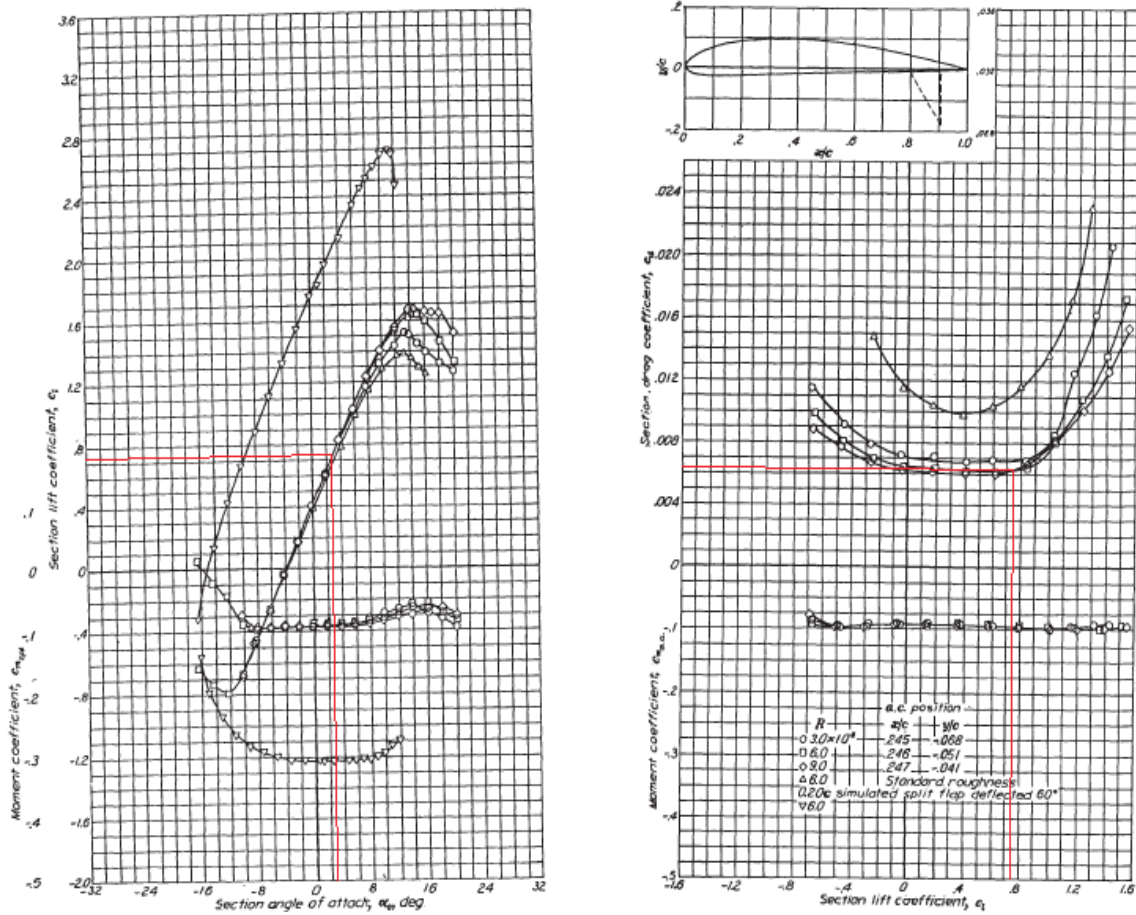
Fig. B. 1 Lift and drag coefficients. NACA 4412. 7000 ft

B.2 NACA 4412. Coefficient obtaining at sea level
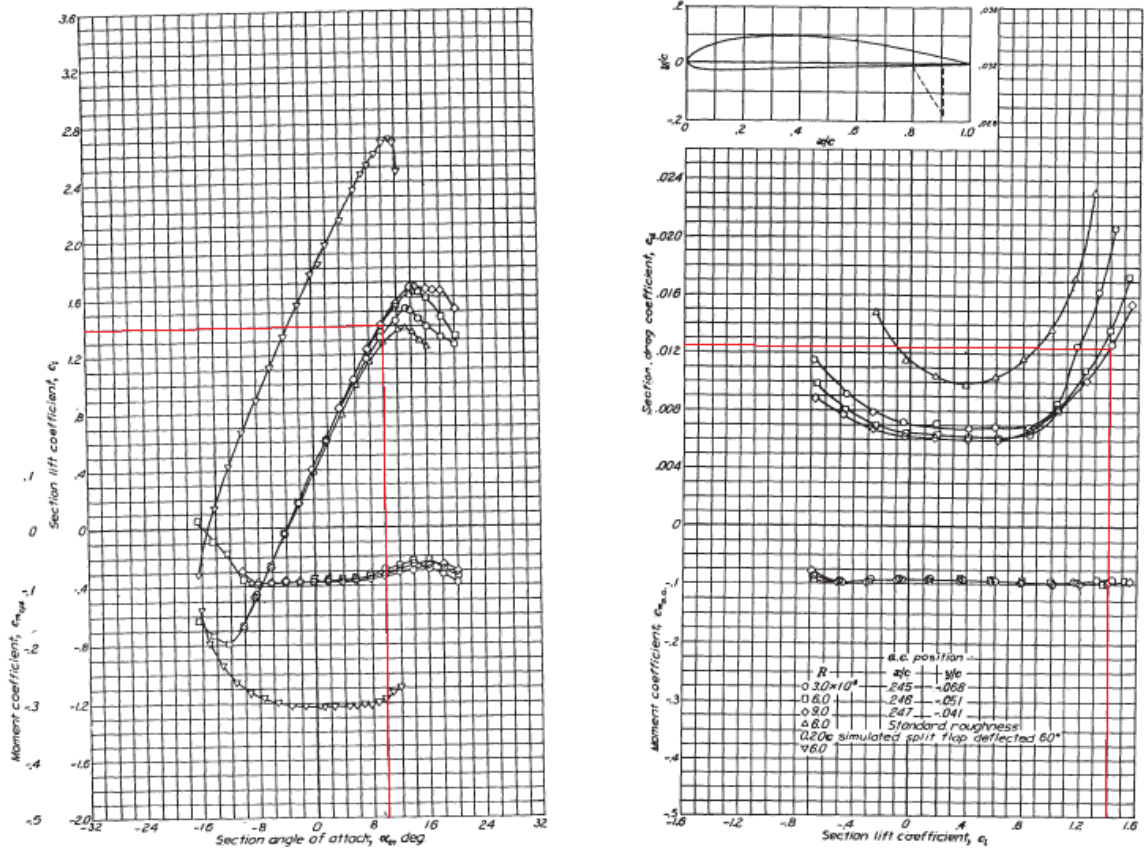
Fig. B. 2 Lift and drag coefficients. NACA 4412. Sea level

B.3 NACA 0009. Coefficient obtaining at 7,000 ft
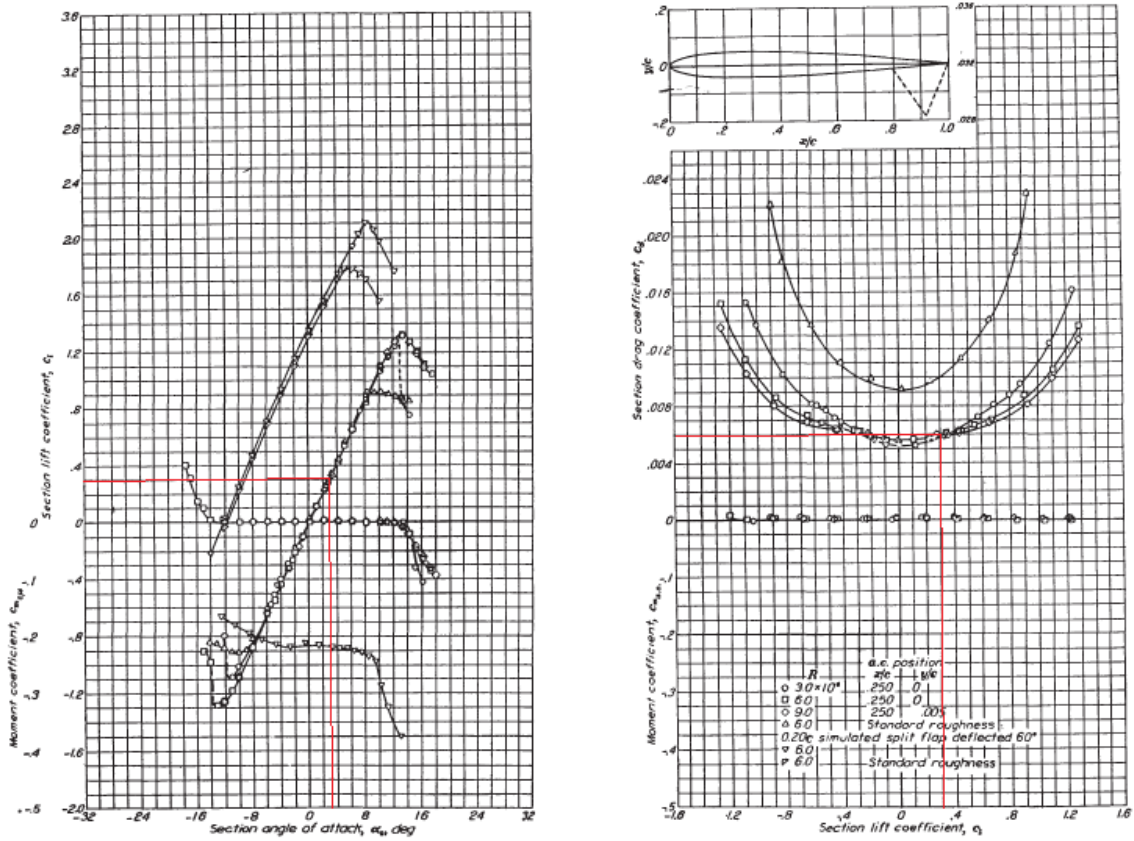
Fig. B. 3 Lift and drag coefficients. NACA 0009. 7000 ft

B.4 NACA 0009. Coefficient obtaining at 7,000 ft
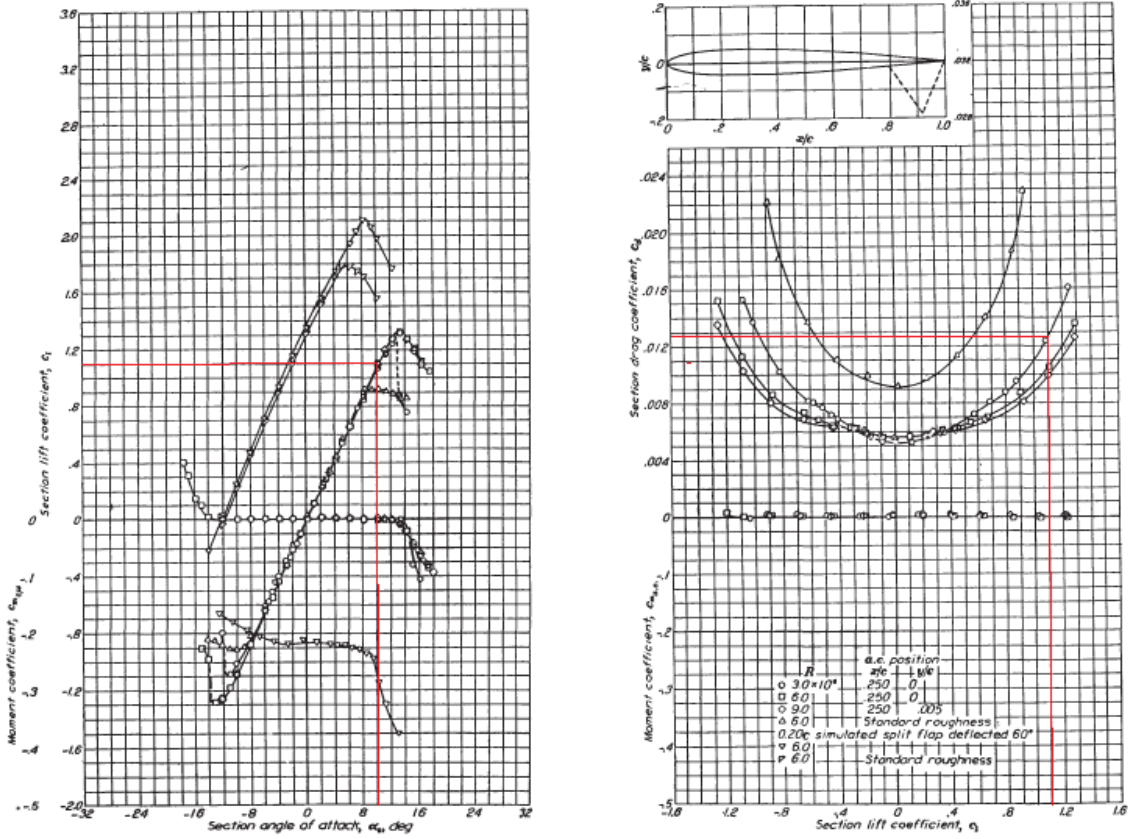
Fig. B. 4 Lift and drag coefficients. NACA 0009. Sea level

ANNEX C – RAT LOCATION SKETCHES

C.1 Tail

It must be taken into account that all sketches are dimensioned into a scale 1:32.
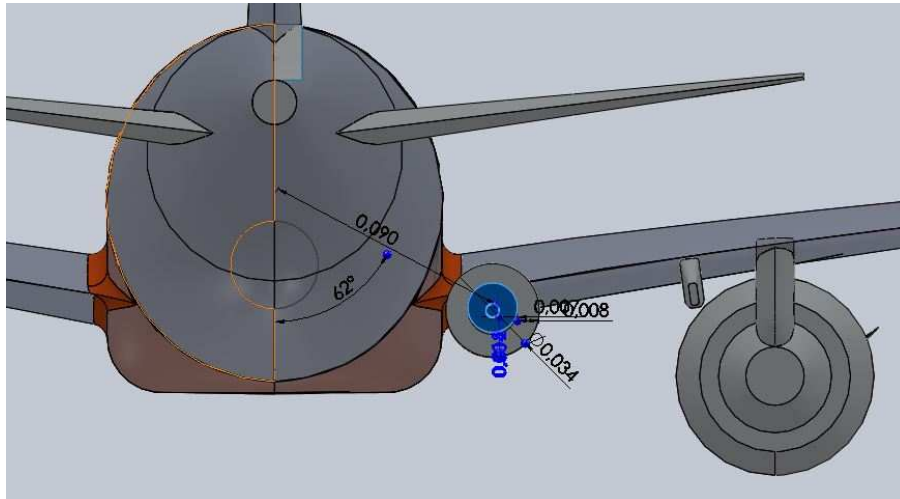
Fig. C. 1 RAT dimensions and location in the tail
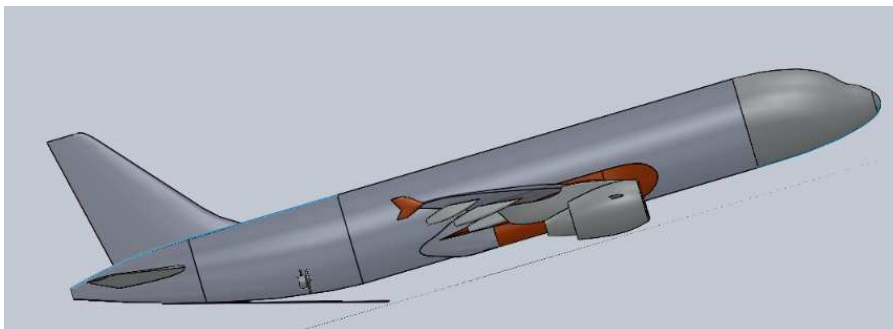
Fig. C. 2 We make sure that the RAT location avoids geometry limitation areas
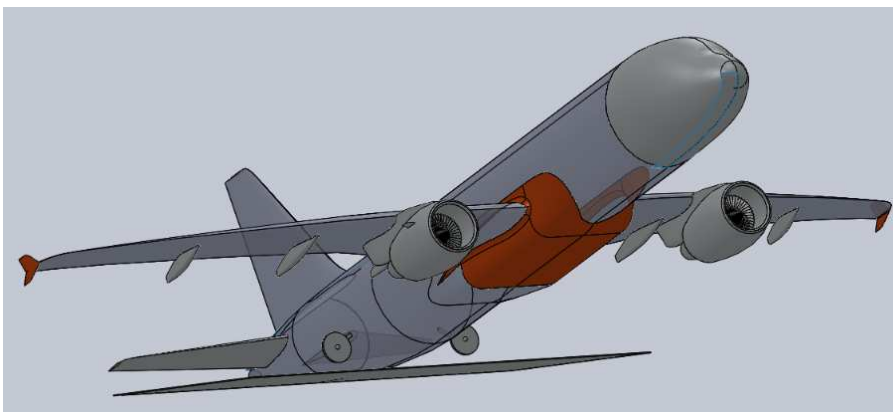
Fig. C. 3 RAT avoids the ground at limiting geometry angle of attack

C.2 Nose
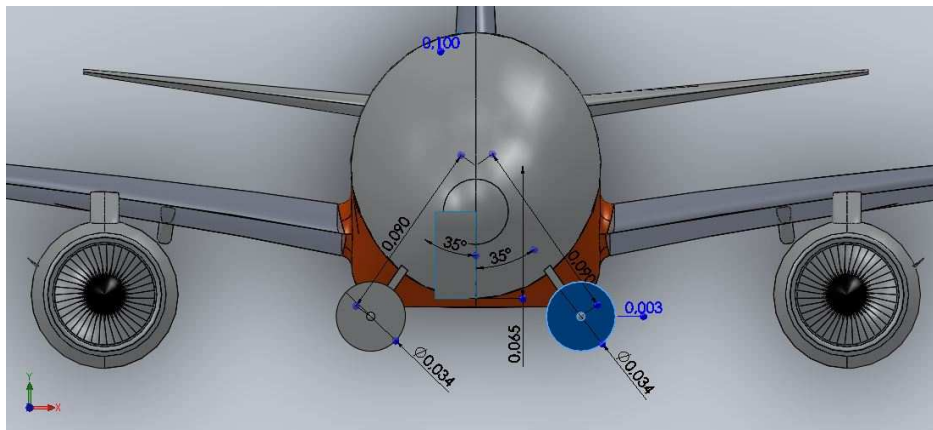
Fig. C. 4 RAT dimensions and location in the nose
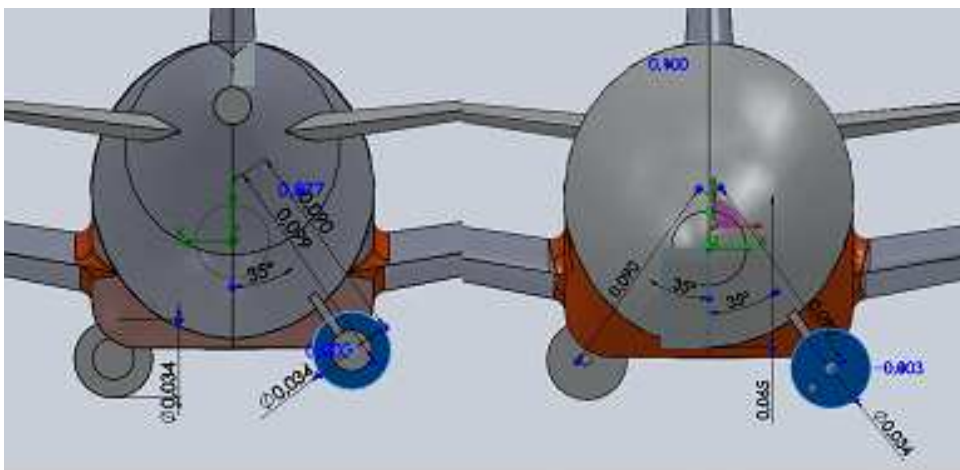
Fig. C. 5 RAT dimensions and location in the nose and tail

C.3 Belly-fairing
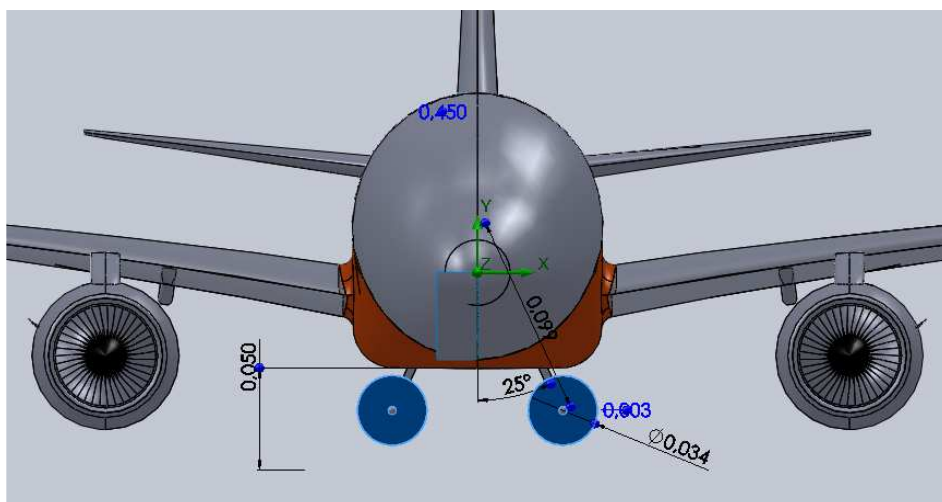
Fig. C. 6 RAT dimensions and location in the belly-fairing

ANNEX D – SIMULATIONS

D.1 RAT located on the tail. Sea Level
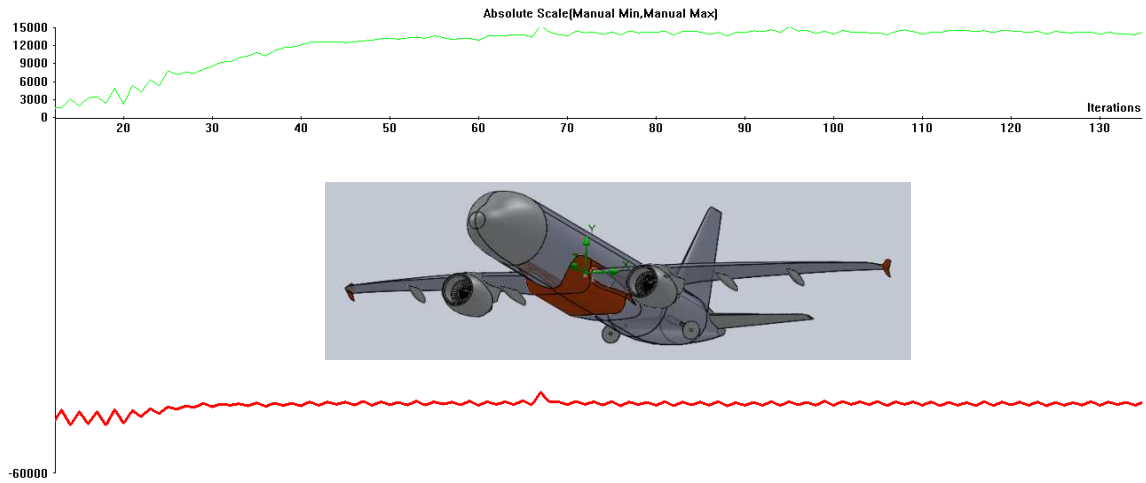
Fig. D. 1 Lift/Drag simulation with RAT in tail at sea level
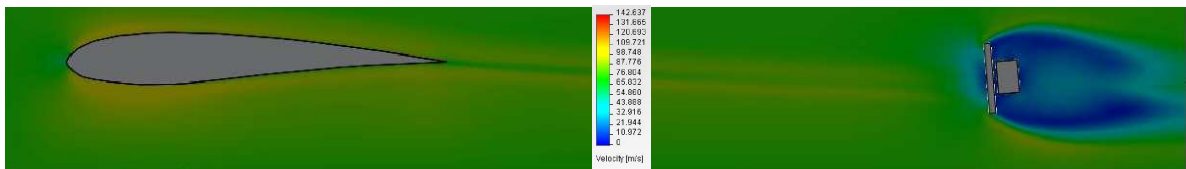
Fig. D. 2 Velocity simulation with RAT in the tail at sea level. General View
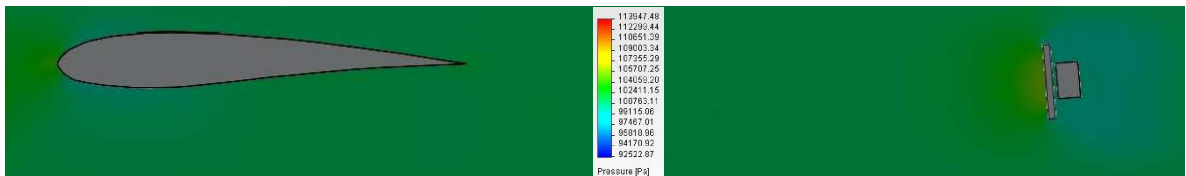
Fig. D. 3 Pressure simulation with RAT in the tail at sea level. General View
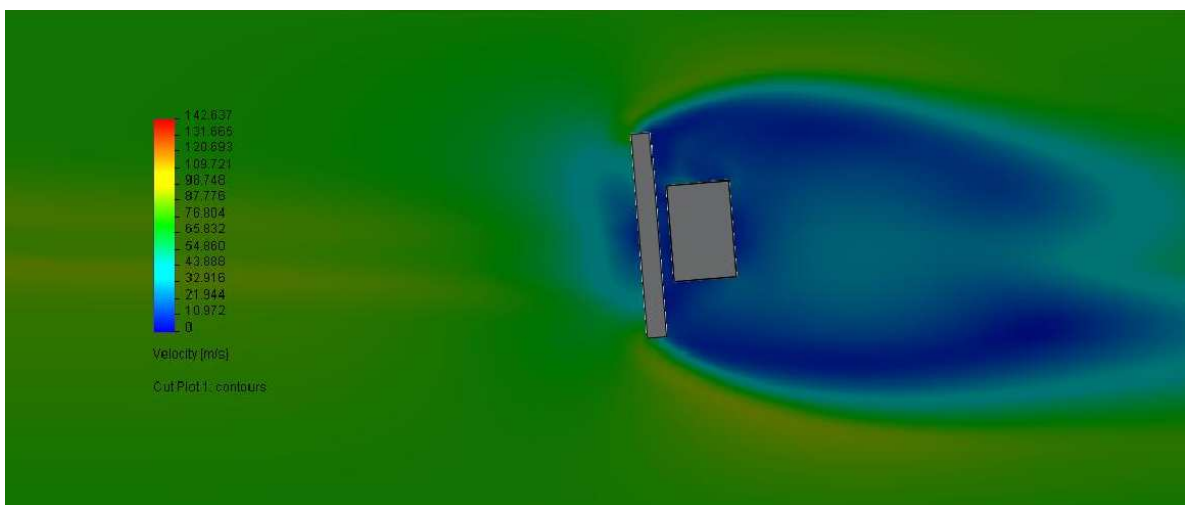
Fig. D. 4 Velocity simulation with RAT at sea level in the tail detailed
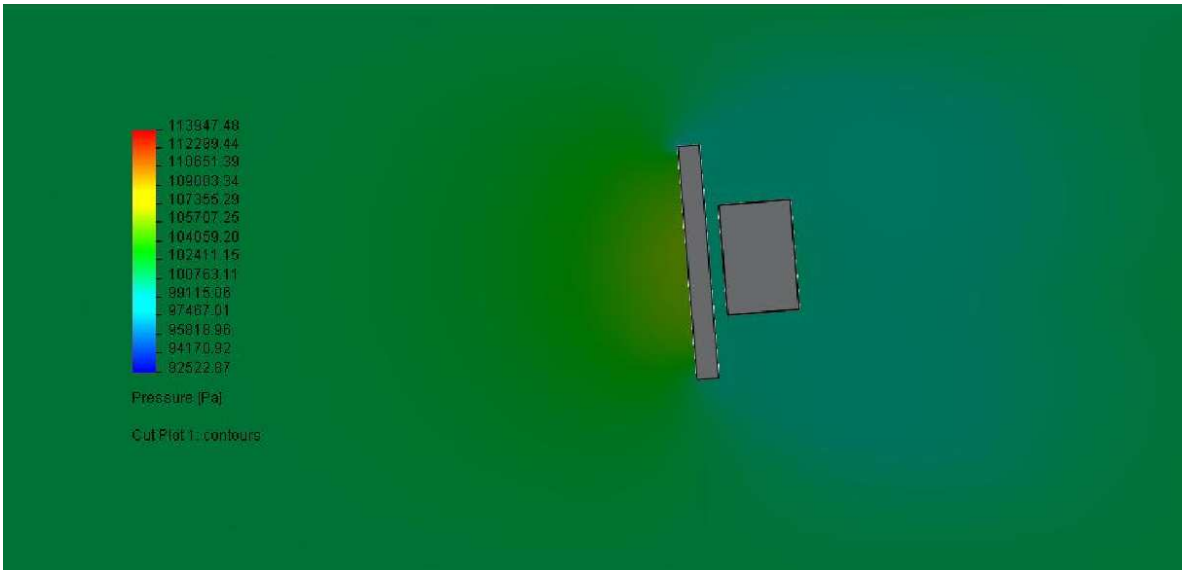
Fig. D. 5 Pressure simulation with RAT at sea level in the tail detailed

D.2 RAT located on the tail. 7,000 ft
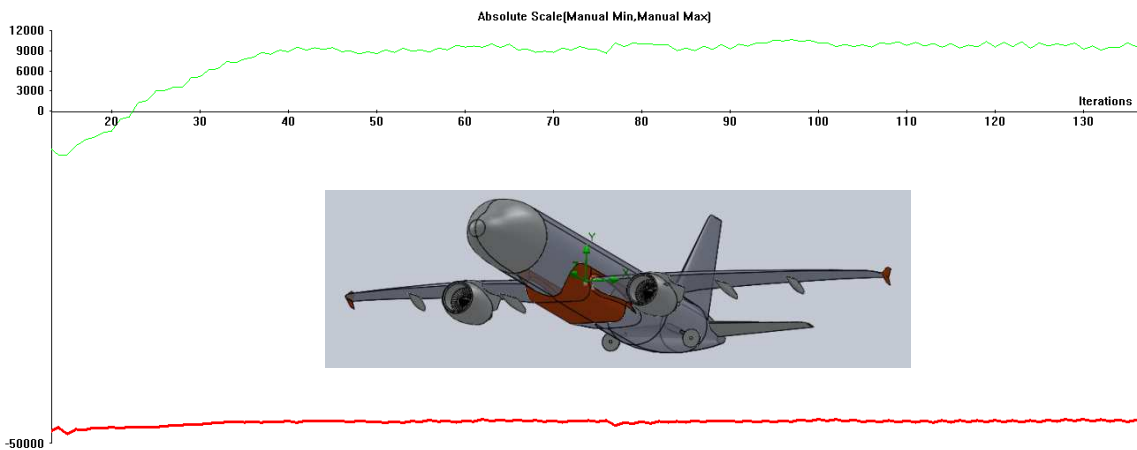
Fig. D. 6 Lift/Drag simulation with RAT in tail at 7,000 ft
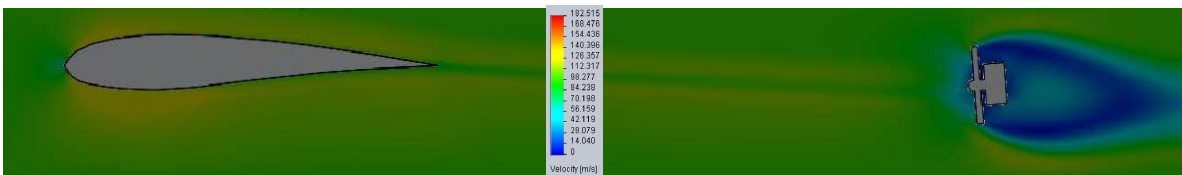
Fig. D. 7 Velocity simulation with RAT in the tail at 7,000 ft. General View
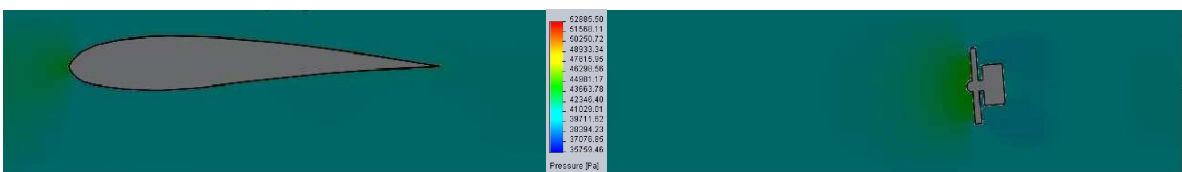
Fig. D. 8 Pressure simulation with RAT in the tail at 7,000 ft. General View
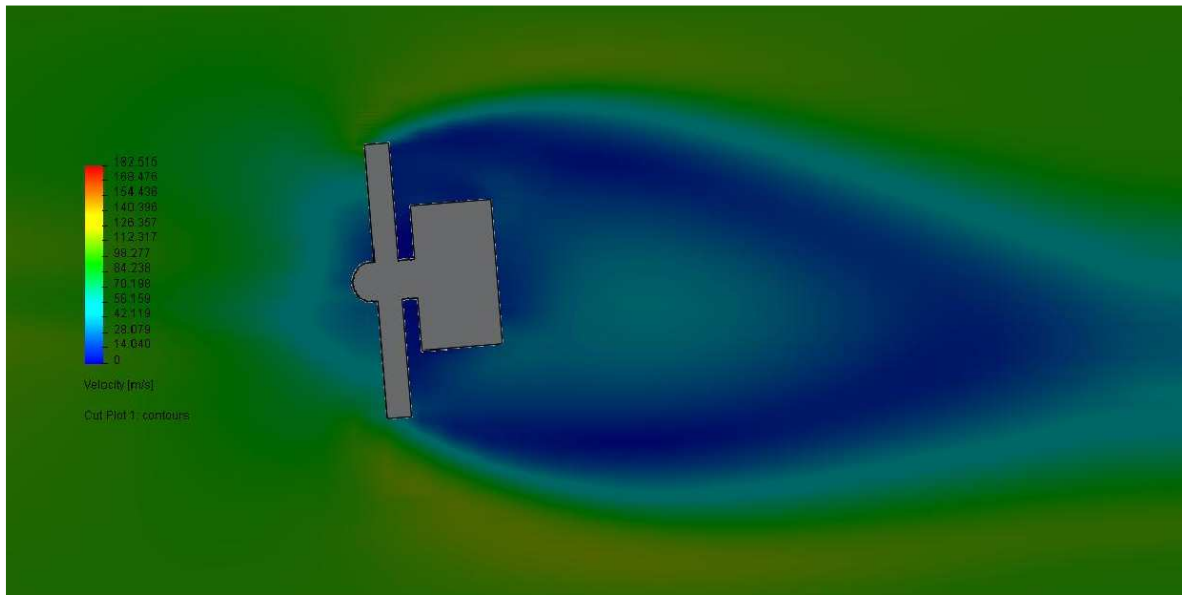
Fig. D. 9 Velocity simulation with RAT at 7,000 ft in the tail detailed
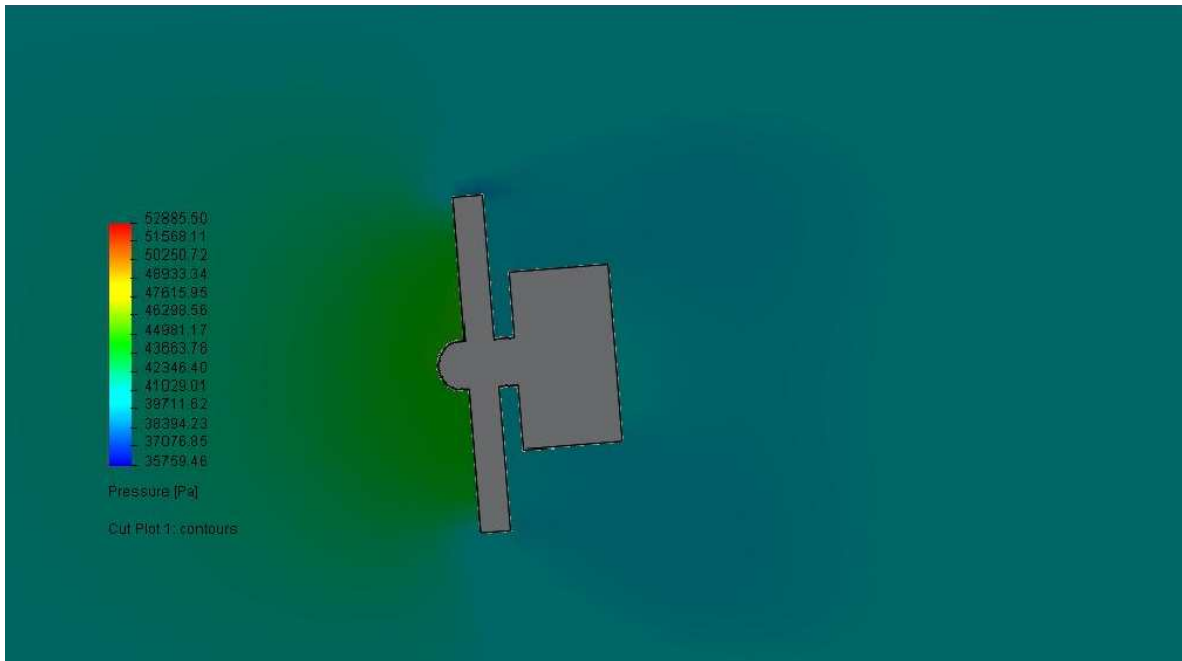
Fig. D. 10 Pressure simulation with RAT at 7,000 ft in the tail detailed

D.3 RAT located on the tail. Sea level with full flaps
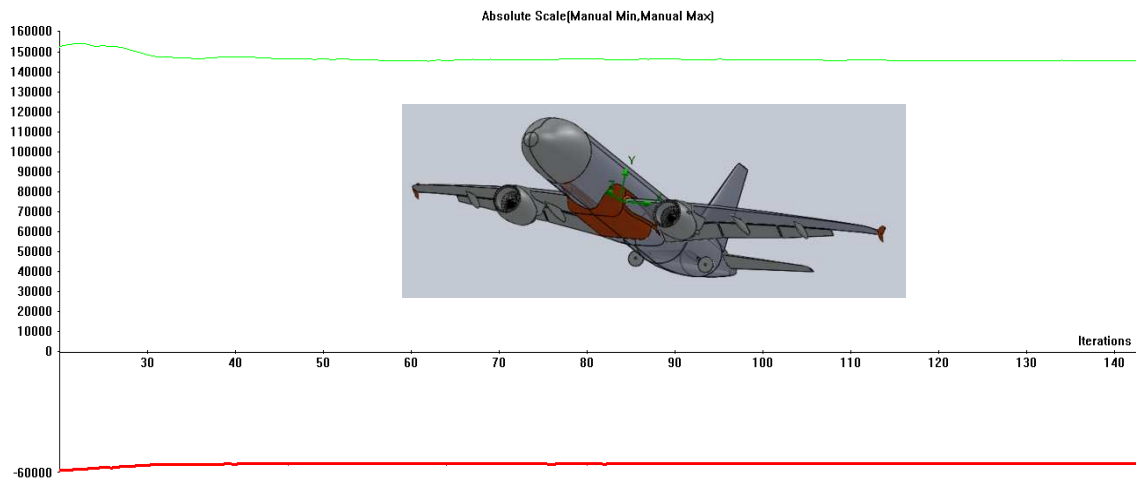
Fig. D. 11 Lift/Drag simulation with RAT in the tail at sea level with full flaps
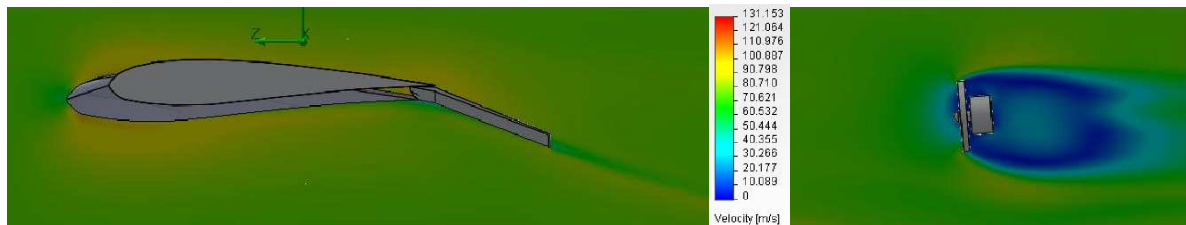
Fig. D. 12 Velocity simulation with RAT in the tail at sea level with full flaps. General View
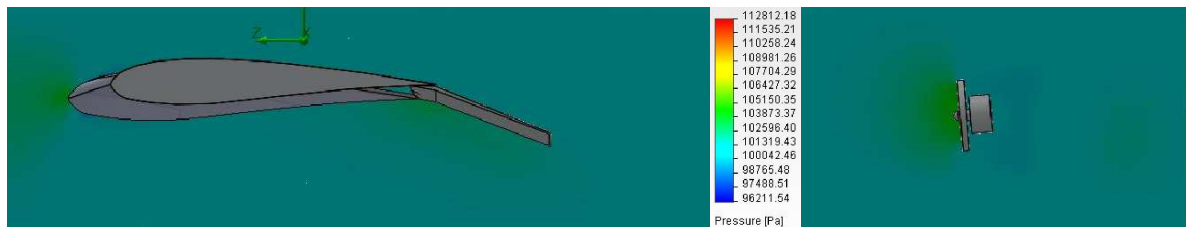
Fig. D. 13 Pressure simulation with RAT in the tail at sea level with full flaps. General View
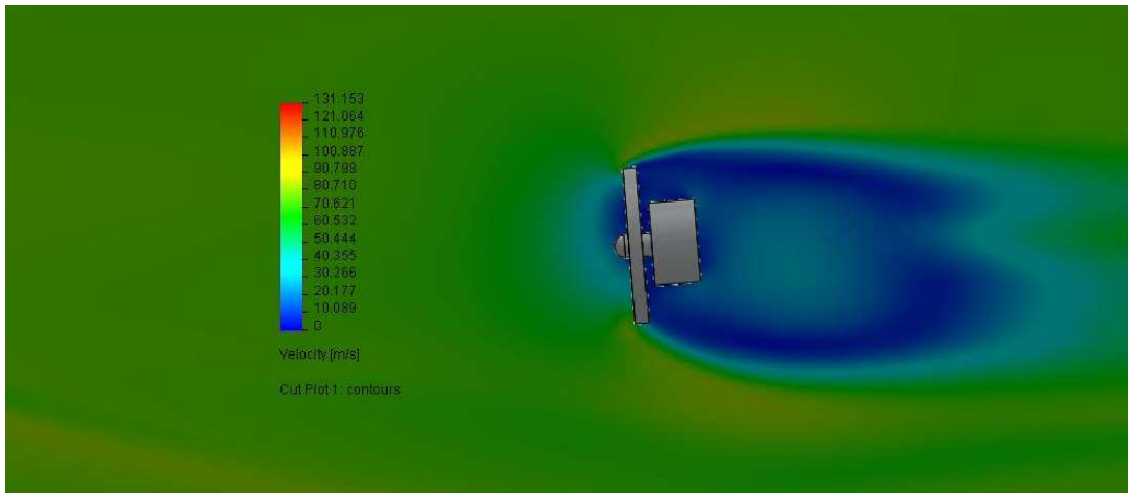
Fig. D. 14 Velocity simulation with RAT in the tail at sea level with full flaps detailed
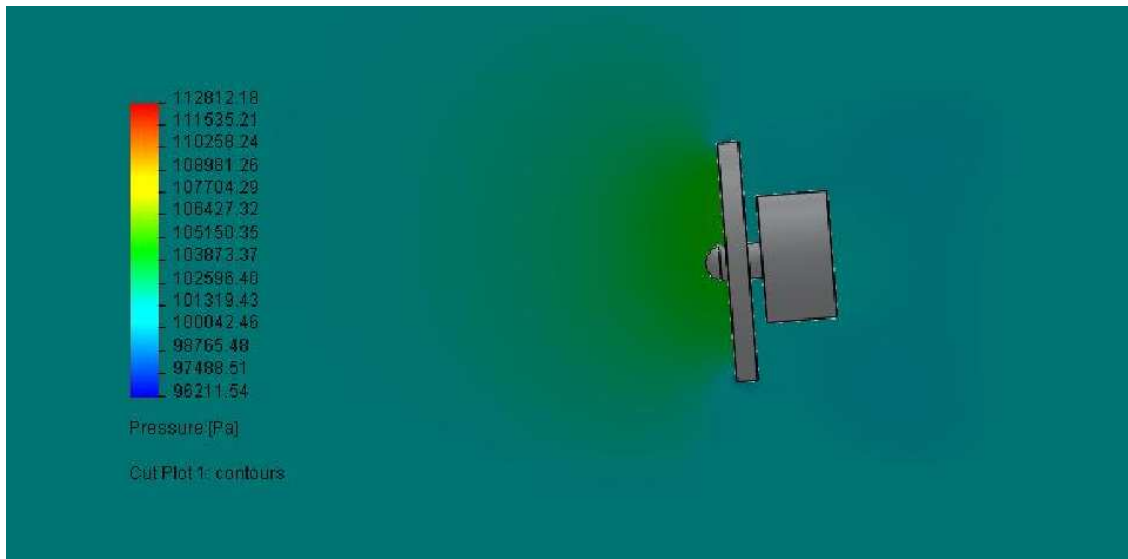
Fig. D. 15 Pressure simulation with RAT in the tail at sea level with full flaps detailed

D.4 RAT located on the nose. Sea level
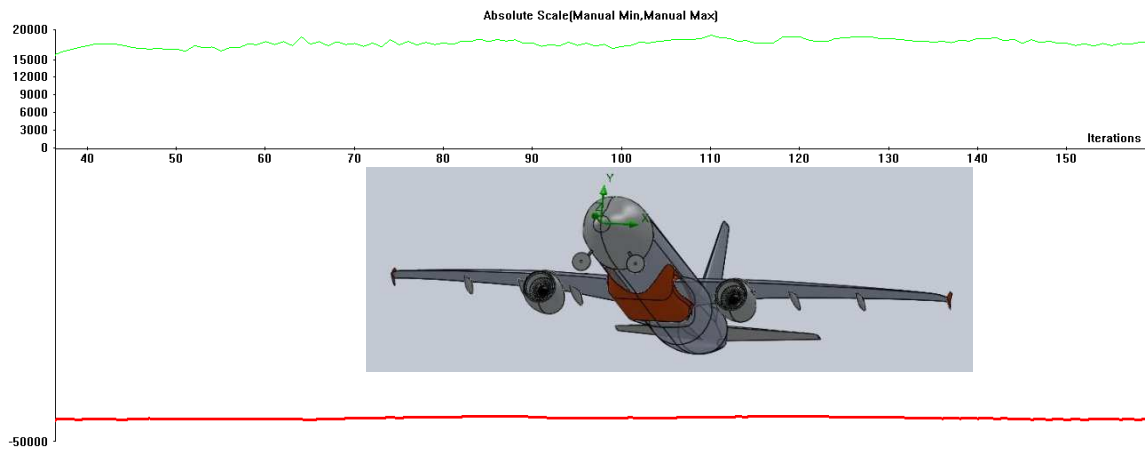
Fig. D. 16 Lift/Drag simulation with RAT in the nose at sea level
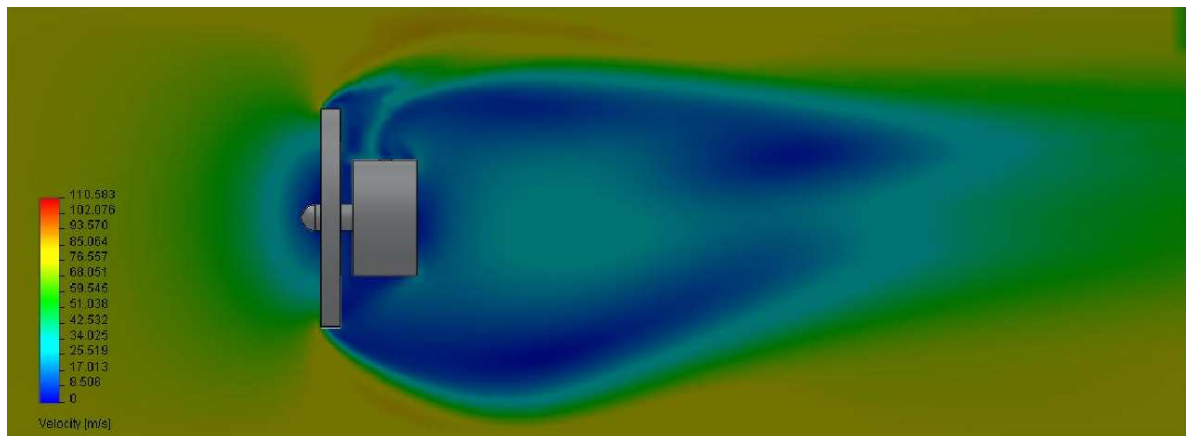
Fig. D. 17 Velocity simulation with the RAT in the nose at sea level in detail
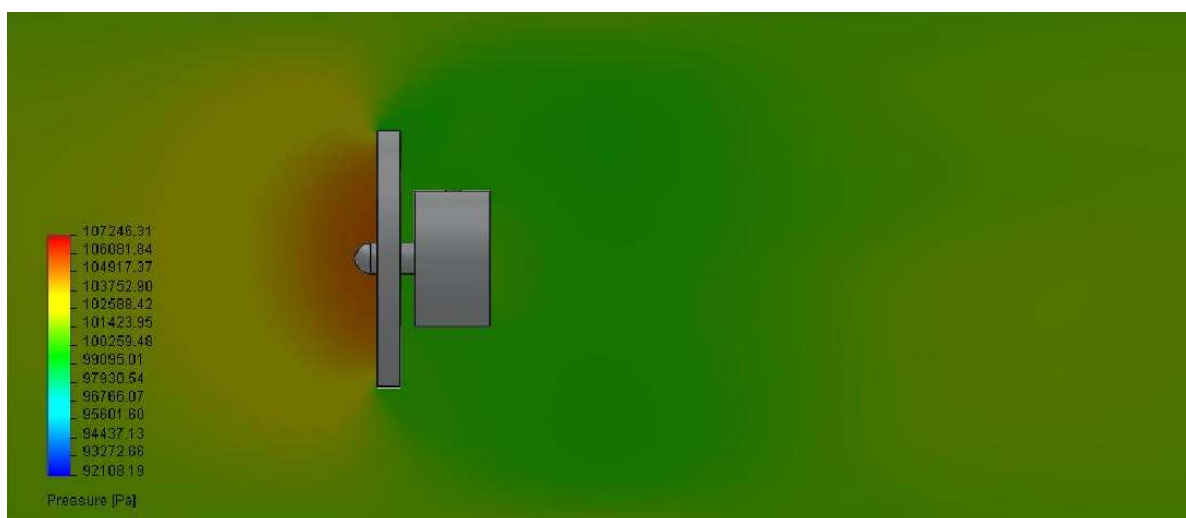
Fig. D. 18 Pressure simulation with the RAT in the nose at sea level in detail

D.5 RAT located on the nose. 7,000 ft
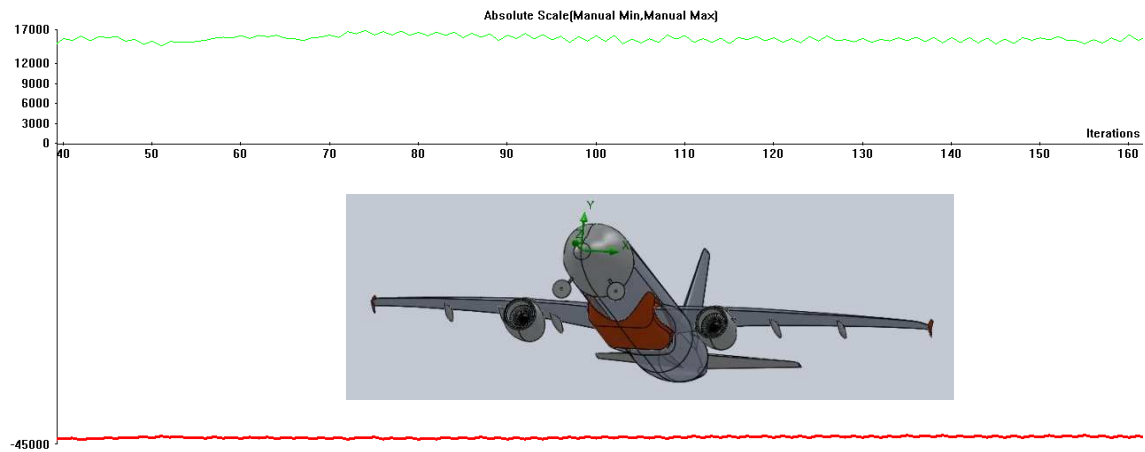
Fig. D. 19 Lift/Drag simulation with RAT in the nose at 7,000 ft
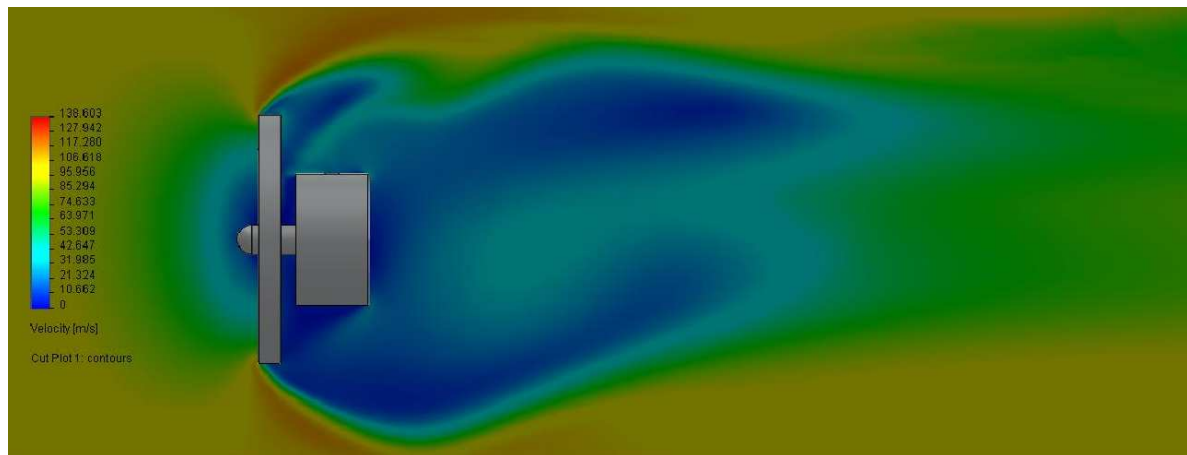
Fig. D. 20 Velocity simulation with the RAT in the nose at 7,000 ft in detail

Fig. D. 21 Pressure simulation with the RAT in the nose at 7,000 ft in detail

D.6 RAT located on the nose and tail. Sea level
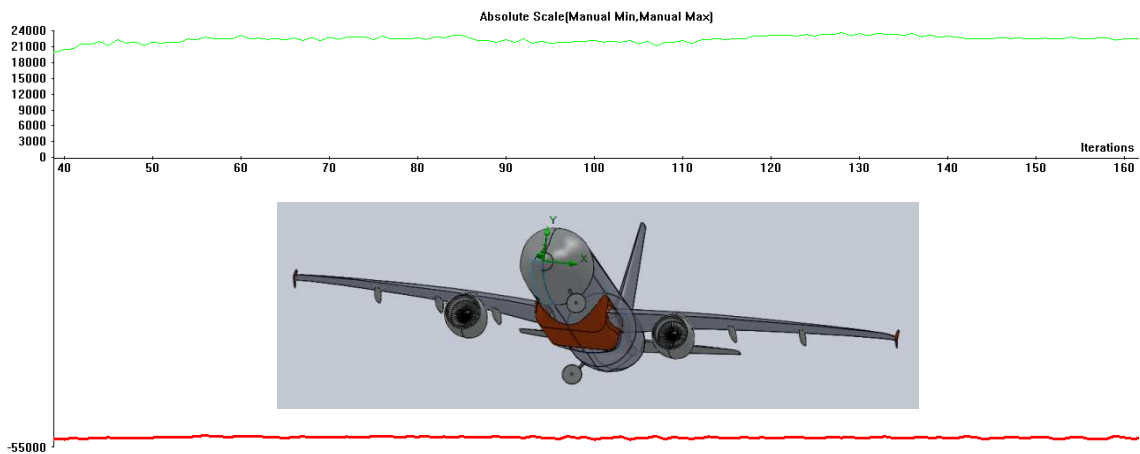
Fig. D. 22 Lift/Drag simulation with RAT in the nose and tail at sea level
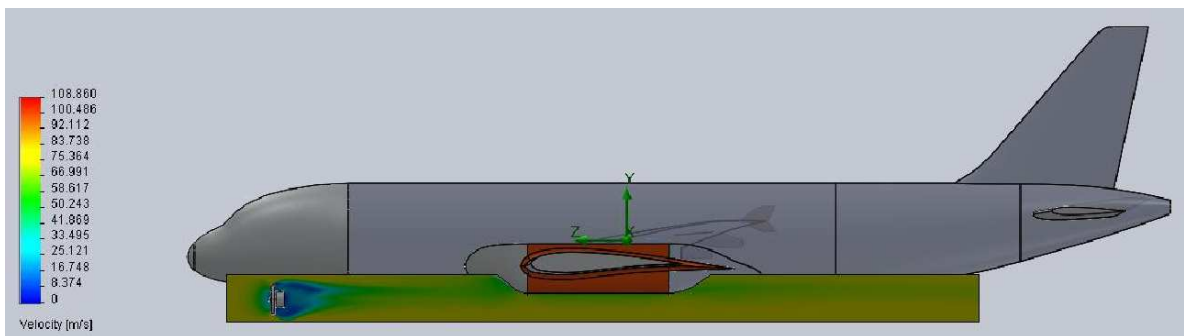
Fig. D. 23 Velocity simulation with RAT in the nose at sea level. General left side view
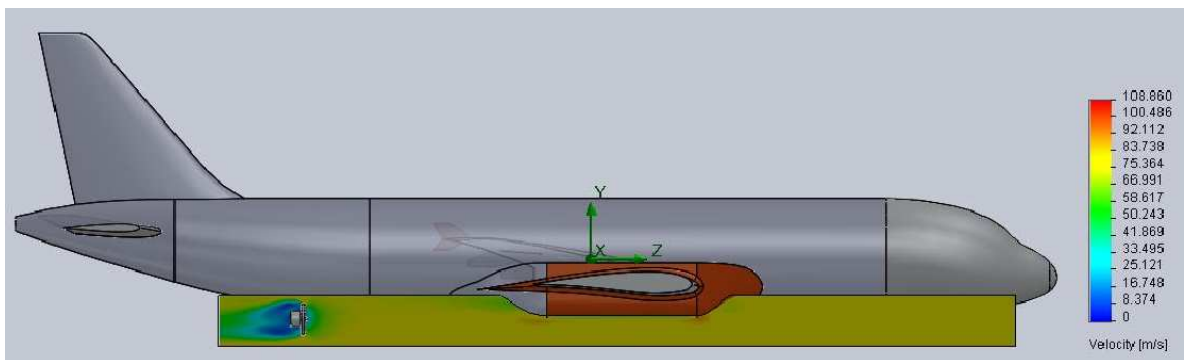
Fig. D. 24 Velocity simulation with RAT in the tail at sea level. General right side view
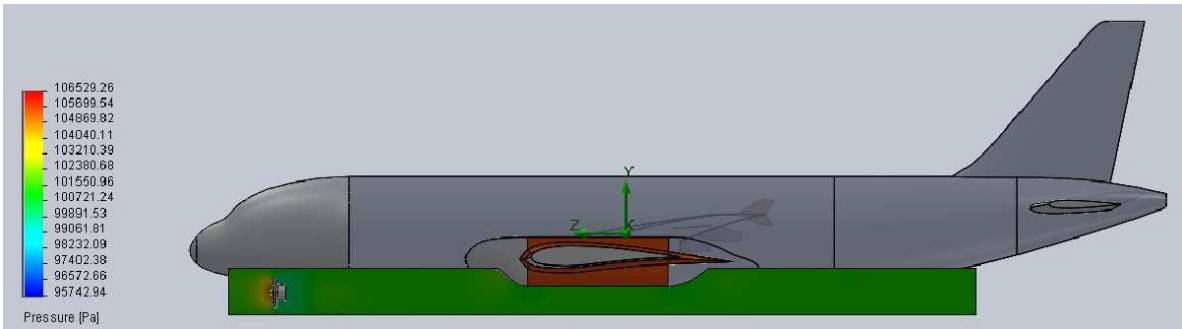
Fig. D. 25 Pressure simulation with RAT in the nose at sea level. General left side view
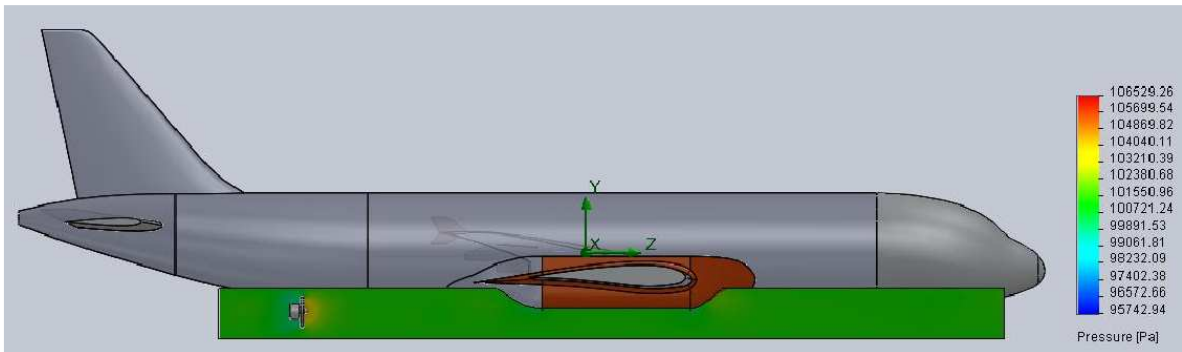
Fig. D. 26 Pressure simulation with RAT in the tail at sea level. General right side view
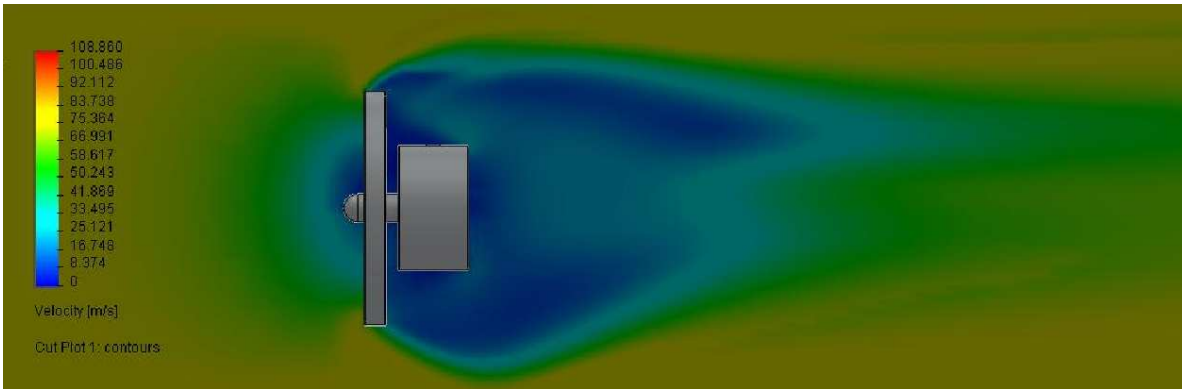
Fig. D. 27 Velocity simulation with the RAT in the nose left side at sea level in detail
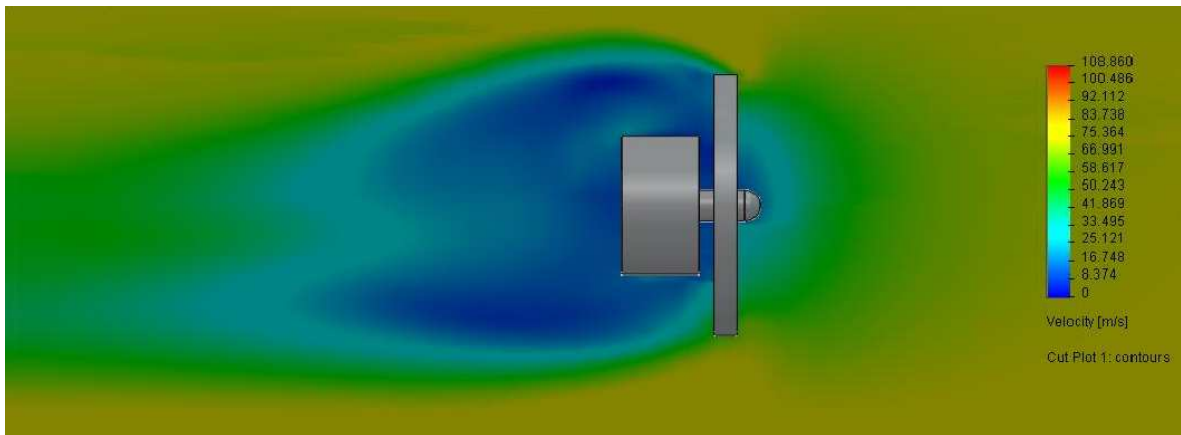
Fig. D. 28 Velocity simulation with the RAT in the tail right side at sea level in detail
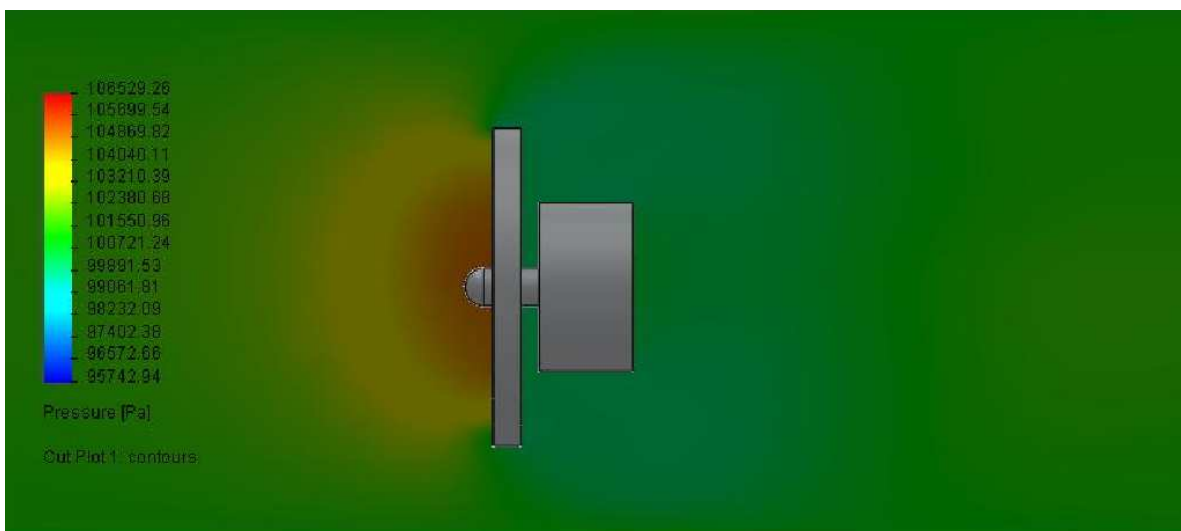
Fig. D. 29 Pressure simulation with the RAT in the nose left side at sea level in detail
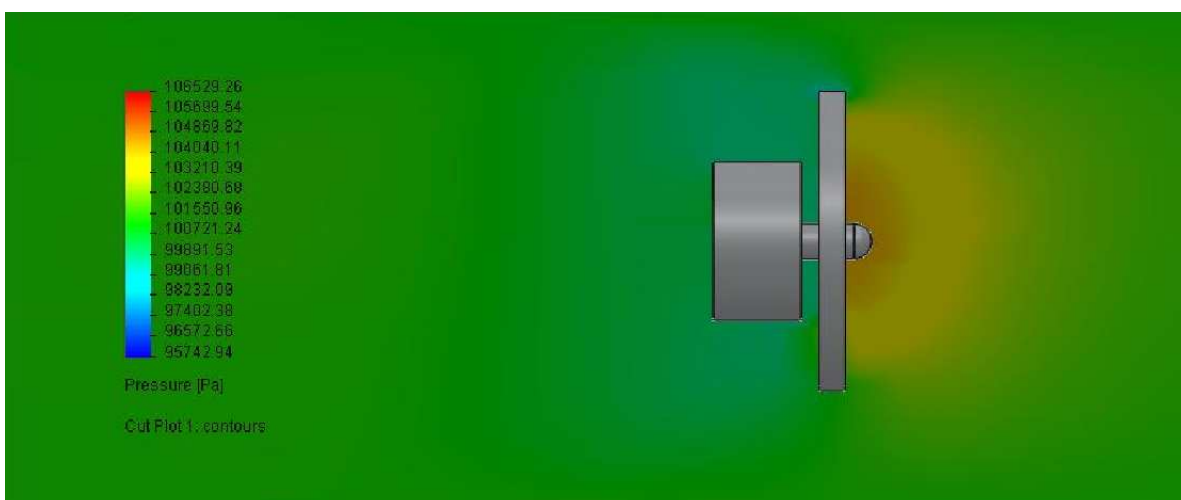
Fig. D. 30 Pressure simulation with the RAT in the tail right side at sea level in detail

D.7 RAT located on the nose and tail. 7,000 ft
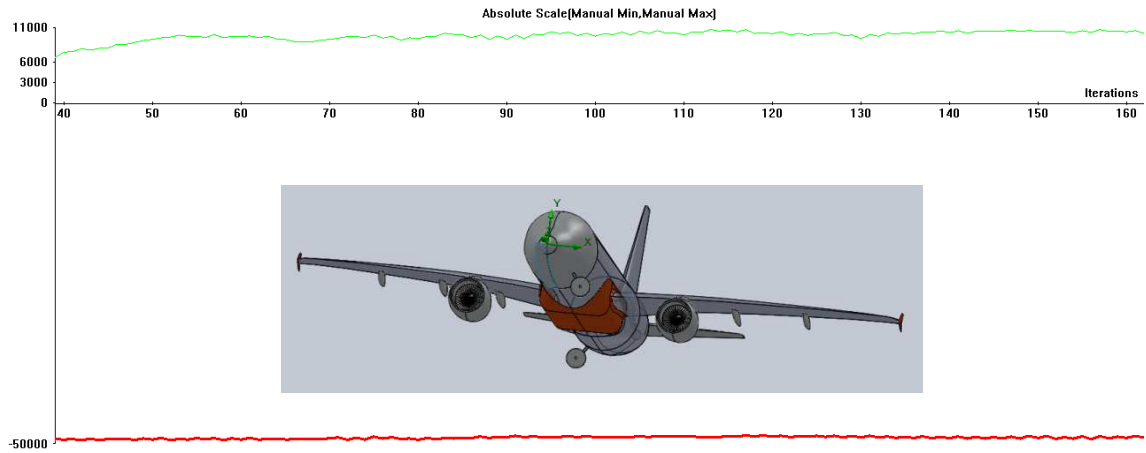
Fig. D. 31 Lift/Drag simulation with RAT in the nose and tail at 7,000 ft
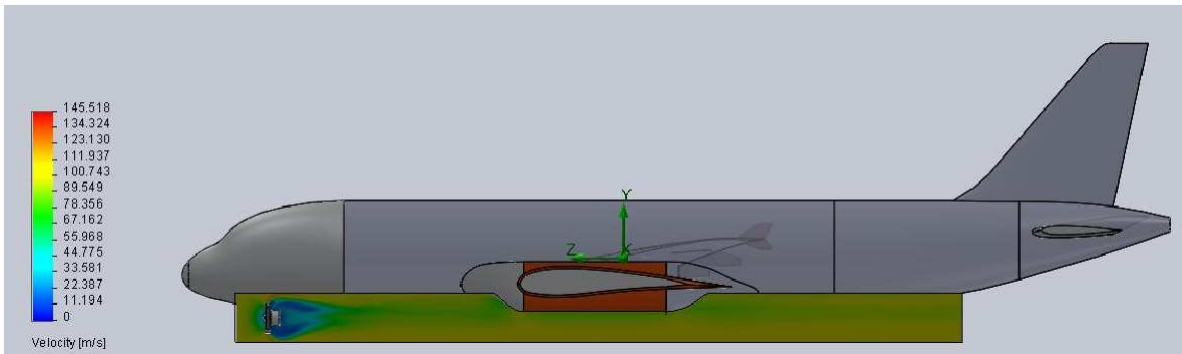
Fig. D. 32 Velocity simulation with RAT in the nose at 7,000 ft. General left side view
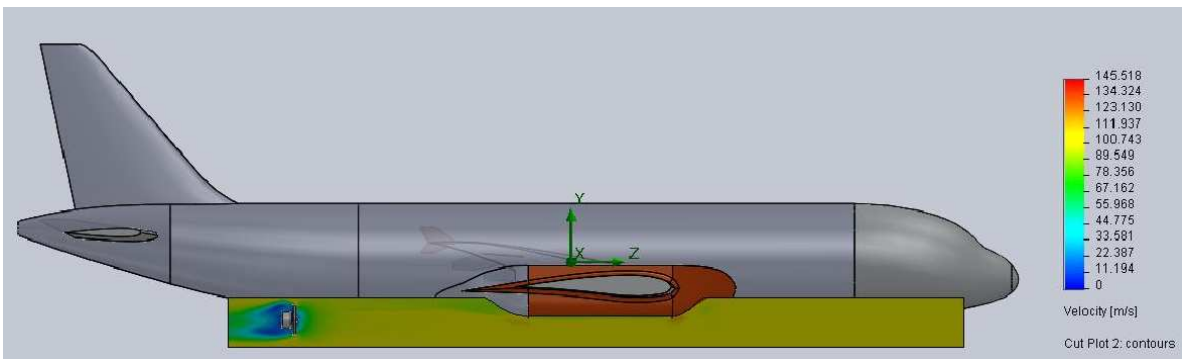
Fig. D. 33 Velocity simulation with RAT in the nose at 7,000 ft. General right side view
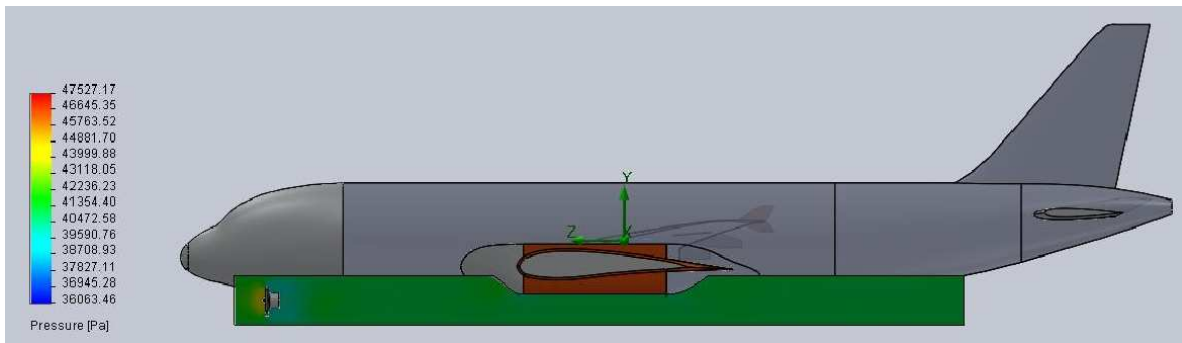
Fig. D. 34 Pressure simulation with RAT in the nose at 7,000 ft. General left side view
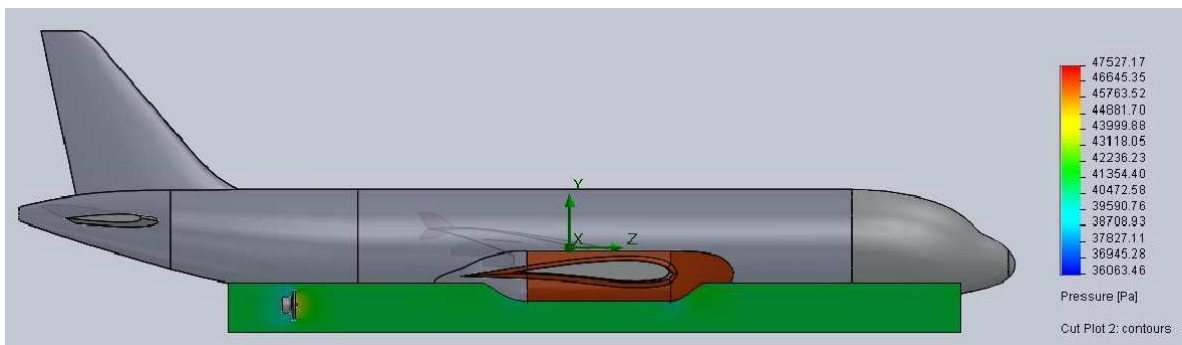
Fig. D. 35 Pressure simulation with RAT in the nose at 7,000 ft. General right side view
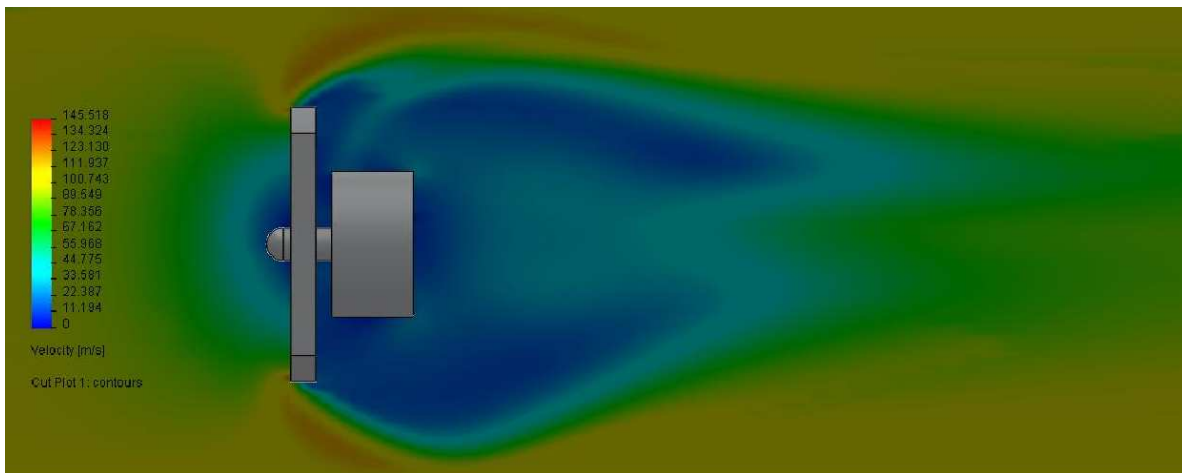
Fig. D. 36 Velocity simulation with the RAT in the nose left side at 7,000 ft in detail
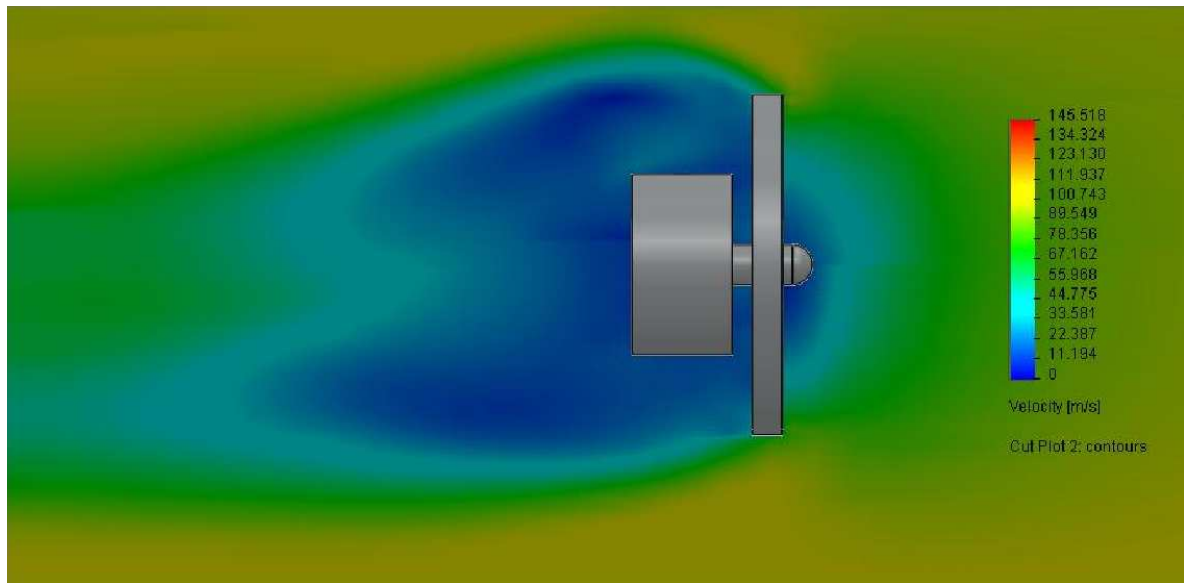
Fig. D. 37 Velocity simulation with the RAT in the nose right side at 7,000 ft in detail
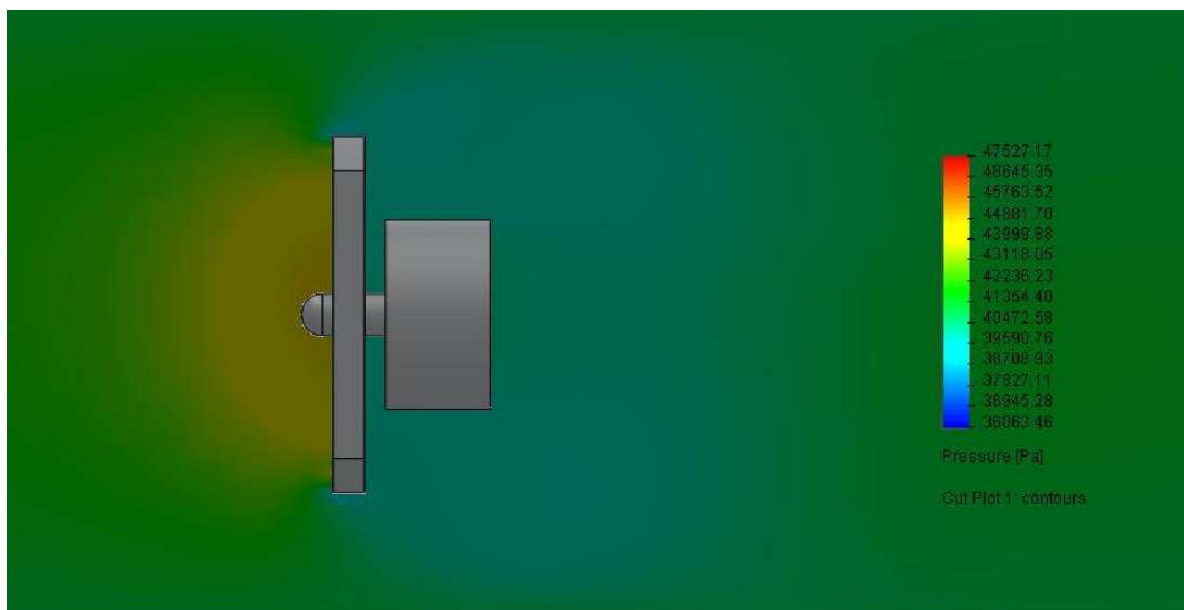
Fig. D. 38 Pressure simulation with the RAT in the nose left side at 7,000 ft in detail
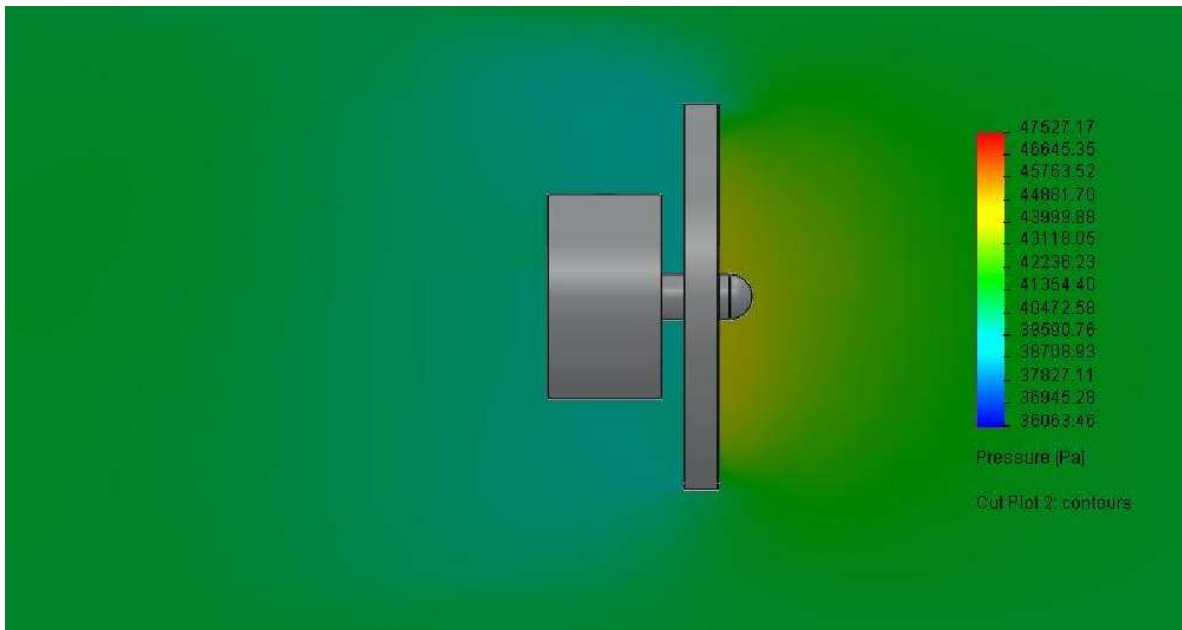
Fig. D. 39 Pressure simulation with the RAT in the nose right side at 7,000 ft in detail

D.8 RAT located on the belly-fairing. Sea level
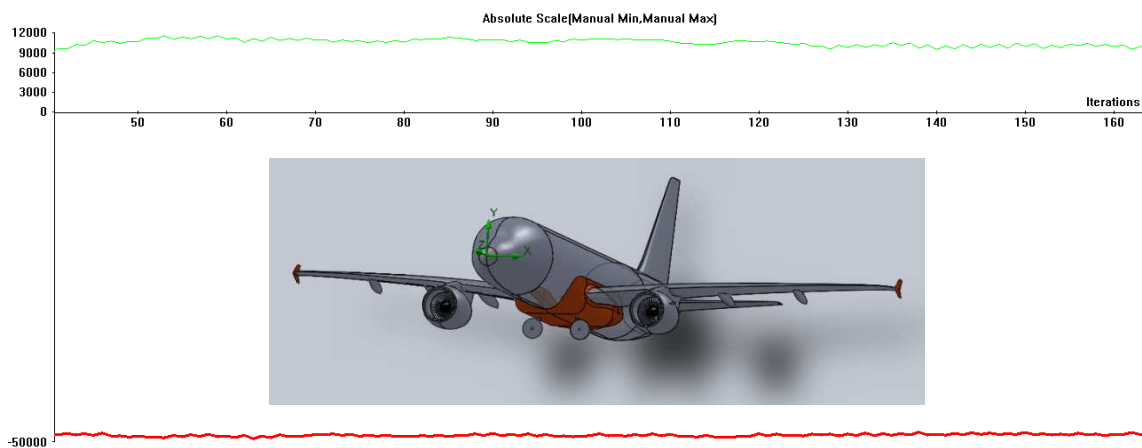
Fig. D. 40 Lift/Drag simulation with RAT in the belly-fairing at sea level
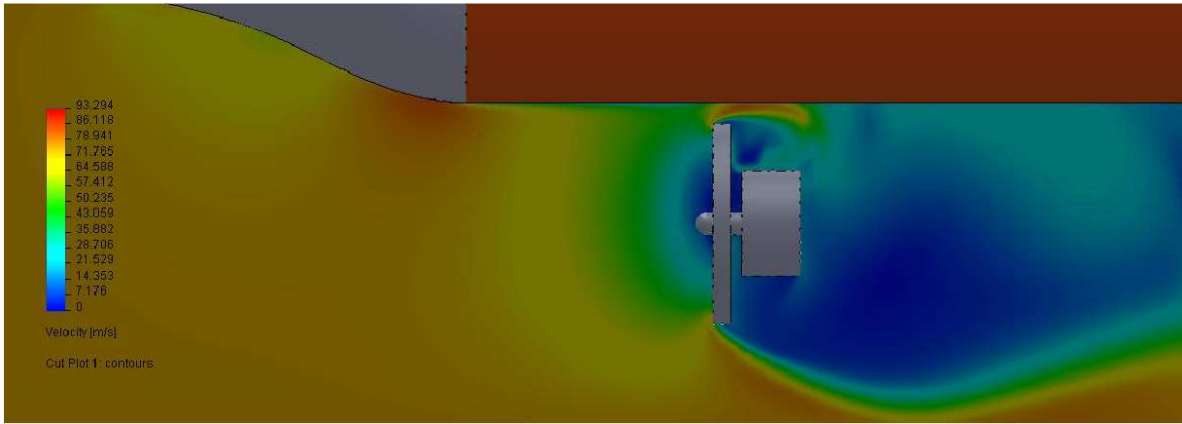
Fig. D. 41 Velocity simulation with the RAT in the belly-fairing at sea level in detail
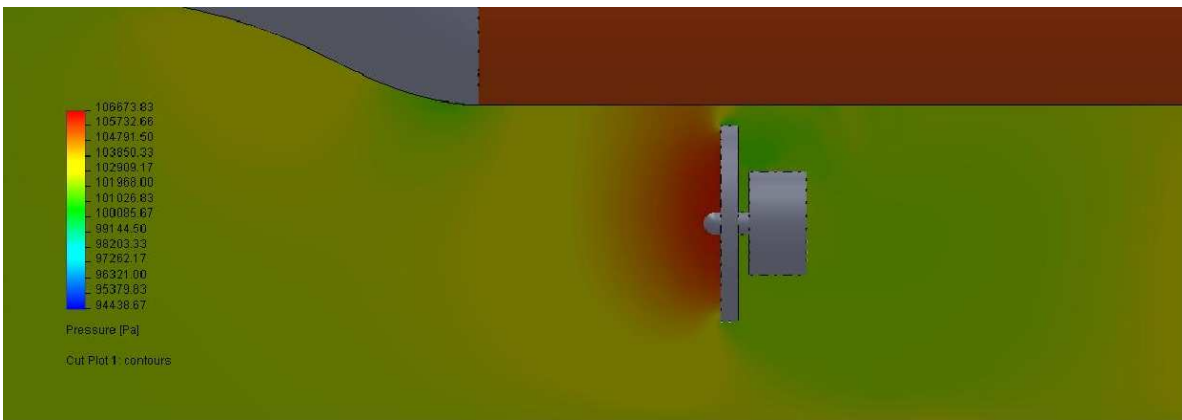
Fig. D. 42 Pressure simulation with the RAT in the belly-fairing at sea level in detail

D.9 RAT located on the belly-fairing. 7,000 ft
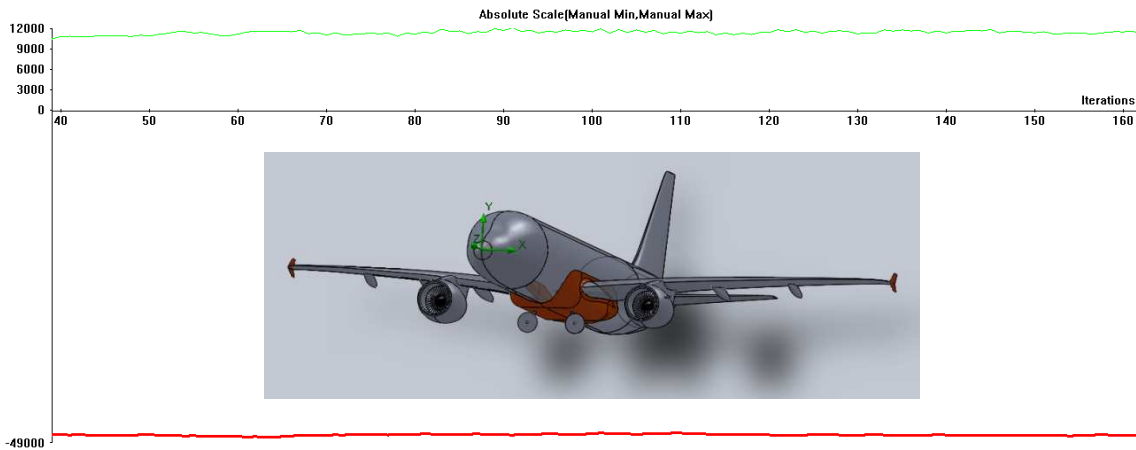
Fig. D. 43 Lift/Drag simulation with RAT in the belly-fairing at 7,000 ft
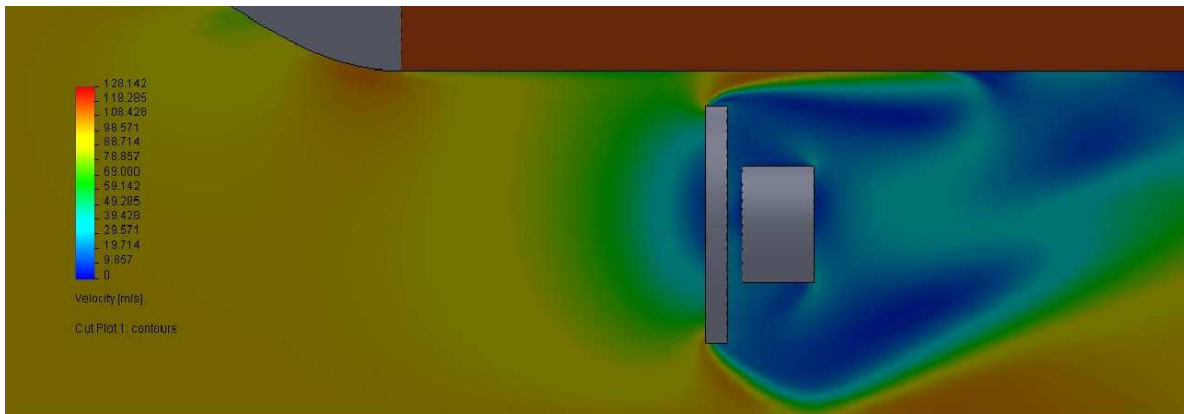
Fig. D. 44 Velocity simulation with the RAT in the belly-fairing at 7,000 ft in detail
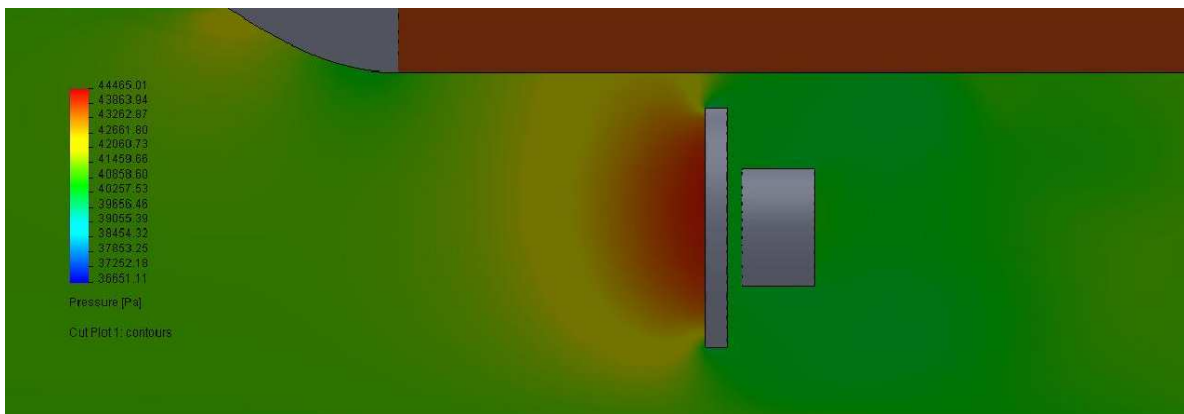
Fig. D. 45 Pressure simulation with the RAT in the belly-fairing at 7,000 ft in detail

D.10 A320 without RAT. Sea Level
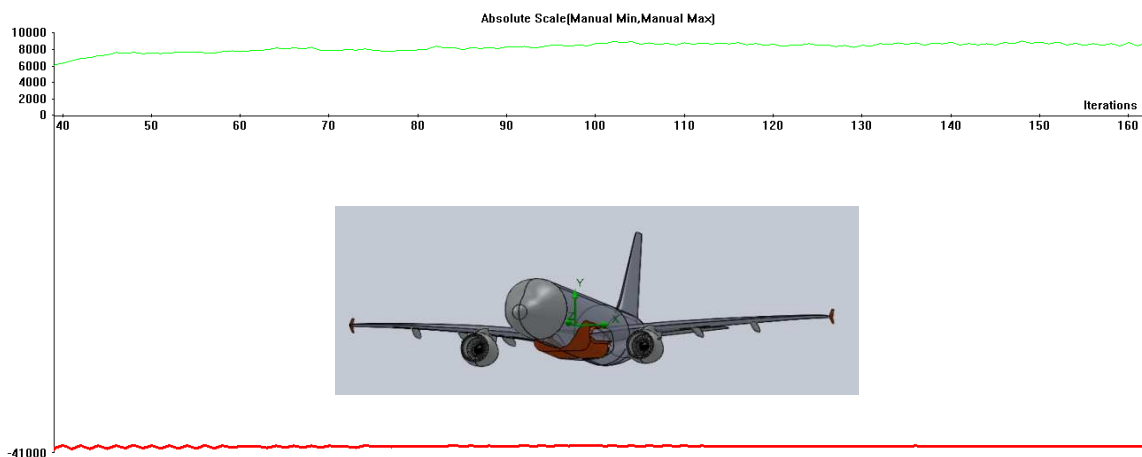
Fig. D. 46 Lift/Drag simulation without RAT at sea level
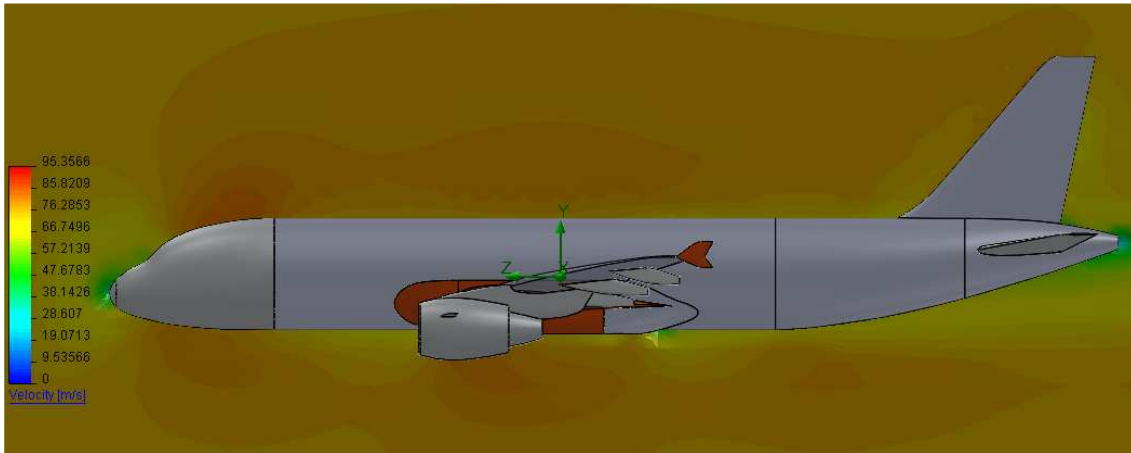
Fig. D. 47 Velocity simulation without RAT at sea level. General view
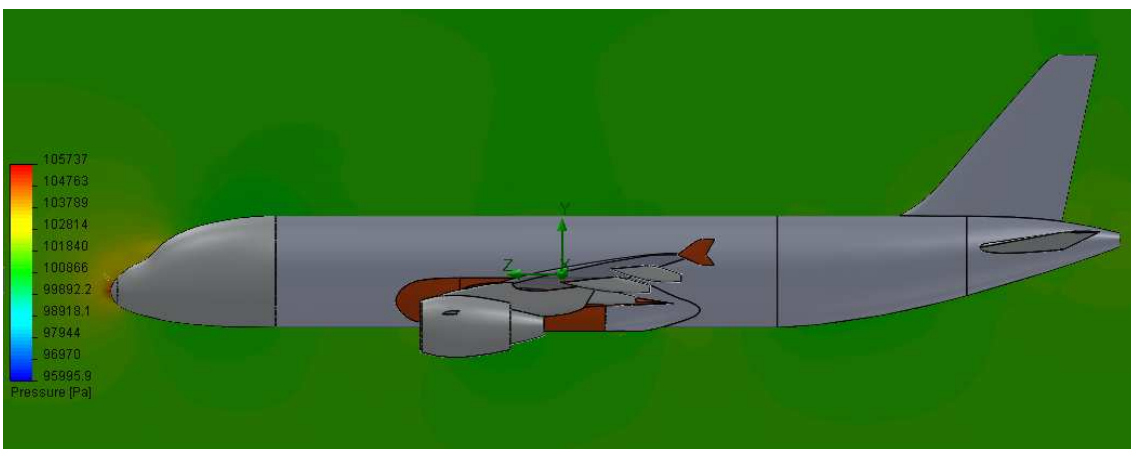
Fig. D. 48 Pressure simulation without RAT at sea level. General view

D.11 A320 without RAT. 7,000 ft
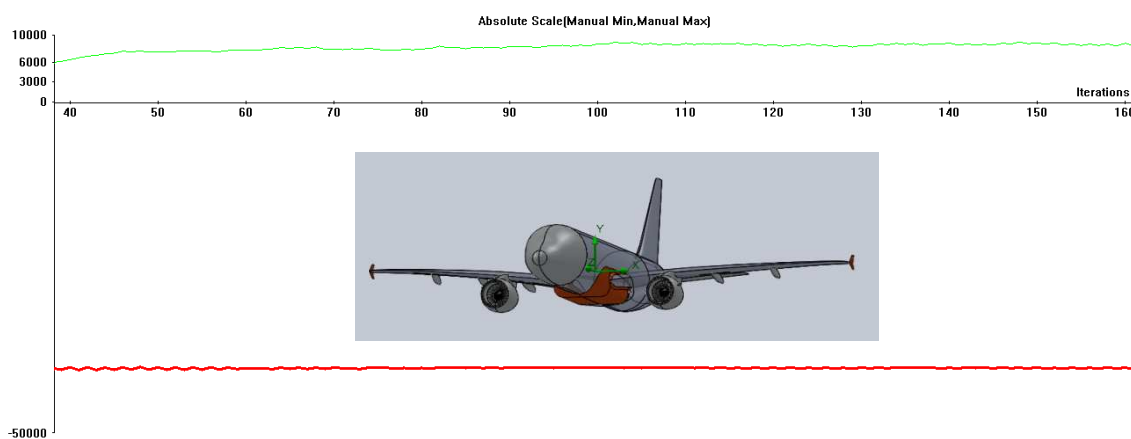
Fig. D. 49 Lift/Drag simulation without RAT at 7,000 ft
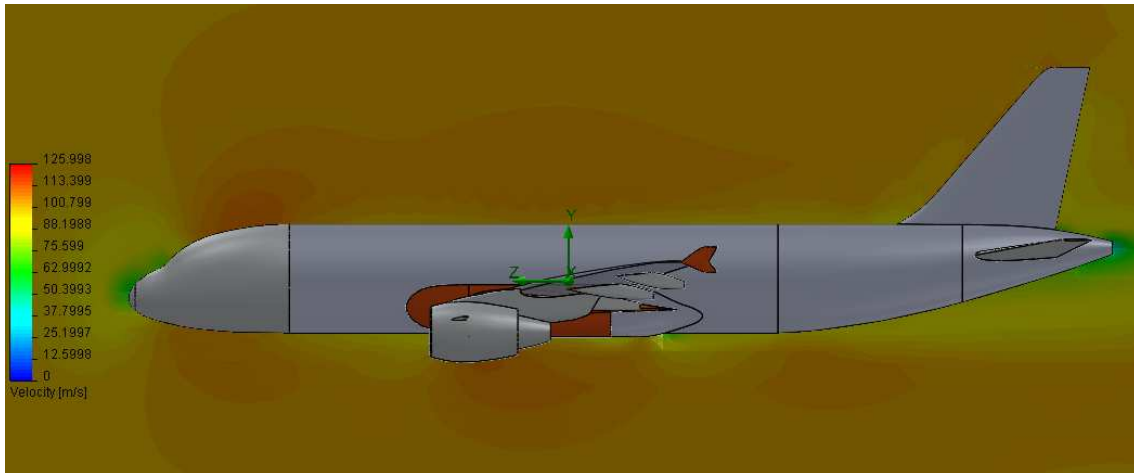
Fig. D. 50 Velocity simulation without RAT at 7,000 ft. General view
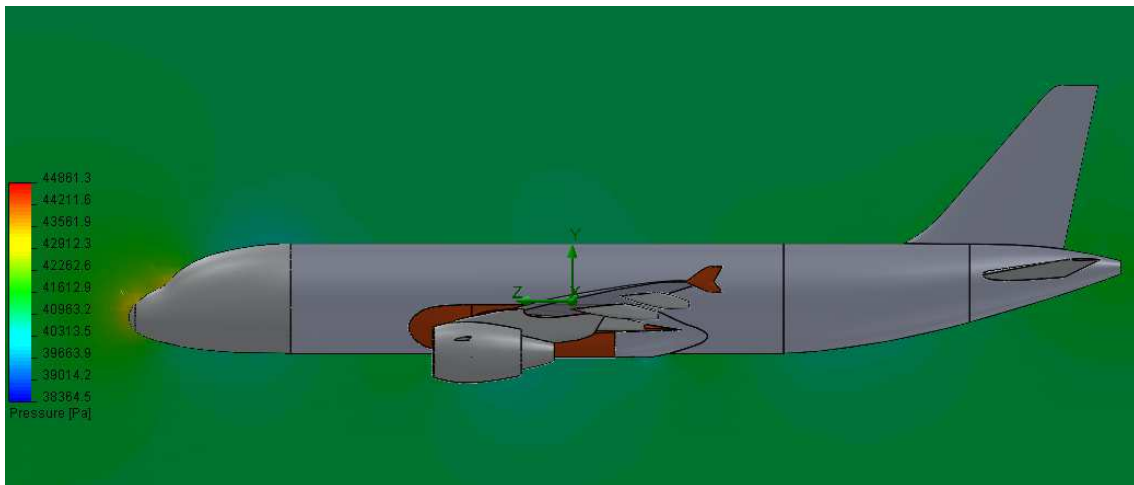
Fig. D. 51 Pressure simulation without RAT at 7,000 ft. General view

ANNEX E – REPORTS

E.1 RAT located on the tail. Sea level report

System Info

Product	Flow Simulation 2010 0.0. Build: 1063
Computer name	ANDREUPARES
User name	Andreu
Processors	Intel(R) Core(TM) i7-2670QM CPU @ 2.20GHz
Memory	3872 MB / 8388607 MB
Operating system	Service Pack 1 (Build 7601)
CAD version	SolidWorks 2010 SP0
CPU speed	2201 (1298) MHz

General Info

Model	C:\Users\Andreu\Documents\Andreu\Universitat\TFC\Treball per capítols\Capítol 4\Sims\Tail\simplificat+rat-tail.SLDPRT
Project name	tail_7000ft (1)
Project path	C:\Users\Andreu\Documents\Andreu\Universitat\TFC\Treball per capítols\Capítol 4\Sims\Tail\10
Units system	SI (m-kg-s)
Analysis type	External (exclude internal spaces)
Exclude cavities without flow conditions	On
Coordinate system	Global coordinate system
Reference axis	Z

INPUT DATA

Initial Mesh Settings
Automatic initial mesh: On
Result resolution level: 6
Advanced narrow channel refinement: Off
Refinement in solid region: Off

Geometry Resolution
Evaluation of minimum gap size: Automatic
Evaluation of minimum wall thickness: Automatic

Computational Domain
Size

X min	-21.4923344 m
X max	22.0998141 m
Y min	-8.31360878 m
Y max	9.41290843 m
Z min	-27.5892194 m
Z max	25.4662 m

Boundary Conditions

2D plane flow	None
At X min	Default
At X max	Default
At Y min	Default
At Y max	Default
At Z min	Default
At Z max	Default

Physical Features
Heat conduction in solids: Off
Time dependent: Off
Gravitational effects: Off
Flow type: Laminar and turbulent
High Mach number flow: Off
Humidity: Off
Default roughness: 0 micrometer
Default wall conditions: Adiabatic wall

Ambient Conditions

Thermodynamic parameters	Static Pressure: 101325 Pa Temperature: 293.2 K
Velocity parameters	Velocity vector Velocity in X direction: 0 m/s Velocity in Y direction: 0 m/s Velocity in Z direction: -75.56 m/s
Turbulence parameters	Turbulence intensity and length Intensity: 0.1 % Length: 0.113583997 m

Material Settings
Fluids
Air

Goals
Global Goals
GG Min Total Pressure 1

Type	Global Goal
Goal type	Total Pressure
Calculate	Minimum value
Coordinate system	Global coordinate system
Use in convergence	On

GG Av Total Pressure 1

Type	Global Goal
Goal type	Total Pressure
Calculate	Average value
Coordinate system	Global coordinate system
Use in convergence	On

GG Max Total Pressure 1

Type	Global Goal
Goal type	Total Pressure
Calculate	Maximum value
Coordinate system	Global coordinate system
Use in convergence	On

GG Min Velocity 1

Type	Global Goal
Goal type	Velocity
Calculate	Minimum value
Coordinate system	Global coordinate system
Use in convergence	On

GG Av Velocity 1

Type	Global Goal

Goal type	Velocity
Calculate	Average value
Coordinate system	Global coordinate system
Use in convergence	On

GG Max Velocity 1

Type	Global Goal
Goal type	Velocity
Calculate	Maximum value
Coordinate system	Global coordinate system
Use in convergence	On

GG Y - Component of Force 1

Type	Global Goal
Goal type	Y - Component of Force
Coordinate system	Global coordinate system
Use in convergence	On

GG Z - Component of Force 1

Type	Global Goal
Goal type	Z - Component of Force
Coordinate system	Global coordinate system
Use in convergence	On

Calculation Control Options
Finish Conditions

Finish conditions	If one is satisfied
Maximum travels	4
Goals convergence	Analysis interval: 0.5

Solver Refinement

Refinement level	1
Refinement criterion	1.5
Unrefinement criterion	0.15
Adaptive refinement in fluid	On
Use global parameter variation	Off
Approximate maximum cells	3200000
Refinement strategy	Tabular refinement
Units	Travels
Relaxation interval	0.2
Refinements	2

Results Saving

Save before refinement	On

Advanced Control Options
Flow Freezing

Flow freezing strategy	Disabled

RESULTS

General Info
Iterations: 290
CPU time: 950 s

Log

Mesh generation started	11:02:39 , Jul 01
Mesh generation normally finished	11:04:15 , Jul 01

Preparing data for calculation	11:04:30 , Jul 01
Calculation started 0	11:04:34 , Jul 01
Refinement 129	11:08:40 , Jul 01
Calculation has converged since the following criteria are satisfied: 289	11:22:17 , Jul 01
Goals are converged 289	
Calculation finished 290	11:22:32 , Jul 01

Calculation Mesh
Basic Mesh Dimensions

Number of cells in X	38
Number of cells in Y	16
Number of cells in Z	48

Number Of Cells

Total cells	78247
Fluid cells	66363
Solid cells	3072
Partial cells	8812
Irregular cells	0
Trimmed cells	224

Maximum refinement level: 2

Goals

Name	Unit	Value	Progress	Use in convergence	Delta	Criteria
GG Min Total Pressure 1	Pa	95400.2	100	On	7.64252475	341.09537
GG Av Total Pressure 1	Pa	104787	100	On	0.109840383	1.06979996
GG Max Total Pressure 1	Pa	112913	100	On	288.230163	421.714965
GG Min Velocity 1	m/s	0	100	On	0	0
GG Av Velocity 1	m/s	75.3237	100	On	0.00145842994	0.0124003533
GG Max Velocity 1	m/s	96.5013	100	On	0.0370347659	0.0801089053
GG Y - Component of Force 1	N	15804.8	100	On	655.245414	658.262079
GG Z - Component of Force 1	N	-42555.9	100	On	89.656266	1650.03255

Min/Max Table

Name	Minimum	Maximum
Pressure [Pa]	95400.2	108604
Temperature [K]	291.41	296.046
Velocity [m/s]	0	94.8362
X – Component of Velocity [m/s]	-51.7145	51.8336
Y – Component of Velocity [m/s]	-54.0797	51.5224
Z – Component of Velocity [m/s]	-93.7228	22.1023
Fluid Temperature [K]	291.41	296.046
Mach Number [ ]	0	0.277076
Shear Stress [Pa]	0	31.1937
Heat Transfer Coefficient [W/m^2/K]	0	0
Surface Heat Flux [W/m^2]	0	0
Density [kg/m^3]	1.13459	1.29208

E.2 RAT located on the tail. 7,000 ft report
General Info

Model	C:\Users\Andreu\Documents\Andreu\Universitat\TFC\Treball per capítols\Capítol 4\Sims\Tail\simplificat+rat-tail.SLDPRT
Project name	tail_7000ft
Project path	C:\Users\Andreu\Documents\Andreu\Universitat\TFC\Treball per capítols\Capítol 4\Sims\Tail\8
Units system	SI (m-kg-s)
Analysis type	External (exclude internal spaces)
Exclude cavities without flow conditions	On
Coordinate system	Global coordinate system
Reference axis	Z

Initial Mesh Settings
Automatic initial mesh: On
Result resolution level: 6
Advanced narrow channel refinement: Off
Refinement in solid region: Off

Geometry Resolution
Evaluation of minimum gap size: Automatic
Evaluation of minimum wall thickness: Automatic

Computational Domain

Size

X min	-22.7243488 m
X max	23.2085719 m
Y min	-8.93764046 m
Y max	10.4650762 m
Z min	-28.4500807 m
Z max	23.8953648 m

Boundary Conditions

2D plane flow	None
At X min	Default
At X max	Default
At Y min	Default
At Y max	Default
At Z min	Default
At Z max	Default

Physical Features
Heat conduction in solids: Off
Time dependent: On
Gravitational effects: On
Flow type: Laminar and turbulent
High Mach number flow: Off
Humidity: Off
Default roughness: 0 micrometer

Gravitational Settings

X component	0 m/s^2

Y component	-9.81 m/s^2
Z component	0 m/s^2

Default wall conditions: Adiabatic wall

Ambient Conditions

Thermodynamic parameters	Temperature: 242.55 K Density: 0.59 kg/m^3
Velocity parameters	Velocity vector Velocity in X direction: 0 m/s Velocity in Y direction: 0 m/s Velocity in Z direction: -100.35 m/s
Turbulence parameters	Turbulence intensity and length Intensity: 0.1 % Length: 0.113583997 m

Material Settings
Fluids
Air

Goals
Global Goals
GG Min Total Pressure 1

Type	Global Goal
Goal type	Total Pressure
Calculate	Minimum value
Coordinate system	Global coordinate system
Use in convergence	On

GG Av Total Pressure 1

Type	Global Goal
Goal type	Total Pressure
Calculate	Average value
Coordinate system	Global coordinate system
Use in convergence	On

GG Max Total Pressure 1

Type	Global Goal
Goal type	Total Pressure
Calculate	Maximum value
Coordinate system	Global coordinate system
Use in convergence	On

GG Min Velocity 1

Type	Global Goal
Goal type	Velocity
Calculate	Minimum value
Coordinate system	Global coordinate system
Use in convergence	On

GG Av Velocity 1

Type	Global Goal
Goal type	Velocity
Calculate	Average value
Coordinate system	Global coordinate system
Use in convergence	On

GG Max Velocity 1

Type	Global Goal
Goal type	Velocity
Calculate	Maximum value
Coordinate system	Global coordinate system
Use in convergence	On

GG Y - Component of Force 1

Type	Global Goal
Goal type	Y - Component of Force
Coordinate system	Global coordinate system
Use in convergence	On

GG Z - Component of Force 1

Type	Global Goal
Goal type	Z - Component of Force
Coordinate system	Global coordinate system
Use in convergence	On

Calculation Control Options
Finish Conditions

Finish conditions	If one is satisfied
Maximum physical time	1 s

Solver Refinement

Refinement level	1
Refinement criterion	1.5
Unrefinement criterion	0.15
Adaptive refinement in fluid	On
Use global parameter variation	Off
Approximate maximum cells	3200000
Refinement strategy	Tabular refinement
Units	Travels
Relaxation interval	0.2
Refinements	2

Results Saving

Save before refinement	On

Advanced Control Options
Flow Freezing

Flow freezing strategy	Disabled

Manual time step: Off

<div align="center">RESULTS</div>

General Info
Iterations: 327
Physical time: 5.40813193 s
CPU time: 644 s

Log

Mesh generation started	23:41:42 , Jun 30
Mesh generation normally finished	23:43:16 , Jun 30
Preparing data for calculation	23:43:29 , Jun 30
Calculation started 0	23:43:34 , Jun 30
Refinement 326	23:54:05 , Jun 30
Calculation has converged since the following criteria are satisfied: 326	23:55:19 , Jun 30

Max. phys. time is reached	326	
Calculation finished	327	23:55:33 , Jun 30

Calculation Mesh
Basic Mesh Dimensions

Number of cells in X	40
Number of cells in Y	17
Number of cells in Z	45

Number Of Cells

Total cells	77549
Fluid cells	66380
Solid cells	2688
Partial cells	8481
Irregular cells	0
Trimmed cells	189

Maximum refinement level: 2
Goals

Name	Unit	Value	Progress	Use in convergence	Delta	Criteria
GG Min Total Pressure 1	Pa	38540.5	55.3	On	230.823723	127.804644
GG Av Total Pressure 1	Pa	44105.5	46.7	On	1.82097748	0.851008765
GG Max Total Pressure 1	Pa	47165.1	64.4	On	608.349107	392.087645
GG Min Velocity 1	m/s	0	100	On	0	0
GG Av Velocity 1	m/s	99.8552	100	On	0.00298514244	0.0165939549
GG Max Velocity 1	m/s	123.944	39.3	On	1.33511318	0.525520946
GG Y - Component of Force 1	N	1261.62	15.6	On	9276.24908	1447.34678
GG Z - Component of Force 1	N	-56087.8	34.5	On	9664.66943	3336.42724

Min/Max Table

Name	Minimum	Maximum
Pressure [Pa]	38540.5	45535.8
Temperature [K]	239.886	247.487
Velocity [m/s]	0	122.853
X – Component of Velocity [m/s]	-59.2489	59.5786
Y – Component of Velocity [m/s]	-62.1996	56.2727
Z – Component of Velocity [m/s]	-122.352	13.314
Fluid Temperature [K]	239.886	247.487
Mach Number [ ]	0	0.395549
Shear Stress [Pa]	0	21.4754
Heat Transfer Coefficient [W/m^2/K]	0	0
Surface Heat Flux [W/m^2]	0	0
Density [kg/m^3]	0.543675	0.64712

E.3 RAT located on the tail. Sea level with full flaps report

General Info

Model	C:\Users\Andreu\Documents\Andreu\Universitat\TFC\Treball

	per capítols\Capítol 4\Sims\Tail\simplificat+rat-tail+flaps.SLDPRT
Project name	sim_obstacle (6)
Project path	C:\Users\Andreu\Documents\Andreu\Universitat\TFC\Treball per capítols\Capítol 4\Sims\Tail\9
Units system	SI (m-kg-s)
Analysis type	External (exclude internal spaces)
Exclude cavities without flow conditions	On
Coordinate system	Global coordinate system
Reference axis	Z

INPUT DATA

Initial Mesh Settings
Automatic initial mesh: On
Result resolution level: 6
Advanced narrow channel refinement: Off
Refinement in solid region: Off

Geometry Resolution
Evaluation of minimum gap size: Automatic
Evaluation of minimum wall thickness: Automatic

Computational Domain
Size

X min	-21.8224182 m
X max	21.0781877 m
Y min	-8.03462293 m
Y max	9.23816362 m
Z min	-26.3371103 m
Z max	23.643896 m

Boundary Conditions

2D plane flow	None
At X min	Default
At X max	Default
At Y min	Default
At Y max	Default
At Z min	Default
At Z max	Default

Physical Features
Heat conduction in solids: Off
Time dependent: On
Gravitational effects: On
Flow type: Laminar and turbulent
High Mach number flow: Off
Humidity: Off
Default roughness: 0 micrometer

Gravitational Settings

X component	0 m/s^2
Y component	-9.81 m/s^2
Z component	0 m/s^2

Default wall conditions: Adiabatic wall

Ambient Conditions

Thermodynamic parameters	Static Pressure: 101325 Pa Temperature: 293.2 K
Velocity parameters	Velocity vector Velocity in X direction: 0 m/s Velocity in Y direction: 0 m/s Velocity in Z direction: -75.56 m/s
Turbulence parameters	Turbulence intensity and length Intensity: 0.1 % Length: 0.113583997 m

Material Settings
Fluids
Air

Goals
Global Goals
GG Min Total Pressure 1

Type	Global Goal
Goal type	Total Pressure
Calculate	Minimum value
Coordinate system	Global coordinate system
Use in convergence	On

GG Av Total Pressure 1

Type	Global Goal
Goal type	Total Pressure
Calculate	Average value
Coordinate system	Global coordinate system
Use in convergence	On

GG Max Total Pressure 1

Type	Global Goal
Goal type	Total Pressure
Calculate	Maximum value
Coordinate system	Global coordinate system
Use in convergence	On

GG Min Velocity 1

Type	Global Goal
Goal type	Velocity
Calculate	Minimum value
Coordinate system	Global coordinate system
Use in convergence	On

GG Av Velocity 1

Type	Global Goal
Goal type	Velocity
Calculate	Average value
Coordinate system	Global coordinate system
Use in convergence	On

GG Max Velocity 1

Type	Global Goal
Goal type	Velocity
Calculate	Maximum value
Coordinate system	Global coordinate system
Use in convergence	On

GG Y - Component of Force 1

Type	Global Goal
Goal type	Y - Component of Force
Coordinate system	Global coordinate system
Use in convergence	On

GG Z - Component of Force 1

Type	Global Goal
Goal type	Z - Component of Force
Coordinate system	Global coordinate system
Use in convergence	On

Calculation Control Options
Finish Conditions

Finish conditions	If one is satisfied
Maximum physical time	1 s

Solver Refinement

Refinement level	1
Refinement criterion	1.5
Unrefinement criterion	0.15
Adaptive refinement in fluid	On
Use global parameter variation	Off
Approximate maximum cells	3200000
Refinement strategy	Tabular refinement
Units	Travels
Relaxation interval	0.2
Refinements	2

Results Saving

Save before refinement	On

Advanced Control Options
Flow Freezing

Flow freezing strategy	Disabled

Manual time step: Off

RESULTS

General Info
Iterations: 313
Physical time: 7.2518814 s
CPU time: 536 s

Log

Mesh generation started	08:41:11 , Jul 01
Mesh generation normally finished	08:42:56 , Jul 01
Preparing data for calculation	08:43:07 , Jul 01
Calculation started 0	08:43:12 , Jul 01
Refinement 312	08:51:42 , Jul 01
Calculation has converged since the following criteria are satisfied: 312	08:53:00 , Jul 01
Max. phys. time is reached 312	
Calculation finished 313	08:53:15 , Jul 01

Calculation Mesh
Basic Mesh Dimensions

Number of cells in X	38

Number of cells in Y	16
Number of cells in Z	43

Number Of Cells

Total cells	71406
Fluid cells	59802
Solid cells	2807
Partial cells	8797
Irregular cells	0
Trimmed cells	271

Maximum refinement level: 2

Goals

Name	Unit	Value	Progress	Use in convergence	Delta	Criteria
GG Min Total Pressure 1	Pa	97851.9	39.8	On	694.53308	276.818669
GG Av Total Pressure 1	Pa	104764	43.5	On	1.90115471	0.827841639
GG Max Total Pressure 1	Pa	108042	79.1	On	750.180393	593.94172
GG Min Velocity 1	m/s	0	100	On	0	0
GG Av Velocity 1	m/s	75.2106	100	On	0.00230341716	0.0100664921
GG Max Velocity 1	m/s	93.7134	16.5	On	1.50449709	0.248887396
GG Y - Component of Force 1	N	157439	10.1	On	12226.6436	1238.08542
GG Z - Component of Force 1	N	-73815.6	14.5	On	18051.3358	2632.53491

Min/Max Table

Name	Minimum	Maximum
Pressure [Pa]	97851	106415
Temperature [K]	291.674	296.034
Velocity [m/s]	0	93.5103
X – Component of Velocity [m/s]	-44.1855	46.0187
Y – Component of Velocity [m/s]	-45.2848	41.8548
Z – Component of Velocity [m/s]	-93.0047	23.4135
Fluid Temperature [K]	291.674	296.034
Mach Number [ ]	0	0.273199
Shear Stress [Pa]	0	57.9255
Heat Transfer Coefficient [W/m^2/K]	0	0
Surface Heat Flux [W/m^2]	0	0
Density [kg/m^3]	1.15997	1.25517

E.4 RAT located on the nose. Sea level report

General Info

Model	C:\Users\Andreu\Documents\Andreu\Universitat\TFC\Treball per capítols\Capítol 4\Sims\Nose\simplificat+rat-nose.SLDPRT
Project name	sim_obstacle (7)
Project path	C:\Users\Andreu\Documents\Andreu\Universitat\TFC\Treball per capítols\Capítol 4\Sims\Nose\3
Units system	SI (m-kg-s)
Analysis type	External (exclude internal spaces)
Exclude cavities without flow conditions	On

Coordinate system	Global coordinate system
Reference axis	Z

INPUT DATA

Initial Mesh Settings
Automatic initial mesh: On
Result resolution level: 6
Advanced narrow channel refinement: Off
Refinement in solid region: Off

Geometry Resolution
Evaluation of minimum gap size: Automatic
Evaluation of minimum wall thickness: Automatic

Computational Domain
Size

X min	-22.5811085 m
X max	21.9873841 m
Y min	-7.18238913 m
Y max	10.3811618 m
Z min	-42.9362408 m
Z max	7.44919847 m

Boundary Conditions

2D plane flow	None
At X min	Default
At X max	Default
At Y min	Default
At Y max	Default
At Z min	Default
At Z max	Default

Physical Features
Heat conduction in solids: Off
Time dependent: On
Gravitational effects: On
Flow type: Laminar and turbulent
High Mach number flow: Off
Humidity: Off
Default roughness: 0 micrometer

Gravitational Settings

X component	0 m/s^2
Y component	-9.81 m/s^2
Z component	0 m/s^2

Default wall conditions: Adiabatic wall
Ambient Conditions

Thermodynamic parameters	Temperature: 242.55 K Density: 0.59 kg/m^3
Velocity parameters	Velocity vector Velocity in X direction: 0 m/s Velocity in Y direction: 0 m/s Velocity in Z direction: -100.35 m/s
Turbulence parameters	Turbulence intensity and length Intensity: 0.1 %

	Length: 0.113583997 m

Material Settings
Fluids
Air

Goals
Global Goals

GG Min Total Pressure 1

Type	Global Goal
Goal type	Total Pressure
Calculate	Minimum value
Coordinate system	Global coordinate system
Use in convergence	On

GG Av Total Pressure 1

Type	Global Goal
Goal type	Total Pressure
Calculate	Average value
Coordinate system	Global coordinate system
Use in convergence	On

GG Max Total Pressure 1

Type	Global Goal
Goal type	Total Pressure
Calculate	Maximum value
Coordinate system	Global coordinate system
Use in convergence	On

GG Min Velocity 1

Type	Global Goal
Goal type	Velocity
Calculate	Minimum value
Coordinate system	Global coordinate system
Use in convergence	On

GG Av Velocity 1

Type	Global Goal
Goal type	Velocity
Calculate	Average value
Coordinate system	Global coordinate system
Use in convergence	On

GG Max Velocity 1

Type	Global Goal
Goal type	Velocity
Calculate	Maximum value
Coordinate system	Global coordinate system
Use in convergence	On

GG Y - Component of Force 1

Type	Global Goal
Goal type	Y - Component of Force
Coordinate system	Global coordinate system
Use in convergence	On

GG Z - Component of Force 1

Type	Global Goal

Goal type	Z - Component of Force
Coordinate system	Global coordinate system
Use in convergence	On

Calculation Control Options
Finish Conditions

Finish conditions	If one is satisfied
Maximum physical time	1 s

Solver Refinement

Refinement level	1
Refinement criterion	1.5
Unrefinement criterion	0.15
Adaptive refinement in fluid	On
Use global parameter variation	Off
Approximate maximum cells	3200000
Refinement strategy	Tabular refinement
Units	Travels
Relaxation interval	0.2
Refinements	2

Results Saving

Save before refinement	On

Advanced Control Options
Flow Freezing

Flow freezing strategy	Disabled

Manual time step: Off

RESULTS

General Info
Iterations: 316
Physical time: 6.82960803 s
CPU time: 538 s

Log

Mesh generation started	16:49:13 , Jul 01
Mesh generation normally finished	16:52:00 , Jul 01
Preparing data for calculation	16:52:14 , Jul 01
Calculation started 0	16:52:22 , Jul 01
Refinement 321	17:07:45 , Jul 01
Calculation has converged since the following criteria are satisfied: 321	17:10:19 , Jul 01
Max. phys. time is reached 321	
Calculation finished 322	17:10:45 , Jul 01

Calculation Mesh
Basic Mesh Dimensions

Number of cells in X	38
Number of cells in Y	16
Number of cells in Z	44

Number Of Cells

Total cells	73456
Fluid cells	61524
Solid cells	3374
Partial cells	8558

Irregular cells	0
Trimmed cells	204

Maximum refinement level: 2

Goals

Name	Unit	Value	Progress	Use in convergence	Delta	Criteria
GG Min Total Pressure 1	Pa	97508.9	100	On	83.5333373	290.636323
GG Av Total Pressure 1	Pa	104740	24	On	4.23777749	1.01987132
GG Max Total Pressure 1	Pa	108110	100	On	335.555918	635.974939
GG Min Velocity 1	m/s	0	100	On	0	0
GG Av Velocity 1	m/s	75.1084	100	On	0.00479003957	0.013056049
GG Max Velocity 1	m/s	92.1797	14.6	On	1.13117012	0.166162446
GG Y - Component of Force 1	N	-2865.08	3.3	On	21511.0408	724.580721
GG Z - Component of Force 1	N	-60520.4	14.9	On	14634.7205	2185.17025

Min/Max Table

Name	Minimum	Maximum
Pressure [Pa]	97508.4	106945
Temperature [K]	291.815	296.026
Velocity [m/s]	0	93.5036
X – Component of Velocity [m/s]	-49.4483	45.5544
Y – Component of Velocity [m/s]	-44.5677	47.5084
Z – Component of Velocity [m/s]	-91.8462	30.4962
Fluid Temperature [K]	291.815	296.026
Mach Number [ ]	0	0.273066
Shear Stress [Pa]	0	26.8854
Heat Transfer Coefficient [W/m^2/K]	0	0
Surface Heat Flux [W/m^2]	0	0
Density [kg/m^3]	1.15631	1.26161

E.5 RAT located on the nose. 7,000 ft report

General Info

Model	C:\Users\Andreu\Documents\Andreu\Universitat\TFC\Treball per capítols\Capítol 4\Sims\Nose\simplificat+rat-nose.SLDPRT
Project name	sim_obstacle (7)
Project path	C:\Users\Andreu\Documents\Andreu\Universitat\TFC\Treball per capítols\Capítol 4\Sims\Nose\3
Units system	SI (m-kg-s)
Analysis type	External (exclude internal spaces)
Exclude cavities without flow conditions	On
Coordinate system	Global coordinate system
Reference axis	Z

INPUT DATA

Initial Mesh Settings
Automatic initial mesh: On
Result resolution level: 6

Advanced narrow channel refinement: Off
Refinement in solid region: Off

Geometry Resolution
Evaluation of minimum gap size: Automatic
Evaluation of minimum wall thickness: Automatic

Computational Domain
Size

X min	-22.5811085 m
X max	21.9873841 m
Y min	-7.18238913 m
Y max	10.3811618 m
Z min	-42.9362408 m
Z max	7.44919847 m

Boundary Conditions

2D plane flow	None
At X min	Default
At X max	Default
At Y min	Default
At Y max	Default
At Z min	Default
At Z max	Default

Physical Features
Heat conduction in solids: Off
Time dependent: On
Gravitational effects: On
Flow type: Laminar and turbulent
High Mach number flow: Off
Humidity: Off
Default roughness: 0 micrometer

Gravitational Settings

X component	0 m/s^2
Y component	-9.81 m/s^2
Z component	0 m/s^2

Default wall conditions: Adiabatic wall
Ambient Conditions

Thermodynamic parameters	Temperature: 242.55 K Density: 0.59 kg/m^3
Velocity parameters	Velocity vector Velocity in X direction: 0 m/s Velocity in Y direction: 0 m/s Velocity in Z direction: -100.35 m/s
Turbulence parameters	Turbulence intensity and length Intensity: 0.1 % Length: 0.113583997 m

Material Settings
Fluids
Air

Goals
Global Goals
GG Min Total Pressure 1

Type	Global Goal
Goal type	Total Pressure
Calculate	Minimum value
Coordinate system	Global coordinate system
Use in convergence	On

GG Av Total Pressure 1

Type	Global Goal
Goal type	Total Pressure
Calculate	Average value
Coordinate system	Global coordinate system
Use in convergence	On

GG Max Total Pressure 1

Type	Global Goal
Goal type	Total Pressure
Calculate	Maximum value
Coordinate system	Global coordinate system
Use in convergence	On

GG Min Velocity 1

Type	Global Goal
Goal type	Velocity
Calculate	Minimum value
Coordinate system	Global coordinate system
Use in convergence	On

GG Av Velocity 1

Type	Global Goal
Goal type	Velocity
Calculate	Average value
Coordinate system	Global coordinate system
Use in convergence	On

GG Max Velocity 1

Type	Global Goal
Goal type	Velocity
Calculate	Maximum value
Coordinate system	Global coordinate system
Use in convergence	On

GG Y - Component of Force 1

Type	Global Goal
Goal type	Y - Component of Force
Coordinate system	Global coordinate system
Use in convergence	On

GG Z - Component of Force 1

Type	Global Goal
Goal type	Z - Component of Force
Coordinate system	Global coordinate system
Use in convergence	On

Calculation Control Options
Finish Conditions

Finish conditions	If one is satisfied
Maximum physical time	1 s

Solver Refinement

Refinement level	1
Refinement criterion	1.5
Unrefinement criterion	0.15
Adaptive refinement in fluid	On
Use global parameter variation	Off
Approximate maximum cells	3200000
Refinement strategy	Tabular refinement
Units	Travels
Relaxation interval	0.2
Refinements	2

Results Saving

Save before refinement	On

Advanced Control Options
Flow Freezing

Flow freezing strategy	Disabled

Manual time step: Off

RESULTS

General Info
Iterations: 322
Physical time: 5.26271118 s
CPU time: 1001 s

Log

Mesh generation started	16:49:13 , Jul 01
Mesh generation normally finished	16:52:00 , Jul 01
Preparing data for calculation	16:52:14 , Jul 01
Calculation started 0	16:52:22 , Jul 01
Refinement 321	17:07:45 , Jul 01
Calculation has converged since the following criteria are satisfied: 321	17:10:19 , Jul 01
Max. phys. time is reached 321	
Calculation finished 322	17:10:45 , Jul 01

Calculation Mesh
Basic Mesh Dimensions

Number of cells in X	40
Number of cells in Y	16
Number of cells in Z	45

Number Of Cells

Total cells	79781
Fluid cells	67978
Solid cells	2968
Partial cells	8835
Irregular cells	0
Trimmed cells	199

Maximum refinement level: 2

Goals

Name	Unit	Value	Progress	Use in convergence	Delta	Criteria
GG Min Total Pressure 1	Pa	38338.6	30.1	On	651.657352	196.722714
GG Av Total Pressure 1	Pa	44090	53.9	On	2.70393594	1.45893817
GG Max Total Pressure 1	Pa	48628.9	12.9	On	2460.42654	318.1603
GG Min Velocity 1	m/s	0	100	On	0	0
GG Av Velocity 1	m/s	99.6564	100	On	0.00401992931	0.0217580002
GG Max Velocity 1	m/s	124.769	8.8	On	5.06181344	0.447758437
GG Y - Component of Force 1	N	619.645	11.1	On	16232.5209	1808.3027
GG Z - Component of Force 1	N	-56442.1	24.2	On	12630.8874	3068.64014

Min/Max Table

Name	Minimum	Maximum
Pressure [Pa]	38338.6	46201.8
Temperature [K]	239.817	247.547
Velocity [m/s]	0	122.332
X – Component of Velocity [m/s]	-56.4961	56.1363
Y – Component of Velocity [m/s]	-78.6164	49.7778
Z – Component of Velocity [m/s]	-121.804	19.9016
Fluid Temperature [K]	239.817	247.547
Mach Number [ ]	0	0.393805
Shear Stress [Pa]	0	34.7905
Heat Transfer Coefficient [W/m^2/K]	0	0
Surface Heat Flux [W/m^2]	0	0
Density [kg/m^3]	0.546248	0.659747

E.6 RAT located on the nose and tail. Sea level report

General Info

Model	C:\Users\Andreu\Documents\Andreu\Universitat\TFC\Treball per capítols\Capítol 4\Sims\Nose\simplificat+rat-nosetail.SLDPRT
Project name	sim_obstacle (10)
Project path	C:\Users\Andreu\Documents\Andreu\Universitat\TFC\Treball per capítols\Capítol 4\Sims\Nose\10
Units system	SI (m-kg-s)
Analysis type	External (exclude internal spaces)
Exclude cavities without flow conditions	On
Coordinate system	Global coordinate system
Reference axis	Z

INPUT DATA

Initial Mesh Settings
Automatic initial mesh: On
Result resolution level: 6
Advanced narrow channel refinement: Off
Refinement in solid region: Off

Geometry Resolution
Evaluation of minimum gap size: Automatic
Evaluation of minimum wall thickness: Automatic

Computational Domain
Size

X min	-22.1371623 m
X max	22.136617 m
Y min	-7.95387799 m
Y max	11.0918251 m
Z min	-28.6827146 m
Z max	23.0001653 m

Boundary Conditions

2D plane flow	None
At X min	Default
At X max	Default
At Y min	Default
At Y max	Default
At Z min	Default
At Z max	Default

Physical Features
Heat conduction in solids: Off
Time dependent: On
Gravitational effects: On
Flow type: Laminar and turbulent
High Mach number flow: Off
Humidity: Off
Default roughness: 0 micrometer

Gravitational Settings

X component	0 m/s^2
Y component	-9.81 m/s^2
Z component	0 m/s^2

Default wall conditions: Adiabatic wall
Ambient Conditions

Thermodynamic parameters	Static Pressure: 101325 Pa Temperature: 293.2 K
Velocity parameters	Velocity vector Velocity in X direction: 0 m/s Velocity in Y direction: 0 m/s Velocity in Z direction: -75.56 m/s
Turbulence parameters	Turbulence intensity and length Intensity: 0.1 % Length: 0.113583997 m

Material Settings
Fluids
Air

Goals
Global Goals

GG Min Total Pressure 1

Type	Global Goal
Goal type	Total Pressure
Calculate	Minimum value
Coordinate system	Global coordinate system
Use in convergence	On

GG Av Total Pressure 1

Type	Global Goal
Goal type	Total Pressure
Calculate	Average value
Coordinate system	Global coordinate system
Use in convergence	On

GG Max Total Pressure 1

Type	Global Goal
Goal type	Total Pressure
Calculate	Maximum value
Coordinate system	Global coordinate system
Use in convergence	On

GG Min Velocity 1

Type	Global Goal
Goal type	Velocity
Calculate	Minimum value
Coordinate system	Global coordinate system
Use in convergence	On

GG Av Velocity 1

Type	Global Goal
Goal type	Velocity
Calculate	Average value
Coordinate system	Global coordinate system
Use in convergence	On

GG Max Velocity 1

Type	Global Goal
Goal type	Velocity
Calculate	Maximum value
Coordinate system	Global coordinate system
Use in convergence	On

GG Y - Component of Force 1

Type	Global Goal
Goal type	Y - Component of Force
Coordinate system	Global coordinate system
Use in convergence	On

GG Z - Component of Force 1

Type	Global Goal
Goal type	Z - Component of Force
Coordinate system	Global coordinate system
Use in convergence	On

Calculation Control Options
Finish Conditions

Finish conditions	If one is satisfied
Maximum physical time	1 s

Solver Refinement

Refinement level	1
Refinement criterion	1.5
Unrefinement criterion	0.15
Adaptive refinement in fluid	On
Use global parameter variation	Off
Approximate maximum cells	3200000
Refinement strategy	Tabular refinement
Units	Travels
Relaxation interval	0.2
Refinements	2

Results Saving

Save before refinement	On

Advanced Control Options
Flow Freezing

Flow freezing strategy	Disabled

Manual time step: Off

RESULTS

General Info
Iterations: 328
Physical time: 7.37250589 s
CPU time: 734 s

Log

Mesh generation started	23:41:48 , Jul 01
Mesh generation normally finished	23:43:23 , Jul 01
Preparing data for calculation	23:43:34 , Jul 01
Calculation started 0	23:43:39 , Jul 01
Refinement 327	23:55:23 , Jul 01
Calculation has converged since the following criteria are satisfied: 327	23:56:46 , Jul 01
Max. phys. time is reached 327	
Calculation finished 328	23:57:03 , Jul 01

Calculation Mesh
Basic Mesh Dimensions

Number of cells in X	37
Number of cells in Y	18
Number of cells in Z	46

Number Of Cells

Total cells	78355
Fluid cells	67760
Solid cells	2421
Partial cells	8174
Irregular cells	0
Trimmed cells	253

Maximum refinement level: 2

Goals

Name	Unit	Value	Progress	Use in convergence	Delta	Criteria
GG Min Total Pressure 1	Pa	98117.9	100	On	401.803253	695.667563
GG Av Total	Pa	104761	24.6	On	3.36682913	0.830317876

Pressure 1						
GG Max Total Pressure 1	Pa	107485	100	On	483.672223	633.545998
GG Min Velocity 1	m/s	0	100	On	0	0
GG Av Velocity 1	m/s	75.2043	100	On	0.00217583392	0.010911281
GG Max Velocity 1	m/s	92.486	10.3	On	2.29878939	0.23777453
GG Y - Component of Force 1	N	4352.08	3.9	On	19057.586	746.920466
GG Z - Component of Force 1	N	-61250	31.1	On	8029.31202	2504.75535

Min/Max Table

Name	Minimum	Maximum
Pressure [Pa]	98117.9	106887
Temperature [K]	291.787	296.035
Velocity [m/s]	0	93.1364
X – Component of Velocity [m/s]	-41.6815	40.2788
Y – Component of Velocity [m/s]	-54.5077	37.6998
Z – Component of Velocity [m/s]	-92.2153	42.5922
Fluid Temperature [K]	291.787	296.035
Mach Number [ ]	0	0.272054
Shear Stress [Pa]	0	32.5702
Heat Transfer Coefficient [W/m^2/K]	0	0
Surface Heat Flux [W/m^2]	0	0
Density [kg/m^3]	1.16142	1.25793

E.7 RAT located on the nose and tail. 7,000 ft report

General Info

Model	C:\Users\Andreu\Documents\Andreu\Universitat\TFC\Treball per capítols\Capítol 4\Sims\Nose\simplificat+rat-nosetail.SLDPRT
Project name	sim_obstacle (11)
Project path	C:\Users\Andreu\Documents\Andreu\Universitat\TFC\Treball per capítols\Capítol 4\Sims\Nose\11
Units system	SI (m-kg-s)
Analysis type	External (exclude internal spaces)
Exclude cavities without flow conditions	On
Coordinate system	Global coordinate system
Reference axis	Z

INPUT DATA

Initial Mesh Settings
Automatic initial mesh: On
Result resolution level: 6
Advanced narrow channel refinement: Off
Refinement in solid region: Off

Geometry Resolution
Evaluation of minimum gap size: Automatic
Evaluation of minimum wall thickness: Automatic

Computational Domain
Size

X min	-20.551245 m
X max	20.7489394 m
Y min	-7.16091936 m
Y max	10.6953458 m
Z min	-25.4288677 m
Z max	24.3830448 m

Boundary Conditions

2D plane flow	None
At X min	Default
At X max	Default
At Y min	Default
At Y max	Default
At Z min	Default
At Z max	Default

Physical Features
Heat conduction in solids: Off
Time dependent: On
Gravitational effects: On
Flow type: Laminar and turbulent
High Mach number flow: Off
Humidity: Off
Default roughness: 0 micrometer

Gravitational Settings

X component	0 m/s^2
Y component	-9.81 m/s^2
Z component	0 m/s^2

Default wall conditions: Adiabatic wall
Ambient Conditions

Thermodynamic parameters	Temperature: 242.55 K Density: 0.59 kg/m^3
Velocity parameters	Velocity vector Velocity in X direction: 0 m/s Velocity in Y direction: 0 m/s Velocity in Z direction: -100.35 m/s
Turbulence parameters	Turbulence intensity and length Intensity: 0.1 % Length: 0.113583997 m

Material Settings
Fluids
Air

Goals
Global Goals

GG Min Total Pressure 1

Type	Global Goal
Goal type	Total Pressure
Calculate	Minimum value
Coordinate system	Global coordinate system
Use in convergence	On

GG Av Total Pressure 1

Type	Global Goal
Goal type	Total Pressure
Calculate	Average value
Coordinate system	Global coordinate system
Use in convergence	On

GG Max Total Pressure 1

Type	Global Goal
Goal type	Total Pressure
Calculate	Maximum value
Coordinate system	Global coordinate system
Use in convergence	On

GG Min Velocity 1

Type	Global Goal
Goal type	Velocity
Calculate	Minimum value
Coordinate system	Global coordinate system
Use in convergence	On

GG Av Velocity 1

Type	Global Goal
Goal type	Velocity
Calculate	Average value
Coordinate system	Global coordinate system
Use in convergence	On

GG Max Velocity 1

Type	Global Goal
Goal type	Velocity
Calculate	Maximum value
Coordinate system	Global coordinate system
Use in convergence	On

GG Y - Component of Force 1

Type	Global Goal
Goal type	Y - Component of Force
Coordinate system	Global coordinate system
Use in convergence	On

GG Z - Component of Force 1

Type	Global Goal
Goal type	Z - Component of Force
Coordinate system	Global coordinate system
Use in convergence	On

Calculation Control Options
Finish Conditions

Finish conditions	If one is satisfied
Maximum physical time	1 s

Solver Refinement

Refinement level	1
Refinement criterion	1.5
Unrefinement criterion	0.15
Adaptive refinement in fluid	On
Use global parameter variation	Off
Approximate maximum cells	3200000

Refinement strategy	Tabular refinement
Units	Travels
Relaxation interval	0.2
Refinements	2

Results Saving

Save before refinement	On

Advanced Control Options
Flow Freezing

Flow freezing strategy	Disabled

Manual time step: Off

RESULTS

General Info
Iterations: 306
Physical time: 5.27651141 s
CPU time: 526 s

Log

Mesh generation started	00:28:31 , Jul 02
Mesh generation normally finished	00:30:12 , Jul 02
Preparing data for calculation	00:30:25 , Jul 02
Calculation started 0	00:30:30 , Jul 02
Refinement 305	00:38:39 , Jul 02
Calculation has converged since the following criteria are satisfied: 305	00:39:57 , Jul 02
Max. phys. time is reached 305	
Calculation finished 306	00:40:10 , Jul 02

Calculation Mesh
Basic Mesh Dimensions

Number of cells in X	37
Number of cells in Y	15
Number of cells in Z	44

Number Of Cells

Total cells	68905
Fluid cells	58579
Solid cells	2370
Partial cells	7956
Irregular cells	0
Trimmed cells	251

Maximum refinement level: 2
Goals

Name	Unit	Value	Progress	Use in convergence	Delta	Criteria
GG Min Total Pressure 1	Pa	37896.8	100	On	30.5365155	165.503189
GG Av Total Pressure 1	Pa	44077.5	67.3	On	2.99500912	2.01824392
GG Max Total Pressure 1	Pa	47848.3	86.1	On	490.91535	423.145865
GG Min Velocity 1	m/s	0	100	On	0	0
GG Av Velocity 1	m/s	99.4425	100	On	0.00562320236	0.0283920474

GG Max Velocity 1	m/s	130.363	10.1	On	3.89091742	0.39634597
GG Y - Component of Force 1	N	15456.1	32.9	On	5529.6444	1820.30494
GG Z - Component of Force 1	N	-62122.2	20.9	On	13250.451	2780.30932

Min/Max Table

Name	Minimum	Maximum
Pressure [Pa]	37896.6	47708.5
Temperature [K]	239.108	247.554
Velocity [m/s]	0	126.064
X – Component of Velocity [m/s]	-63.2355	72.524
Y – Component of Velocity [m/s]	-58.8376	53.4961
Z – Component of Velocity [m/s]	-124.742	29.7431
Fluid Temperature [K]	239.108	247.554
Mach Number [ ]	0	0.406745
Shear Stress [Pa]	0	24.8753
Heat Transfer Coefficient [W/m^2/K]	0	0
Surface Heat Flux [W/m^2]	0	0
Density [kg/m^3]	0.541412	0.671736

E.8 RAT located on the belly-fairing. Sea level report

General Info

Model	C:\Users\Andreu\Documents\Andreu\Universitat\TFC\Treball per capítols\Capítol 4\Sims\Belly-fairing\simplificat+rat-belly.SLDPRT
Project name	sim_obstacle (5)
Project path	C:\Users\Andreu\Documents\Andreu\Universitat\TFC\Treball per capítols\Capítol 4\Sims\Belly-fairing\1
Units system	SI (m-kg-s)
Analysis type	External (exclude internal spaces)
Exclude cavities without flow conditions	On
Coordinate system	Global coordinate system
Reference axis	Z

INPUT DATA

Initial Mesh Settings
Automatic initial mesh: On
Result resolution level: 6
Advanced narrow channel refinement: Off
Refinement in solid region: Off

Geometry Resolution
Evaluation of minimum gap size: Automatic
Evaluation of minimum wall thickness: Automatic

Computational Domain
Size

X min	-22.0119054 m
X max	22.7167138 m
Y min	-6.76266152 m
Y max	11.4207588 m
Z min	-44.1180866 m
Z max	10.7604728 m

Boundary Conditions

2D plane flow	None
At X min	Default
At X max	Default
At Y min	Default
At Y max	Default
At Z min	Default
At Z max	Default

Physical Features

Heat conduction in solids: Off
Time dependent: On
Gravitational effects: On
Flow type: Laminar and turbulent
High Mach number flow: Off
Humidity: Off
Default roughness: 0 micrometer

Gravitational Settings

X component	0 m/s^2
Y component	-9.81 m/s^2
Z component	0 m/s^2

Default wall conditions: Adiabatic wall

Ambient Conditions

Thermodynamic parameters	Static Pressure: 101325 Pa Temperature: 293.2 K
Velocity parameters	Velocity vector Velocity in X direction: 0 m/s Velocity in Y direction: 0 m/s Velocity in Z direction: -75.56 m/s
Turbulence parameters	Turbulence intensity and length Intensity: 0.1 % Length: 0.114580803 m

Material Settings
Fluids
Air

Goals
Global Goals

GG Min Total Pressure 1

Type	Global Goal
Goal type	Total Pressure
Calculate	Minimum value
Coordinate system	Global coordinate system
Use in convergence	On

GG Av Total Pressure 1

Type	Global Goal
Goal type	Total Pressure
Calculate	Average value
Coordinate system	Global coordinate system
Use in convergence	On

GG Max Total Pressure 1

Type	Global Goal
Goal type	Total Pressure
Calculate	Maximum value
Coordinate system	Global coordinate system
Use in convergence	On

GG Min Velocity 1

Type	Global Goal
Goal type	Velocity
Calculate	Minimum value
Coordinate system	Global coordinate system
Use in convergence	On

GG Av Velocity 1

Type	Global Goal
Goal type	Velocity
Calculate	Average value
Coordinate system	Global coordinate system
Use in convergence	On

GG Max Velocity 1

Type	Global Goal
Goal type	Velocity
Calculate	Maximum value
Coordinate system	Global coordinate system
Use in convergence	On

GG Y - Component of Force 1

Type	Global Goal
Goal type	Y - Component of Force
Coordinate system	Global coordinate system
Use in convergence	On

GG Z - Component of Force 1

Type	Global Goal
Goal type	Z - Component of Force
Coordinate system	Global coordinate system
Use in convergence	On

Calculation Control Options
Finish Conditions

Finish conditions	If one is satisfied
Maximum physical time	1 s

Solver Refinement

Refinement level	1
Refinement criterion	1.5
Unrefinement criterion	0.15
Adaptive refinement in fluid	On
Use global parameter variation	Off
Approximate maximum cells	3200000
Refinement strategy	Tabular refinement
Units	Travels
Relaxation interval	0.2
Refinements	2

Results Saving

Save before refinement	On

Advanced Control Options

Flow Freezing

Flow freezing strategy	Disabled

Manual time step: Off

RESULTS

General Info

Iterations: 328
Physical time: 7.46894867 s
CPU time: 623 s

Log

Mesh generation started	18:26:04 , Jul 01
Mesh generation normally finished	18:27:41 , Jul 01
Preparing data for calculation	18:27:49 , Jul 01
Calculation started 0	18:27:54 , Jul 01
Refinement 327	18:38:08 , Jul 01
Calculation has converged since the following criteria are satisfied: 327	18:39:27 , Jul 01
Max. phys. time is reached 327	
Calculation finished 328	18:39:42 , Jul 01

Calculation Mesh
Basic Mesh Dimensions

Number of cells in X	39
Number of cells in Y	17
Number of cells in Z	46

Number Of Cells

Total cells	82725
Fluid cells	70720
Solid cells	2953
Partial cells	9052
Irregular cells	0
Trimmed cells	147

Maximum refinement level: 2

Goals

Name	Unit	Value	Progress	Use in convergence	Delta	Criteria
GG Min Total Pressure 1	Pa	97225.6	57.3	On	520.930224	298.911494
GG Av Total Pressure 1	Pa	104740	55.5	On	1.83828521	1.02106161
GG Max Total Pressure 1	Pa	107871	73	On	819.443083	598.49882
GG Min Velocity 1	m/s	0	100	On	0	0
GG Av Velocity 1	m/s	75.1049	100	On	0.00322908066	0.013004518
GG Max Velocity 1	m/s	102.487	1.9	On	12.5653455	0.24888411
GG Y - Component of Force 1	N	-12611.4	3.8	On	23034.7029	880.918713
GG Z - Component of Force 1	N	-61017.3	15.8	On	12313.5642	1949.35866

Min/Max Table

Name	Minimum	Maximum
Pressure [Pa]	97225.6	106127
Temperature [K]	290.818	296.016
Velocity [m/s]	0	95.6459
X – Component of Velocity [m/s]	-47.1476	43.8193
Y – Component of Velocity [m/s]	-41.797	43.32
Z – Component of Velocity [m/s]	-94.7401	25.4801
Fluid Temperature [K]	290.818	296.016
Mach Number [ ]	0	0.279297
Shear Stress [Pa]	0	26.8187
Heat Transfer Coefficient [W/m^2/K]	0	0
Surface Heat Flux [W/m^2]	0	0
Density [kg/m^3]	1.14412	1.25044

E.9 RAT located on the belly-fairing. 7,000 ft report

General Info

Model	C:\Users\Andreu\Documents\Andreu\Universitat\TFC\Treball per capítols\Capítol 4\Sims\Belly-fairing\simplificat+rat-belly.SLDPRT
Project name	sim_obstacle (6)
Project path	C:\Users\Andreu\Documents\Andreu\Universitat\TFC\Treball per capítols\Capítol 4\Sims\Belly-fairing\2
Units system	SI (m-kg-s)
Analysis type	External (exclude internal spaces)
Exclude cavities without flow conditions	On
Coordinate system	Global coordinate system
Reference axis	Z

INPUT DATA

Initial Mesh Settings
Automatic initial mesh: On
Result resolution level: 6
Advanced narrow channel refinement: Off
Refinement in solid region: Off

Geometry Resolution
Evaluation of minimum gap size: Automatic
Evaluation of minimum wall thickness: Automatic

Computational Domain
Size

X min	-23.1865865 m
X max	22.6227398 m
Y min	-8.03131669 m
Y max	12.4074906 m
Z min	-43.8503063 m
Z max	6.26179077 m

Boundary Conditions

2D plane flow	None
At X min	Default
At X max	Default
At Y min	Default
At Y max	Default
At Z min	Default
At Z max	Default

Physical Features
Heat conduction in solids: Off
Time dependent: On
Gravitational effects: On
Flow type: Laminar and turbulent
High Mach number flow: Off
Humidity: Off
Default roughness: 0 micrometer

Gravitational Settings

X component	0 m/s^2
Y component	-9.81 m/s^2
Z component	0 m/s^2

Default wall conditions: Adiabatic wall
Ambient Conditions

Thermodynamic parameters	Temperature: 242.55 K Density: 0.59 kg/m^3
Velocity parameters	Velocity vector Velocity in X direction: 0 m/s Velocity in Y direction: 0 m/s Velocity in Z direction: -100.35 m/s
Turbulence parameters	Turbulence intensity and length Intensity: 0.1 % Length: 0.114580803 m

Material Settings
Fluids
Air

Goals
Global Goals

GG Min Total Pressure 1

Type	Global Goal
Goal type	Total Pressure
Calculate	Minimum value
Coordinate system	Global coordinate system
Use in convergence	On

GG Av Total Pressure 1

Type	Global Goal
Goal type	Total Pressure
Calculate	Average value
Coordinate system	Global coordinate system
Use in convergence	On

GG Max Total Pressure 1

Type	Global Goal
Goal type	Total Pressure
Calculate	Maximum value
Coordinate system	Global coordinate system
Use in convergence	On

GG Min Velocity 1

Type	Global Goal

Goal type	Velocity
Calculate	Minimum value
Coordinate system	Global coordinate system
Use in convergence	On

GG Av Velocity 1

Type	Global Goal
Goal type	Velocity
Calculate	Average value
Coordinate system	Global coordinate system
Use in convergence	On

GG Max Velocity 1

Type	Global Goal
Goal type	Velocity
Calculate	Maximum value
Coordinate system	Global coordinate system
Use in convergence	On

GG Y - Component of Force 1

Type	Global Goal
Goal type	Y - Component of Force
Coordinate system	Global coordinate system
Use in convergence	On

GG Z - Component of Force 1

Type	Global Goal
Goal type	Z - Component of Force
Coordinate system	Global coordinate system
Use in convergence	On

Calculation Control Options
Finish Conditions

Finish conditions	If one is satisfied
Maximum physical time	1 s

Solver Refinement

Refinement level	1
Refinement criterion	1.5
Unrefinement criterion	0.15
Adaptive refinement in fluid	On
Use global parameter variation	Off
Approximate maximum cells	3200000
Refinement strategy	Tabular refinement
Units	Travels
Relaxation interval	0.2
Refinements	2

Results Saving

Save before refinement	On

Advanced Control Options
Flow Freezing

Flow freezing strategy	Disabled

Manual time step: Off

RESULTS

General Info

Iterations: 328
Physical time: 5.46544857 s
CPU time: 614 s

Log

Mesh generation started	18:58:21 , Jul 01
Mesh generation normally finished	18:59:56 , Jul 01
Preparing data for calculation	19:00:06 , Jul 01
Calculation started 0	19:00:11 , Jul 01
Refinement 327	19:10:22 , Jul 01
Calculation has converged since the following criteria are satisfied: 327	19:11:35 , Jul 01
Max. phys. time is reached 327	
Calculation finished 328	19:11:48 , Jul 01

Calculation Mesh
Basic Mesh Dimensions

Number of cells in X	39
Number of cells in Y	18
Number of cells in Z	44

Number Of Cells

Total cells	76808
Fluid cells	65876
Solid cells	2720
Partial cells	8212
Irregular cells	0
Trimmed cells	232

Maximum refinement level: 2

Goals

Name	Unit	Value	Progress	Use in convergence	Delta	Criteria
GG Min Total Pressure 1	Pa	38078	36.5	On	409.353566	149.610496
GG Av Total Pressure 1	Pa	44103.7	46.6	On	3.06510889	1.42941468
GG Max Total Pressure 1	Pa	46716.7	34.9	On	1212.60017	423.960706
GG Min Velocity 1	m/s	0	100	On	0	0
GG Av Velocity 1	m/s	99.9658	100	On	0.00240618767	0.0139342689
GG Max Velocity 1	m/s	121.916	21.9	On	1.56712589	0.343544024
GG Y - Component of Force 1	N	-888.244	14.2	On	12863.8588	1834.5705
GG Z - Component of Force 1	N	-56523.1	36.7	On	8763.91894	3224.5593

Min/Max Table

Name	Minimum	Maximum
Pressure [Pa]	38078	46080.2
Temperature [K]	240.168	247.548
Velocity [m/s]	0	123.65
X – Component of Velocity [m/s]	-70.7875	63.7172

Y – Component of Velocity [m/s]	-59.812	60.833
Z – Component of Velocity [m/s]	-121.596	31.6339
Fluid Temperature [K]	240.168	247.548
Mach Number [ ]	0	0.398001
Shear Stress [Pa]	0	29.8596
Heat Transfer Coefficient [W/m^2/K]	0	0
Surface Heat Flux [W/m^2]	0	0
Density [kg/m^3]	0.536531	0.649173

E.10 A320 without RAT. Sea level report

General Info

Model	C:\Users\Andreu\Documents\Andreu\Universitat\TFC\Treball per capítols\Capítol 4\Sims\simplificat.SLDPRT
Project name	sim_obstacle (2)
Project path	C:\Users\Andreu\Documents\Andreu\Universitat\TFC\Treball per capítols\Capítol 4\Sims\2
Units system	SI (m-kg-s)
Analysis type	External (exclude internal spaces)
Exclude cavities without flow conditions	On
Coordinate system	Global coordinate system
Reference axis	Z

INPUT DATA

Initial Mesh Settings
Automatic initial mesh: On
Result resolution level: 6
Advanced narrow channel refinement: Off
Refinement in solid region: Off

Geometry Resolution
Evaluation of minimum gap size: Automatic
Evaluation of minimum wall thickness: Automatic

Computational Domain
Size

X min	-22.7830319 m
X max	23.2426001 m
Y min	-8.5377722 m
Y max	12.9964298 m
Z min	-28.1721994 m
Z max	22.8733359 m

Boundary Conditions

2D plane flow	None
At X min	Default
At X max	Default
At Y min	Default
At Y max	Default
At Z min	Default
At Z max	Default

Physical Features
Heat conduction in solids: Off
Time dependent: On
Gravitational effects: On

Flow type: Laminar and turbulent
High Mach number flow: Off
Humidity: Off
Default roughness: 0 micrometer

Gravitational Settings

X component	0 m/s^2
Y component	-9.81 m/s^2
Z component	0 m/s^2

Default wall conditions: Adiabatic wall
Ambient Conditions

Thermodynamic parameters	Temperature: 242.55 K Density: 0.59 kg/m^3
Velocity parameters	Velocity vector Velocity in X direction: 0 m/s Velocity in Y direction: 0 m/s Velocity in Z direction: -100.35 m/s
Turbulence parameters	Turbulence intensity and length Intensity: 0.1 % Length: 0.113583997 m

Material Settings
Fluids
Air

Goals
Global Goals
GG Min Total Pressure 1

Type	Global Goal
Goal type	Total Pressure
Calculate	Minimum value
Coordinate system	Global coordinate system
Use in convergence	On

GG Av Total Pressure 1

Type	Global Goal
Goal type	Total Pressure
Calculate	Average value
Coordinate system	Global coordinate system
Use in convergence	On

GG Max Total Pressure 1

Type	Global Goal
Goal type	Total Pressure
Calculate	Maximum value
Coordinate system	Global coordinate system
Use in convergence	On

GG Min Velocity 1

Type	Global Goal
Goal type	Velocity
Calculate	Minimum value
Coordinate system	Global coordinate system
Use in convergence	On

GG Av Velocity 1

Type	Global Goal
Goal type	Velocity
Calculate	Average value
Coordinate system	Global coordinate system
Use in convergence	On

GG Max Velocity 1

Type	Global Goal
Goal type	Velocity
Calculate	Maximum value
Coordinate system	Global coordinate system
Use in convergence	On

GG Y - Component of Force 1

Type	Global Goal
Goal type	Y - Component of Force
Coordinate system	Global coordinate system
Use in convergence	On

GG Z - Component of Force 1

Type	Global Goal
Goal type	Z - Component of Force
Coordinate system	Global coordinate system
Use in convergence	On

Calculation Control Options
Finish Conditions

Finish conditions	If one is satisfied
Maximum physical time	1 s

Solver Refinement

Refinement level	1
Refinement criterion	1.5
Unrefinement criterion	0.15
Adaptive refinement in fluid	On
Use global parameter variation	Off
Approximate maximum cells	3200000
Refinement strategy	Tabular refinement
Units	Travels
Relaxation interval	0.2
Refinements	2

Results Saving

Save before refinement	On

Advanced Control Options
Flow Freezing

Flow freezing strategy	Disabled

Manual time step: Off

RESULTS

General Info
Iterations: 335
Physical time: 6.6260849 s
CPU time: 652 s

Log

Mesh generation started	15:13:08 , Jul 02
Mesh generation normally finished	15:14:39 , Jul 02
Preparing data for calculation	15:14:47 , Jul 02
Calculation started 0	15:14:52 , Jul 02
Refinement 346	15:26:46 , Jul 02
Calculation has converged since the following criteria are satisfied: 346	15:28:00 , Jul 02
Max. phys. time is reached 346	
Calculation finished 347	15:28:15 , Jul 02

Calculation Mesh
Basic Mesh Dimensions

Number of cells in X	39
Number of cells in Y	19
Number of cells in Z	44

Number Of Cells

Total cells	84586
Fluid cells	71040
Solid cells	3952
Partial cells	9594
Irregular cells	0
Trimmed cells	164

Maximum refinement level: 2
Goals

Name	Unit	Value	Progress	Use in convergence	Delta	Criteria
GG Min Total Pressure 1	Pa	95995.9	14.9	On	2001.15475	298.522257
GG Av Total Pressure 1	Pa	104764	20.5	On	3.13654993	0.6442506
GG Max Total Pressure 1	Pa	107291	63.4	On	543.173155	344.89948
GG Min Velocity 1	m/s	0	100	On	0	0
GG Av Velocity 1	m/s	75.4437	100	On	0.000555661943	0.0044751039
GG Max Velocity 1	m/s	94.9686	16.9	On	2.78526902	0.471993438
GG Y - Component of Force 1	N	-4747.68	3.7	On	16775.515	631.236605
GG Z - Component of Force 1	N	-56489.9	21.9	On	11174.2244	2451.2347

Min/Max Table

Name	Minimum	Maximum
Pressure [Pa]	95995.9	105737
Temperature [K]	291.556	295.941
Velocity [m/s]	0	95.3566
X – Component of Velocity [m/s]	-44.8716	44.836
Y – Component of Velocity [m/s]	-61.002	45.991
Z – Component of Velocity [m/s]	-94.3402	24.1403
Fluid Temperature [K]	291.556	295.941
Mach Number [ ]	0	0.278625
Shear Stress [Pa]	0	27.5055
Heat Transfer Coefficient	0	0

[W/m^2/K]		
Surface Heat Flux [W/m^2]	0	0
Density [kg/m^3]	1.1306	1.24415

E.11 A320 without RAT. 7,000 ft report

General Info

Model	C:\Users\Andreu\Documents\Andreu\Universitat\TFC\Treball per capítols\Capítol 4\Sims\simplificat.SLDPRT
Project name	sim_obstacle (2)
Project path	C:\Users\Andreu\Documents\Andreu\Universitat\TFC\Treball per capítols\Capítol 4\Sims\2
Units system	SI (m-kg-s)
Analysis type	External (exclude internal spaces)
Exclude cavities without flow conditions	On
Coordinate system	Global coordinate system
Reference axis	Z

INPUT DATA

Initial Mesh Settings
Automatic initial mesh: On
Result resolution level: 6
Advanced narrow channel refinement: Off
Refinement in solid region: Off

Geometry Resolution
Evaluation of minimum gap size: Automatic
Evaluation of minimum wall thickness: Automatic

Computational Domain
Size

X min	-22.7830319 m
X max	23.2426001 m
Y min	-8.5377722 m
Y max	12.9964298 m
Z min	-28.1721994 m
Z max	22.8733359 m

Boundary Conditions

2D plane flow	None
At X min	Default
At X max	Default
At Y min	Default
At Y max	Default
At Z min	Default
At Z max	Default

Physical Features
Heat conduction in solids: Off
Time dependent: On
Gravitational effects: On
Flow type: Laminar and turbulent
High Mach number flow: Off
Humidity: Off
Default roughness: 0 micrometer

Gravitational Settings

X component	0 m/s^2
Y component	-9.81 m/s^2
Z component	0 m/s^2

Default wall conditions: Adiabatic wall
Ambient Conditions

Thermodynamic parameters	Temperature: 242.55 K Density: 0.59 kg/m^3
Velocity parameters	Velocity vector Velocity in X direction: 0 m/s Velocity in Y direction: 0 m/s Velocity in Z direction: -100.35 m/s
Turbulence parameters	Turbulence intensity and length Intensity: 0.1 % Length: 0.113583997 m

Material Settings
Fluids
Air

Goals
Global Goals
GG Min Total Pressure 1

Type	Global Goal
Goal type	Total Pressure
Calculate	Minimum value
Coordinate system	Global coordinate system
Use in convergence	On

GG Av Total Pressure 1

Type	Global Goal
Goal type	Total Pressure
Calculate	Average value
Coordinate system	Global coordinate system
Use in convergence	On

GG Max Total Pressure 1

Type	Global Goal
Goal type	Total Pressure
Calculate	Maximum value
Coordinate system	Global coordinate system
Use in convergence	On

GG Min Velocity 1

Type	Global Goal
Goal type	Velocity
Calculate	Minimum value
Coordinate system	Global coordinate system
Use in convergence	On

GG Av Velocity 1

Type	Global Goal
Goal type	Velocity
Calculate	Average value
Coordinate system	Global coordinate system
Use in convergence	On

GG Max Velocity 1

Type	Global Goal
Goal type	Velocity
Calculate	Maximum value
Coordinate system	Global coordinate system
Use in convergence	On

GG Y - Component of Force 1

Type	Global Goal
Goal type	Y - Component of Force
Coordinate system	Global coordinate system
Use in convergence	On

GG Z - Component of Force 1

Type	Global Goal
Goal type	Z - Component of Force
Coordinate system	Global coordinate system
Use in convergence	On

Calculation Control Options
Finish Conditions

Finish conditions	If one is satisfied
Maximum physical time	1 s

Solver Refinement

Refinement level	1
Refinement criterion	1.5
Unrefinement criterion	0.15
Adaptive refinement in fluid	On
Use global parameter variation	Off
Approximate maximum cells	3200000
Refinement strategy	Tabular refinement
Units	Travels
Relaxation interval	0.2
Refinements	2

Results Saving

Save before refinement	On

Advanced Control Options
Flow Freezing

Flow freezing strategy	Disabled

Manual time step: Off

RESULTS

General Info
Iterations: 347
Physical time: 5.17374648 s
CPU time: 725 s

Log

Mesh generation started	15:13:08 , Jul 02
Mesh generation normally finished	15:14:39 , Jul 02
Preparing data for calculation	15:14:47 , Jul 02
Calculation started 0	15:14:52 , Jul 02
Refinement 346	15:26:46 , Jul 02
Calculation has converged since the following	15:28:00 , Jul 02

criteria are satisfied:	346	
Max. phys. time is reached	346	
Calculation finished	347	15:28:15 , Jul 02

Calculation Mesh
Basic Mesh Dimensions

Number of cells in X	40
Number of cells in Y	20
Number of cells in Z	46

Number Of Cells

Total cells	88719
Fluid cells	76079
Solid cells	3418
Partial cells	9222
Irregular cells	0
Trimmed cells	164

Maximum refinement level: 2
Goals

Name	Unit	Value	Progress	Use in convergence	Delta	Criteria
GG Min Total Pressure 1	Pa	38364.5	35.8	On	648.91084	232.722956
GG Av Total Pressure 1	Pa	44115.7	84.8	On	1.91692909	1.62681018
GG Max Total Pressure 1	Pa	45885.3	100	On	46.982306	335.297836
GG Min Velocity 1	m/s	0	100	On	0	0
GG Av Velocity 1	m/s	100.195	100	On	0.00208960673	0.00725364894
GG Max Velocity 1	m/s	131.603	3.7	On	9.44261245	0.358191225
GG Y - Component of Force 1	N	-6032.06	14.2	On	15245.6437	2176.8243
GG Z - Component of Force 1	N	-49130.9	36.7	On	8920.92395	3276.50688

Min/Max Table

Name	Minimum	Maximum
Pressure [Pa]	38364.5	44861.3
Temperature [K]	238.942	247.381
Velocity [m/s]	0	125.998
X – Component of Velocity [m/s]	-54.7378	54.2203
Y – Component of Velocity [m/s]	-63.5256	59.1818
Z – Component of Velocity [m/s]	-125.08	24.5861
Fluid Temperature [K]	238.942	247.381
Mach Number [ ]	0	0.406673
Shear Stress [Pa]	0	27.5546
Heat Transfer Coefficient [W/m^2/K]	0	0
Surface Heat Flux [W/m^2]	0	0
Density [kg/m^3]	0.546509	0.631575

ANNEX F – SPECIFICATIONS

F.1 Hamilton Sundstrand A320 RAT model ERPS06M

RAM AIR TURBINE MODULE

Speed and Direction of Rotation
Direction of Rotation (looking aft).. Clockwise
Minimum Airspeed at the Turbine for Rated Output .... 135.5 KEAS
Governed Turbine Speed (minimum/maximum) .... 4,800/6,600 rpm
Turbine/Hydraulic Pump Speed Ratio.. 1:1.09

Environmental Conditions
Maximum Operational Altitude... 41,000 ft (12.5 km)
Ambient Temperature Range .... -85°F to 194°F (-65°C to 90°C)

Weight and Overall Dimensions
Weight (Including 6.1 lb (2.77 kg) for Stow Panel)........................... 180.0 lb (81.65 kg)
Height .... 48 inch (1,220 mm)
Length .... 26 inch (660 mm)
Width.. 7 inch (178 mm)
Turbine Diameter .... 29.5 inch (749.3 mm)

HYDRAULIC PUMP

Hydraulic Fluid .... per NSA 307.110

Hydraulic Pump Output
Rated Flow Capacity.. 21.6 gpm (81.8 lpm)
Discharge Pressure .... 2,640 psi (18,202 kPa)
Operational Speed .... 4,500 to 6,950 rpm
Displacement (nominal) .... 0.9 cipr (94.75 ccpr)

Weight and Overall Dimensions
Weight .... 14.0 lbs (6.4 kg)
Height .... 5.6 inch (142.24 mm)
Length... 8.15 inch (207.01 mm)
Width... 6.4 inch (162.56 mm Mounting Flange AND10261)

ACTUATOR

Operating Pressure .... 2,610 to 3,000 psi (17,995 - 20,684 kPa)
Stroke .... 6.85 inch (173.99 mm)

Weight and Overall Dimensions
Weight (dry) .... 32.0 lbs (14.51 kg)
Length... 31 inch (787 mm)
Diameter .... 4.9 inch (124.46 mm)